STUDIES ON THE REGULATION OF THE CENTRAL MELANOCORTIN SYSTEM BY INFLAMMATORY CYTOKINES

by

Jarrad M. Scarlett

A DISSERTATION

Presented to the Neuroscience Graduate Program

and the Oregon Health & Science University

School of Medicine

in partial fulfillment of

the requirements for the degree of

Doctor of Philosophy

June 2007

School of Medicine
Oregon Health & Science University

CERTIFICATE OF APPROVAL

This is to certify that the Ph.D. dissertation of

Jarrad M. Scarlett

has been approved

[redacted]

Mentor/Advisor

[redacted]

Member

[redacted]

Member

[redacted]

Member

[redacted]

Member

TABLE OF CONTENTS

LIST OF FIGURES AND TABLES

Chapter 1. Introduction

Chapter 2. Regulation of central melanocortin signaling by interleukin-1β

LIST OF ABBREVIATIONS

α-MSH	α-melanocyte-stimulating hormone
A^{VY}	Variable yellow allele
A^{Y}	Lethal yellow allele
ACTH	Adrenocorticotropic hormone
AgRP	Agouti-related peptide
AP	Area postrema
ARC	Arcuate nucleus of the hypothalamus
BBB	Blood-brain barrier
CART	Cocaine and amphetamine-related transcript
CCK	Cholecystokinin
CHF	Chronic heart failure
CNS	Central nervous system
CNTF	Ciliary neurotrophic factor
COPD	Chronic obstructive pulmonary disease
COX1	Cyclooxygenase-1
COX2	Cyclooxygenase-2
db	Diabetic gene
DIO	Diet-induced obesity
DMH	Dorsomedial nucleus of the hypothalamus

DMV	Dorsal motor nucleus of vagus
EGFP	Enhanced green fluorescent protein
FACS	Flow cytometry and cell sorting
GABA	Gamma-aminobutyric acid
GH	Growth hormone
GHS-R	Growth hormone secretagogue receptor
HPA	Hypothalamic-pituitary-adrenal
ICE	IL-1β-converting enzyme
IFN-γ	Interferon-γ
IL-1β	Interleukin-1β
IL-1α	Interleukin-1α
IL-1R	IL-1 receptor
IL-1RI	Type I IL-1 receptor
IL-1RKO	IL-1R knockout mice
IL-1ra	IL-1 receptor antagonist
IL-1raKO	IL-1ra knockout mice
IL-1RAcP	IL-1R accessory protein
IL-6	Interleukin-6
IL-8	Interleukin-8
IL-10	Interleukin-10
IPSC	Inhibitory post-synaptic current
kDA	Kilodalton
LBM	Lean body mass

LIF	Leukemia inhibitory factor
LPS	Lipopolysaccharide
LHA	Lateral hypothalamic area
MC(1-5)-R	Melanocortin(1-5)-receptor
MC3-RKO	MC3-R knockout mouse
MC4-RKO	MC4-R knockout mouse
MCH	Melanin-concentrating hormone
MCH-KO	MCH knockout mouse
NF-κB	Nuclear factor-kappa B
NMU	Neuromedin U
NPY	Neuropeptide Y
NTS	Nucleus of the solitary tract
ob	Obese gene
OB-Rb	Leptin receptor (long form)
PC1	Prohormone convertase-1
PC2	Prohormone convertase-2
PeVN	Periventricular nucleus
POMC	Proopiomelancortin
PVN	Paraventricular nucleus
Sapphire	Tau-sapphire fusion protein
SLC-1	Somatostatin-like 1 receptor
SOCS-3	Suppressor-of-cytokine–signaling 3

STAT3	Signal-transducer and activator of transcription 3
Th_1	T helper 1 lymphocyte
Th_2	T helper 2 lymphocyte
TNF-α	Tumor necrosis factor alpha
TTX	Tetrodotoxin
VMH	Ventromedial hypothalamic nucleus
WT	Wild-type

ACKNOWLEDGMENTS

Although only a single individual is awarded a Ph.D for the completion of a dissertation, it is crucial to understand that this accomplishment was not, and could not have been accomplished alone. I am sincerely grateful to many people for their support (scientific, personal, emotional and financial) throughout my undergraduate and graduate education that made this achievement possible.

First, I would like to thank Dr. Robert Steiner and Dr. Donald Clifton, my first true mentors at the University of Washington who ignited my passion for science and research. I am forever indebted to both of them for helping bring focus and direction to my professional career. I would also like to acknowledge Dr. Matthew Cunningham who as a graduate student served as my primary teacher for three years. My growth and development as a scientist are a direct reflection of his efforts and I continue to be grateful for the extreme fortune that I had in being taught by him.

Thanks to my thesis advisor and current mentor Dr. Daniel Marks whose enthusiasm for science, keen scientific mind and breadth of knowledge made this dissertation possible. It was another stroke of good fortune that I came to OHSU at the same time that he was establishing his lab. I firmly believe that the choice of a mentor, above all other decisions made during graduate school, is the most important and I firmly believe that I could not have made a better choice than having Dan as my mentor.

Thank you to all the present and past members of the Marks lab who provided much assistance and make the lab a fun and enjoyable place to be. It has given me great joy to see the lab grow and develop over the past five years. In particular, I would like to thank Darren Bowe, Ayesha Batra and Peter Levasseaur for their contributions to this dissertation. Each is outstanding individual and scientist who I have been fortunate to work with.

My thanks to my thesis committee, Dr. Malcolm Low, Dr. Kevin Grove, Dr. Michael Cowley and Dr. Peter Kurre for their advice, encouragement and participation in my scientific endeavors.

Finally, I would like to thank my wife Julie, and my parents Warren and Linda Scarlett. You have truly "lived" the graduate school experience with me, celebrating accomplishments and successes and providing comfort and encouragement during setbacks. For all that you have done for me, I dedicate this dissertation to you.

PREFACE

I have prepared my dissertation in accordance with the guidelines set forth by the Graduate Program of the School of Medicine, Oregon Health and Science University. My thesis is comprised of a general introduction, three chapters of original data, and a final section consisting of summary and conclusions. The references throughout the entire thesis are listed together at the end of the manuscript and conform to the style of *Endocrinology*.

Chapter 2 is a manuscript as it appears in the original paper published in the journal *Endocrinology*. Chapter 3 is a manuscript as it has been prepared for submission to the journal *Endocrinology*. Chapter 4 is a manuscript as it has been prepared for submission to the journal *Circulation*. The appendix contains additional data regarding the regulation of the central melanocortin system by Leukemia Inhibitory Factor.

The electrophysiology experiments described in Chapter 2 were performed by Dr. Erin Jobst.

The radioimmunoassays for the peptide secretion studies described in Chapters 2 and 3 were performed by Dr. Pablo Enriori.

ABSTRACT

Disorders in food intake and energy homeostasis, characterized by anorexia and increased metabolic rate, are frequent manifestations in animals with acute and chronic diseases. Proinflammatory cytokines released in response to pathophysiological conditions are hypothesized to mediate these responses by acting upon neural systems in the brain that are involved in the regulation of feeding behavior and energy homeostasis. The central melanocortin system is a well-characterized neural system that has a key role in the regulation of feeding behavior and energy homeostasis. Recently, studies have demonstrated that blockade of central melancortin signaling attenuates cytokine and illness-induced anorexia suggesting that the central melanocortin system might have an important role in mediating the anorectic effects of cytokines. The goal of this thesis was to investigate the ability of individual cytokines to regulate the activity of the central melanocortin system and to characterize the response of the central melanocortin system to acute and chronic inflammatory states.

In the first part of this thesis work, we investigated the ability of interleukin-1β (IL-1β) to regulate central melanocortin signaling. We demonstrated that proopiomelanocortin (POMC) neurons in the arcuate nucleus of the hypothalamus (ARC) co-expressed the type I interleukin-1 receptor (IL-1R) and that intracerebroventricular (i.c.v.) injection of IL-1β induced the expression of Fos protein in ARC POMC neurons. IL-1β increased the frequency of action potentials of ARC POMC neurons. The release of α-melanocyte-stimulating hormone (α-MSH) from hypothalamic explants was increased by IL-1β in a dose-dependent fashion that was not blocked by inhibitors of

prostaglandin synthesis. These data suggest that IL-1β may increase central melanocortin signaling by directly activating ARC POMC neurons.

In the second part of this thesis work, we investigated the regulation of agouti-related protein (AgRP) during acute and chronic disease processes. We demonstrated that AgRP mRNA expression was increased during acute inflammation induced by injection of lipopolysaccharide and during chronic inflammation in rodent models of cancer and renal failure. AgRP neurons were found to co-express IL-1R and i.c.v. IL-1β induced the expression of Fos protein in AgRP neurons. The release of AgRP from hypothalamic explants was decreased by IL-1β in a dose-dependent fashion that was not blocked by inhibitors of prostaglandin synthesis. These data suggest that the secretion of AgRP is decreased in response to proinflammatory signals released during inflammatory states, while simultaneously the biosynthetic capacity of AgRP neurons to produce AgRP is increased. This data suggests that AgRP neurons may participate with ARC POMC neurons in mediating the anorexic and metabolic responses to acute and chronic disease processes.

In the final part of this thesis work, we investigated the role of the central melanocortin system in the pathogenesis of cardiac cachexia, a wasting disease that often develops in patients with congestive heart failure (CHF). We demonstrated that genetic and pharmacologic blockade of the central melanocortin system attenuated the development of cardiac cachexia in two independent rodent models of CHF.

Collectively, the data presented in this thesis support the central melanocortin system as being a key mediator of cytokine signaling and suggest that compounds that block central melancortin signaling may have potential therapeutic use in treating disorders in

food intake and energy homeostasis that occur in humans with acute and chronic diseases.

CHAPTER 1

INTRODUCTION

1. Significance and Rationale

The regulation of energy homeostasis is one of the most important physiological tasks that animals must perform to ensure survival. Energy intake and energy expenditure are precisely controlled in response to changes in energy stores by complex and redundant neural systems in the brain. One neural system with a well-characterized role in the regulation of energy homeostasis is the central melanocortin system. The central melanocortin system has the capability to sense and integrate a vast array of hormonal, neuronal, and nutrient signals of energy balance and issues commands to behavioral and autonomic effector circuits to maintain energy homeostasis (1). The dramatic increase in the prevalence of obesity in western countries has fueled interest in characterizing the response of the central melanocortin system to signals of energy balance as genetic disruptions in melanocortin signaling are associated with the development of obesity in rodents and humans (2, 3). However, feeding and metabolic-related pathologies are not limited to excess energy intake. Pathologies that cause insufficient energy intake and metabolic dysregulation are frequent challenges that animals face.

Proper energy intake and balanced metabolism are essential for normal growth, development and maintenance of health. Disorders in energy homeostasis, characterized by anorexia and involuntary weight loss develop in animals with acute and chronic diseases and lead to malnutrition and weight loss. The young and elderly are especially vulnerable to disruptions in energy balance and experience poor growth and health maintenance as a result. In many chronic disease states, a pathological syndrome of

anorexia and loss of fat and lean body mass known as cachexia arises (4) and the severity of cachexia is highly correlated with an increase in patient morbidity and mortality (4, 5). Investigations into the etiology of disorders in energy homeostasis that develop during acute and chronic disease states suggest that the cytokines that are released in response to inflammatory stimuli act on the central nervous system to alter the activity of neural systems that regulate appetite and energy homeostasis (6, 7).

The focus of this thesis was to characterize the response of the central melanocortin system to individual proinflammatory cytokines to gain an understanding of how the activity of this key neural system is regulated during inflammatory states. In addition, I examined the effect of blockade of melanocortin signaling on the pathogenesis and progression of cachexia in rodent models of congestive heart failure. Collectively, these studies have advanced our understanding of how the central melanocortin system is regulated by inflammatory cytokines and demonstrated that blockade of melanocortin signaling is a viable target for the theraupeutic treatment of cachexia of chronic disease.

2. Illness-Induced Disruptions in Energy Homeostasis

2.1 Anorexia of Acute Illness and Inflammation

Anorexia is a component of "sickness behavior", a coordinated set of behavioral and physiological changes that develop in animals in response to infection and tissue injury.

Additional signs of sickness include fever, weakness, and malaise and this constellation of signs are thought to represent an organized strategy employed by animals to combat infection and inflammation (8). Proinflammatory cytokines exerting their effects on the central nervous system (CNS) are hypothesized to mediate the signs of sickness behavior (6, 7). Unlike starvation, where a protective neuroendocrine response to restricted caloric intake causes decreased energy expenditure and consumption of fat as the preferential metabolic substrate (9), the neuroendocrine response to illness-induced anorexia seems maladaptive as it promotes increased metabolism and the catabolism of muscle and fat for metabolic fuels (10, 11). The teleology of the anorexic response to cytokines has been difficult to reconcile with the high metabolic cost of mounting the febrile response. For example, in humans, the metabolic rate needs to be raised by 13% to generate a 1 °C raise in core body temperature (12). One hypothesis is that anorexia spares energy that would be required for foraging for food and prevents a weakened animal from risking exposure to a potential predator. Supporting this hypothesis is data showing that lipopolysaccharide (LPS) and interleukin-1β (IL-1β)-treated rats stop seeking a lever that when pressed provides food, but still eat food pellets that are presented to them (13, 14). A second hypothesis is that anorexia may represent a specialized behavioral adaptation to fight bacterial infections. The production and activity of macrophages and lymphocytes, key components of the immune system response to bacterial infection, are increased by starvation (15). In addition, data suggests that a strong T helper 2 (Th_2) compared to a T helper 1 (Th_1) lymphocyte response promotes clearance of bacterial infection. Anorexia prevents feeding induced increases of vagal and hormonal output from the gut that are correlated with a reduced Th_2/ Th_1 ratio (16). These results suggest that acutely, anorexia

might constitute an adaptive strategy in fighting acute bacterial infections. However, prolonged reduction in food intake and an increase in metabolic rate that lead to depletion of body fat and protein stores can be detrimental to the health and survival of an animal as is seen in the anorexia-cachexia syndrome.

2.2 Cachexia of Chronic Disease

Cachexia is a wasting syndrome first described in chronic heart failure (CHF) patients by Hippocrates 2300 years ago (17). Cachexia has long been recognized as a serious complication of many chronic illnesses including cancer, renal failure, liver failure, chronic obstructive pulmonary disease (COPD) and CHF (4). The cardinal features of cachexia are involuntary weight loss, relative anorexia and hypermetabolism (18, 19). Unlike a state of starvation, where the body mounts a protective response to restricted caloric intake by decreasing energy expenditure and consuming fat as the preferential metabolic substrate, cachexia is characterized by an inappropriate increase in metabolism and catabolism of lean body mass (LBM) (20). The subsequent negative energy and nitrogen balance results in a progressive loss of LBM and multi-organ dysfunction (17). These factors are thought to be the primary causes of morbidity and mortality in cachectic patients, and are associated with reduced quality of life scores and overall poorer outcomes (5, 19). Treatments to combat cachexia have focused on increasing nutritional intake by enteral or parenteral means, but these have proven to be largely ineffective due to the anorexia, early satiety and metabolic resistance to the accumulation of LBM exhibited by cachectic patients (21, 22). Steroids remain the most widely used

pharmacologic agents in cachectic patients. Prednisolone and dexamethasone have been shown to significantly stimulate appetite, however these effects are short lived and have not been shown to prevent weight loss (23, 24). The progestational agent megestrol acetate has been extensively studied after the observation that its use resulted in weight-gain in breast cancer patients. Significant increases in body weight and patient-reported quality of life scores have been recorded in patients with cancer and AIDS-associated cachexia treated with megestrol acetate. However, subsequent studies revealed that the increases in body weight were achieved through increased fat and water mass and not LBM (25, 26).

A shared characteristic of chronic diseases associated with the development of cachexia is increased production of proinflammatory cytokines. Elevated circulating levels of tumor necrosis factor alpha (TNF-α), and interleukin-6 (IL-6) in patients with cardiac cachexia are the strongest predictor for pathological weight loss (27, 28). In cancer cachexia, IL-1β, IL-6, leukemia inhibitory factor (LIF) and TNF-α have been shown to be produced by tumor cells in tissue culture and *in vivo* (29, 30). Central administration of these cytokines in rodents is effective in recapitulating the cardinal features of cachexia including: anorexia, weight loss, increased energy expenditure and catabolism of fat and LBM (31, 32). These findings suggest that there are systems within the brain that are sufficient to promote the cachectic state in response to cytokines. In the periphery, data demonstrates that cytokines can act directly on muscle cells to disrupt the normal balance that exists between anabolic and catabolic pathways (33). Expression of nuclear factor-kappa B (NF-κB) in muscle is increased by IL-1β and TNF-α (34).

Increased NF-κB expression in muscle promotes muscle degeneration by accelerating protein breakdown through ubiquitin-dependent proteolysis (35) and preventing muscle repair by decreasing the expression of the transcription factor MyoD (36). Collectively, these data support the hypothesis that the coordinated behavioral and metabolic responses that occur in the clinical syndrome of cachexia likely involve the synergistic effects of combinations of cytokines acting in both the brain and periphery.

3. Neural Control of Feeding and Energy Homeostasis

3.1 Hypothalamic Arcuate Nucleus

In 1954 Eliot Stellar published his revolutionary essay "*The Physiology of Motivation*" in which he outlined a "dual center" model to describe feeding behavior. Stellar proposed that in the hypothalamus there were reciprocally acting centers that controlled feeding, an excitatory center to initiate feeding and an inhibitory center to terminate feeding (37). Thereafter, a series of classic electrolytic and mechanical ablation studies in the mammalian brain confirmed that there were distinct regions within the hypothalamus that had key roles in the regulation of energy homeostasis [reviewed in (38)]. To this day, the basic neuroanatomical layout of the hypothalamus that was established during this period remains central to our understanding of hypothalamic feeding circuits. One region of the hypothalamus identified by ablation studies that has continued to be the focus of intense studies is the arcuate nucleus of the hypothalamus (ARC).

The ARC is located at the base of hypothalamus between the floor of the third ventricle and the median eminence and extends rostro-caudally from the optic chiasm to the mammillary bodies. The ARC has extensive reciprocal connections with other hypothalamic nuclei including the dorsomedial nucleus of the hypothalamus (DMH), the lateral hypothalamic area (LHA), the ventromedial hypothalamic nucleus (VMH), and the paraventricular nucleus (PVN) (38). Ablation studies revealed that lesions of each of these nuclei results in severe disturbances in feeding and energy homeostasis (38-40). Axon terminals of many ARC neurons are localized in the median eminence, a circumventricular organ lacking an intact blood-brain barrier (BBB) (41). Furthermore, following systemic injection, several different dyes and markers are found to accumulate rapidly in cells in the arcuate nucleus and median eminence, suggesting that the capillaries in this region are specialised for exchange of molecules. Collectively, these observations suggest that multiple mechanims may allow the ARC to have increased access to circulating signals of energy balance including hormones, cytokines and macronutrients (42). Lesions of the ARC produce hyperphagia and obesity in animals. This experimental observation prompted the hypothesis that that this region of the ventromedial hypothalamus served as a "satiety center" (38, 43). However, subsequent studies have also revealed that portions of the ARC can act as "appetite stimulating" centers as well (42). As will be discussed in detail below, it is now appreciated that there are two primary neuropeptide-expressing neuronal populations within the ARC that have reciprocal effects on energy balance. A feeding inhibitory population that is comprised of neurons co-expressing proopiomelancortin (POMC) and cocaine and amphetamine-related transcript (CART), and an appetite-stimulating population that is comprised of

neurons co-expressing neuropeptide Y (NPY) and agouti-related peptide (AgRP) (44, 45). Additional neuropeptides that are postulated to have plays roles in the regulation of appetite and energy homeostasis that are expressed in the ARC include: galanin, galanin-like peptide, orexin, brain-derived neurotrophic factor, melanin concentrating hormone, endocannabinoids, corticotropin releasing factor, glucagon-like peptide and kisspeptin.

3.2 Parabiosis Experiments Identify a Neurohumoral Link

After lesion studies had demonstrated that the hypothalamus contained distinct centers that regulated food intake the next task for investigators to accomplish was determining how these centers worked. It was hypothesized that these centers were sensitive to changes in the energy stores of the body following either energy expenditure, or energy intake and adjusted eating behavior accordingly using a system of "feedback" control. However, the type of signal that provided this feedback and the path by which it reached the hypothalamus was unknown. The first answer to these questions came from a series of studies in parabiotic rats. Lesions of the VMH in one member of the parabiotic pair induced hyperphagia and obesity in that animal, whereas the unlesioned member became hypophagic and underweight (39, 40). The results of these experiments suggested that a circulating factor produced in the lesioned rat had signaled the hypothalamus of the unlesioned rat to reduce its own food intake. Although it was unknown what this circulating factor might be, it was hypothesized by Kennedy in 1953 (based on his observations that animals made adjustments to feeding in relation to the amount of stored body fat) that the centers of the hypothalamus might be sensitive to the concentration of a

metabolite that existed in equilibrium with stored fat (46). This hypothesis was supported by another series of parabiosis experiments in two spontaneously obese strains of mice, the *obese* (Lep^{ob}/Lep^{ob}) mouse and *diabetic* (Lep^{db}/Lep^{db}) mouse. Parabiosis experiments found that *ob/ob* partners of *db/db* mice experienced hypophagia, weight loss, hypoglycemia, and often died within 4 weeks after the parabiosis surgery from metabolic exhaustion (47). Similar responses were reported for wild-type mice parabiosed to *db/db* mice (48), and it was concluded that both wild-type and *ob/ob* mice had normal satiety centers that were responsive to a satiety factor produced by *db/db* mice. The similarity of the obesity syndromes observed in the *ob/ob* and *db/db* mice also led to the hypothesis that the two different genes influenced the same satiety mechanism: *ob/ob* mice had a normal satiety center but were unable to produce the circulating satiety factor, whereas *db/db* mice produced the satiety factor, but had a defective satiety center. In 1994, the *ob* gene encoding the protein leptin was cloned (49), and in the following year its receptor (OB-R) was cloned from the *db* locus (50). These findings confirmed the existence of a neurohumoral link whereby centers in the brain that control food intake and energy homeostasis can sense and respond to circulating signals of energy balance.

3.3 Brainstem Mechanisms

Most research has focused on the ARC as the primary site in the brain where signals of energy status are integrated and efferent circuits that coordinate the responses to maintain energy homeostasis are engaged. However, data exists that also supports a role for hindbrain nuclei, in particular the nucleus of the solitary tract (NTS), in performing these

same tasks. The first central projection for gustatory and gastrointestinal afferents is the NTS and studies using decerebrate rats have demonstrated that this nucleus issues commands to local motor circuits that control meal size (51-53). In common with the ARC, the NTS is in close anatomical proximity to and directly innervated by the area postrema (AP), a circumventricular organ (54, 55) suggesting that this site may have direct access to circulating signals of energy balance. Although AgRP cell bodies are absent, the NTS does contain cell bodies expressing neuropeptides with demonstrated roles in the regulation of food intake and energy metabolism including: NPY, POMC, CART, neuromedin U (NMU), and preproglucagon (1, 56, 57).

4. Proinflammatory Cytokines

Cytokines are large 8-60 kDa polypeptides classically associated with the regulation of immune and inflammatory processes. Functionally, cytokines are classified as being either proinflammatory (stimulatory) or anti-inflammatory (inhibitory). Cytokines exhibit pleiotropy and redundancy, meaning a cytokine can have multiple functions and these functions can be mimicked in part by other cytokines (58). Historically, features used to differentiate a cytokine from an endocrine hormone were the source and location of actions of these proteins. Cytokines are primarily synthesized by cells of the immune system and function predominately as autocrine, or paracrine regulators of local tissue processes during tissue injury and inflammation (58). Hormones are produced by specialized cells within ductless glands and function predominately as regulators of system processes (59). However, experimental data has demonstrated that these

distinctions are frequently blurred. For example, studies have demonstrated that in addition to cytokines, lymphocytes are able to produce and secrete a number of hormones including: adrenocorticotropic hormone (ACTH), prolactin, insulin-like growth factor, endorphins and growth hormone (GH) (60-62). Conversely, cytokines and their receptors are expressed by almost all known cell types (including neurons and endocrine cells) (63, 64) and can regulate processes such as production of fever far from their site of production (65). Collectively, these findings have established that cytokines possess hormone-like capabilities to act as key regulators of local and systemic responses to disease and inflammation.

Although there is evidence supporting a role for cytokines in regulating basal neurological processes such as sleep (66, 67) and energy homeostasis (68-71), expression of cytokines in the brain is very low in the absence of infection, or inflammation. However, expression of multiple cytokines is markedly increased in response to inflammation from peripheral sources. Peripheral injections of LPS have been shown to increase the expression of IL-1α, IL-1β, IL-6, TNF-α and LIF in the brain [reviewed in (7)]. In the brain, the proinflammatory cytokines IL-1β and TNF-α have been shown to potently stimulate their own production as well as increasing the synthesis of other inflammatory cytokines such as IL-6, interleukin-8 (IL-8) and LIF (72, 73). This provides a mechanism for amplification of cytokine signaling in the brain in response to peripheral sources of inflammation. Anorexia has been described following the central administration of multiple inflammatory cytokines (IL-1β, IL-6, IL-8, TNF-α and LIF)

(31, 32), however this thesis work primarily focused on studying the interaction between IL-1β and the central melanocortin system.

5. Interleukin-1: An Immuno-Neuro-Endocrine Link

5.1 Synthesis of IL-1α and IL-1β

IL-1, also known as lymphocyte activating factor, B-cell differentiation factor, or endogenous pyrogen is a 17 kDA peptide that is a "prototypic" proinflammatory cytokine (74, 75). There are two forms of IL-1, IL-1α and IL-1β, that are agonists of the IL-1 receptor (IL-1R) (76). A third member of the IL-1 family, IL-1 receptor antagonist (IL-1ra), is an endogenous inhibitor of IL-1 that binds IL-1R, but does not trigger signaling (77). After synthesis, IL-1α remains mainly intracellular whereas IL-1β is cleaved by IL-1β-converting enzyme (ICE) and secreted from the cell (78). In a healthy brain, trace expression of IL-1β is detected in glia, neurons, cerebrovascular cells and circulating immune cells [reviewed in (79)]. Expression of IL-1β in the brain, mainly in the hypothalamus, is markedly increased in response to disease and inflammation both in the periphery and within the CNS itself (80-83).

5.2 Interleukin-1 Receptors

IL-1R is a glycoprotein expressed on the surface of cells that is a complex of two chains, the type I IL-1 receptor (IL-1RI) and the IL-1R accessory protein (IL-1RAcP) (84). IL-

1RI is a membrane bound receptor that binds the agonist ligands IL-1α and IL-1β (85). IL-1RAcP is membrane bound chain that does not bind to either IL-1α and IL-1β, but instead is recruited to the IL-1/IL-1RI complex and is required for efficient signal transduction (86). Binding of IL-1β to IL-1R increases cellular production of NF-κB, a transcription factor that that plays a key role in regulating the cellular response to inflammation (84). In the brain, IL-1R is expressed primarily by non-neuronal cells including endothelial cells, glial cells, and macrophages (87). Only a few neuronal cell groups express IL-1R, however these groups are predominately found in areas associated with energy homeostasis and behavior including the ARC, NTS, AP, basolateral nucleus of the amygdala, hippocampus, and the trigeminal and hypoglossal motor nuclei (87, 88). Expression of IL-1R in the hypothalamus and hindbrain is increased by acute inflammation induced by single injections of LPS (89), or IL-1β (90) and by chronic inflammation due to tumor growth (83).

5.3 Regulation of the Neuroendocrine Axis by IL-1β

The first described physiological role for IL-1β in the brain was the stimulation of fever, an adaptive host defense response to infections and other inflammatory stimuli (91). Injection of picomolar quantities of IL-1β into the brain elicits marked fever in rodents by regulating the activity of thermosensitive neurons in the anterior and preoptic hypothalamus (92). IL-1β-induced fever is attenuated by salicylates and aspirin-like anti-inflammatory drugs that prevent prostaglandin synthesis by antagonizing that activity of cyclooxygenase (COX)1 and COX2 (93). IL-1β also potently increases the activity of

the hypothalamic-pituitary-adrenal (HPA) axis leading to elevated plasma levels of ACTH (94). In addition to promoting fever and activating the HPA axis, IL-1β also has an increasingly recognized role in the regulation of feeding behavior and energy homeostasis. IL-1β potently suppresses food intake when injected peripherally and centrally (95, 96) and unlike IL-1β-mediated fever, the anorexic effect of IL-1β is not completely blocked by inhibition of prostaglandin synthesis (97, 98). Expression of c-fos mRNA is observed in the ARC (**Figure 1**) and NTS (**Figure 2**) in response to peripheral injections of IL-1β (99). In the ARC, IL-1β induces the expression of c-fos immunoreactivity in both POMC and NPY neurons suggesting a role for the hypothalamic melanocortin system in mediating the feeding and metabolic effects of IL-1β (100). Chronic disruption studies indicate that in addition to mediating the feeding and metabolic effects of acute inflammation, IL-1 signaling also has an important role in mediating long-term energy homeostasis. IL-1R knockout mice (IL-1RKO) develop maturity-onset obesity and this metabolic phenotype is preceded by decreased leptin sensitivity, fat utilization, and locomotor activity (69). Conversely, IL-1ra knockout mice (IL-1raKO) have a lean phenotype due to decreased fat mass, related to both a defect in adipogenesis and an increase in energy expenditure (70). IL-1β mRNA expression in the ARC is increased by leptin and central injections of IL-1ra suppress the anorexic and pyrogenic effects of leptin (101). Collectively, these findings strongly support the hypothesis that IL-1β-mediated signaling plays an important role in mediating food intake and energy homeostasis in both basal and inflammatory states.

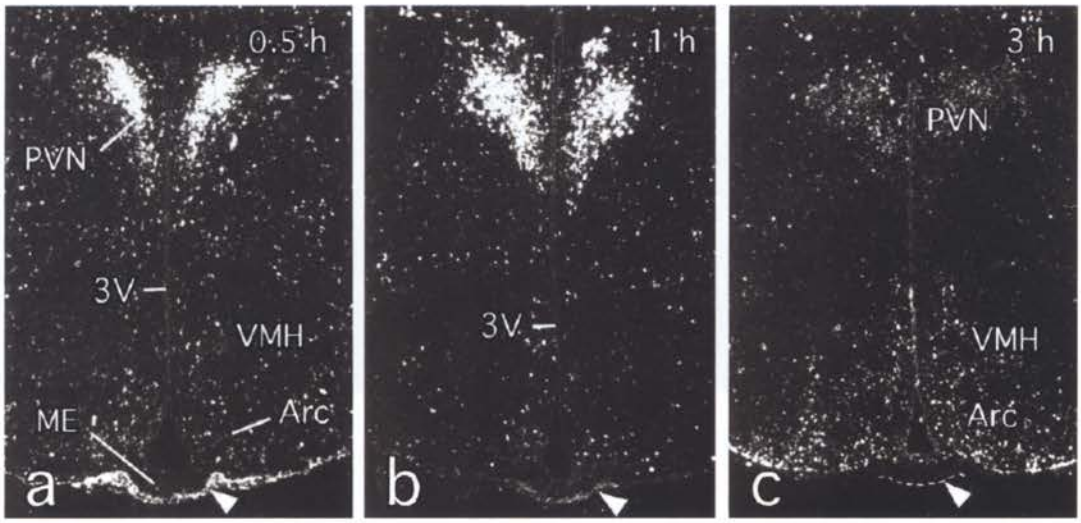

Figure 1-1. Darkfield photomicrographs of *c-fos* mRNA-positive cells in coronal brain sections of the hypothalamus after i.v. injection of IL-1β. Time points after injection are 0.5 hour (a), 1 hour (b), and 3 hours (c). Arrowheads point to the outer edge of the median eminence (ME). 3V, third ventricle; Arc, arcuate nucleus; PVN, paraventricular nucleus; VMH, ventromedial nucleus of the hypothalamus. Figure modified from Herkenham, 1998.

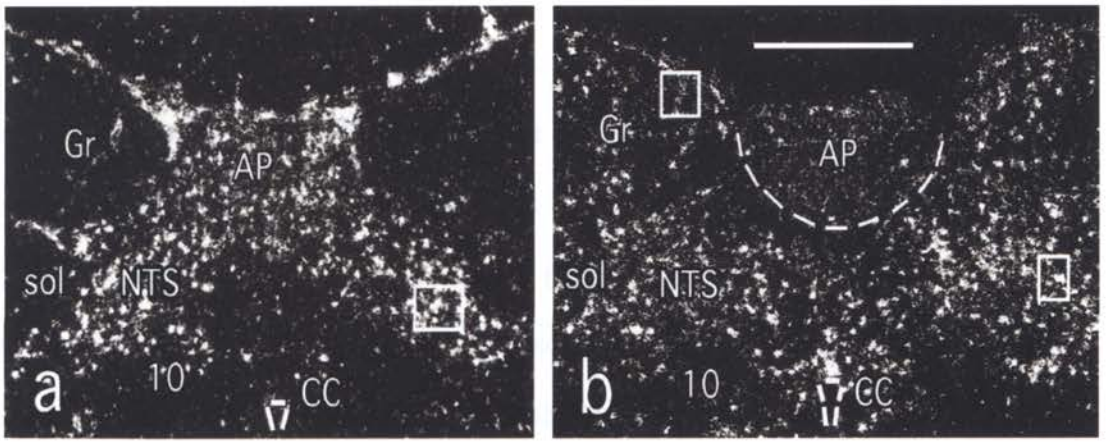

Figure 1-2. Darkfield photomicrographs at the level of the area postrema (AP) and the nucleus of the solitary tract (NTS) showing *c-fos* mRNA-positive cells at 0.5 hour (a) and 3 hours (b) after i.v. injection of IL-1β. CC, central canal; sol, solitary tract; 10, dorsal motor nucleus of the vagus. Dashed line in b marks the border between the AP and the NTS. Figure modified from Herkenham, 1998.

6. Leptin

The ability of cytokines to have key roles in the regulation of energy homeostasis has been demonstrated from studies involving leptin. Leptin, a 16-kDa protein hormone that has the conformational structure of a 4-α-helical bundle cytokine, was cloned from the mouse *obesity* (*ob*) gene and is produced and released primarily by white adipose tissue (49). Administration of leptin to *ob/ob* mice decreased food intake and body weight and also normalized endocrine status (102, 103). Humans with null mutations in the *ob/ob* gene have phenotypes similar to *ob/ob* mice (severe obesity, hyperphagia and hyperinsulinaemia) (104). Treatment of these patients with exogenous leptin is effective in correcting this phenotype (105). The metabolic effects of leptin are mediated by its binding to the long form of its receptor (OB-Rb; isoform that includes the intracellular signaling portion of the receptor). Mutations in this receptor were found to underlie the hyperphagic and obese phenotype of the *db/db* mouse and this phenotype was not corrected with leptin replacement (106, 107). OB-Rb is a single membrane-spanning class I cytokine receptor that is closely related to the gp130 signal-transducing component of the IL-6, LIF and ciliary neurotrophic factor (CNTF) receptors (50). In rodents, OB-Rb is expressed in numerous brain regions including the cortex, hippocampus, thalamus, and hindbrain, but the highest expression is seen in the hypothalamus. In the hypothalamus, OB-Rb is expressed in the ARC, VMH, DMH and ventral premammillary nuclei with the highest expression measured in the ARC (108-111). The pattern of expression of OB-Rb in the human brain is similar to that reported

in rodents (112) and mutations in human OB-Rb result in hyperphagia, obesity and neuroendocrine derangements (113). These data are consistent with the hypothesis that the primary role of leptin is to signal the brain about the overall nutritional state of the animal and demonstrate that in both rodents and humans intact leptin and leptin-signaling via OB-Rb are essential for the regulation of food intake and energy homeostasis.

7. The Central Melanocortin System

7.1 Early Studies of Melanocortins in the Periphery

Interest in investigating the role of the melanocortin system in the regulation of energy homeostasis was initially ignited by studies investigating the role of the melanocortin system in the regulation of coat color in mice. Coat color in mice is determined by the relative production of two major categories of melanin polymers in melanocytes, brown-black eumelanins and yellow-red pheomelanins (114). Regulation of the eumelanin-pheomelanin switch occurs via the interaction of two allelic series, the *extension* locus on chromosome 16 and the *agouti* locus on chromosome 2 (115, 116). Mice with dominant *agouti* alleles, such as the lethal yellow (A^{Y}) and variable yellow (A^{VY}) alleles, have reduced eumelanin production and yellow coat fur (117, 118). In 1992, the *extension* locus was discovered to encode the melancortin-1 receptor (MC1-R) (119). MC1-R is expressed on melanocytes and activation of MC1-R by α-melanocyte-stimulating hormone (α-MSH), a melanocortin peptide product of the POMC gene, produced a dark-colored coat in mice by stimulating the synthesis of eumelanins (120). In the same year,

the cloning of the *agouti* gene revealed that it encoded a 131-amino acid secreted protein (121, 122). A subsequent study demonstrated that *agouti* was a competitive antagonist of the MC1-R (123). The same study also revealed that *agouti* was a potent competitive antagonist of the melanocortin-4 receptor (MC4-R) (123). This result was surprising as the principal site of MC4-R expression is in the CNS (124, 125). This discovery prompted renewed interest in mice with the dominant A^{Y} and A^{VY} mutations as a prominent phenotype displayed by these mice was the agouti obesity syndrome, characterized by hyperphagia, obesity, hyperinsulinemia, and increased body length (117, 118). Antagonism of MC4-R signaling by ectopic expression of *agouti* in the CNS was hypothesized to be responsible for the agouti obesity syndrome displayed by A^{Y} and A^{VY} mice. This hypothesis was supported by studies showing MC4-R mRNA was expressed in regions of the CNS known to involved in autonomic and endocrine function, including the hypothalamus, NTS, and the dorsal motor nucleus of vagus (DMV) (125). Collectively, data from these studies provided compelling support for the hypotheis that melanocortin signaling in the CNS played an important role in the regulation of energy homeostasis.

7.2 Neuroanatomy of Central Melanocortin System

The POMC gene encodes a 32 kilodalton (kDa) propeptide that is predominantly expressed in the pituitary gland, skin, immune system and brain (126). In the brain, post-translational cleavage of the POMC propeptide by a family of serine proteases, the prohormone convertases (PC1 and PC2), produces two different classes of bioactive

peptides, the melanocortins and β-endorphins (127). The melanocortin peptides, which include adrenocorticotropic hormone (ACTH) and α-, β- and γ-melanocyte-stimulating hormones (MSH) mediate their effects by binding to members of a family of five G protein-coupled melanocortin receptors (MC1-R through MC5-R) [reviewed in (1)]. Two melanocortin receptor subtypes, MC3-R and MC4-R are highly expressed in the brain and are supported by data as being the primary mediators of the behavioral and metabolic effects of melanocortin peptides in the brain (128). Expression of POMC in the brain is limited to neurons located in the ARC and the NTS (45, 129). Fibers from ARC POMC neurons have a wide projection field that includes regions in the forebrain, midbrain and hindbrain (1). Within the hypothalamus, most nuclei receive projections from ARC POMC neurons with the densest projections made in the PVN, the periventricular nucleus (PeVN) and the perifornical regions. Fibers from NTS POMC neurons project to hindbrain nuclei, rostrally to the PVN, and the spinal cord. Dual innervation by ARC and NTS POMC fibers occurs in the rostral NTS, parabrachial nucleus, locus coeruleus, DMV, and the lateral reticular nucleus, suggesting that coordination exists between the hypothalamic and brainstem melanocortin systems in the regulation of activity in these nuclei.

Opposing the actions of melanocortin peptides in the brain is AgRP, an endogenous competitive antagonist/inverse-agonist at the MC3-R and MC4-R (130). AgRP was identified by virtue of its sequence similarity to *agouti* and neuroanatomical studies revealed that in the brain, AgRP is expressed exclusively by neurons in the ARC where it is colocalized with the orexigenic neuropeptide, NPY, and the inhibitory neurotransmitter

gamma-aminobutyric acid (GABA) (131, 132). Ubiquitous overexpression of AgRP in transgenic mice recapitulated the obesity and increased body length phenotype displayed by A^{Y} and A^{VY} mice (130), supporting the hypothesis that the agouti obesity syndrome was likely caused by the ability of ectopic *agouti* to mimic AgRP. Loss of AgRP, NPY and GABA signaling by inducible ablation of AgRP/NPY neurons in adult mice causes immediate and severe anorexia in these animals (133). Immunocytochemical studies revealed that AgRP-containing fibers project to many, but not all sites in the CNS that receive projections from POMC-containing fibers (134). Notably, little to no AgRP fiber staining is detected in the NTS (44, 134) (**Figure 3**). These findings demonstrate that the central melanocortin system has reciprocal anorexigenic and orexigenic components and these components make this system ideal for playing a key role in the regulation of feeding behavior and energy homeostasis.

The development of two lines of transgenic mice; one created using the neuronal POMC promoter to drive expression of enhanced green fluorescent protein (POMC-EGFP) (135), and the other created using NPY genomic elements to drive expression of tau-sapphire (green fluorescent protein variant) fusion protein (NPY-Sapphire) (136) have proven key to elucidating the neuronal architecture and complex interactions of the central melanocortin system. The ability to visually identify these neurons in brain slices and primary culture due to their fluorescent properties has made possible pioneering studies investigating their response to signals of energy balance (135-138). In the ARC, electrophysiological recordings and multi-label immunohistochemistry revealed that GABA-secreting ARC AgRP/NPY neurons form synapses with ARC POMC neurons

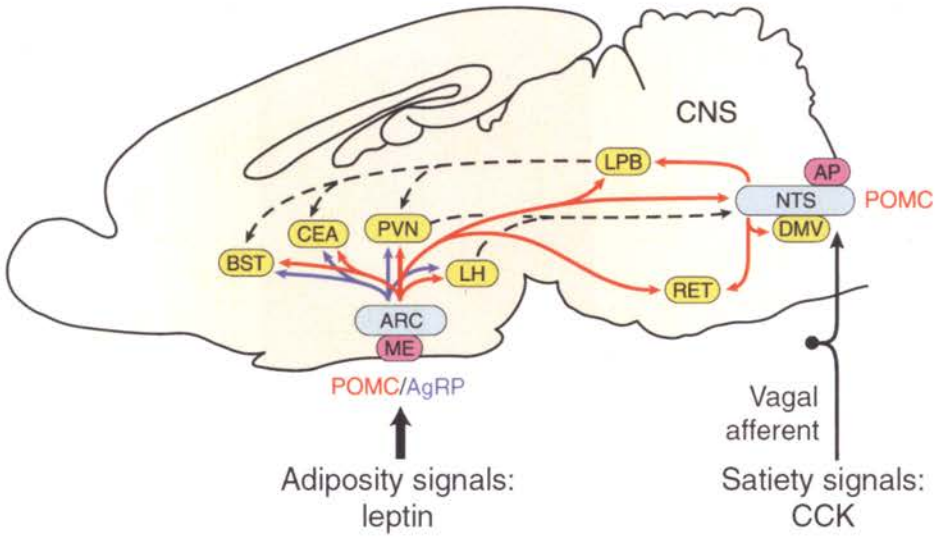

Figure 1-3. Schematic of the central melanocortin system. POMC neurons in the ARC and the NTS of the brainstem and AgRP neruons in the ARC are both adjacent to circumventricular organs and receive and integrate signals from adipostatic factors and satiety factors, respectively. Red arrows, representative POMC projections; blue arrows, representative AgRP projections; dashed arrows, secondary projections linking POMC neurons in hypothalamus and brainstem with common effector sites; AP, area postrema; ARC, arcuate nucleus; BST, bed nucleus of the stria terminalus; CEA, central nucleus of the amygdala; DMV, dorsal motor nucleus of the vagus; LH, lateral hypothalamic area; LPB, lateral parabrachial nucleus; ME, median eminence; NTS, nucleus tractus solitarius; PVN, paraventricular nucleus of the hypothalamus; RET, reticular nucleus. Figure modified from Fan, 2004.

(135). GABA-mediated inhibitory post-synaptic currents (IPSCs) and mini-IPSCs recorded from ARC POMC neurons are reduced by NPY and agonists of the NPY Y2 presynaptic autoreceptor in both the presence and absence of tetrodotoxin (TTX) indicating that the observed effect is due to decreased GABA release from NPY presynaptic terminals (135, 139) (**Figure 4**). Studies with the selective MC3-R agonist, D-Trp^{8}-γMSH revealed that MC3-R is an autoinhibitory receptor expressed on ARC POMC neurons (135), a key finding for future studies investigating the role of this receptor in illness-induced anorexia and cachexia (discussed below). POMC-EGFP mice were used in many of the experiments that I conducted for the work presented in this thesis demonstrating how valuable these animals continue to be to researchers investigating the role of the central melanocortin system in disorders of energy homeostasis.

7.3 Genetic Studies of Central Melanocortin System

The most compelling evidence for the central melanocortin system having a pivotal role in the regulation of feeding behavior and energy homeostasis has come from genetic studies of knockout and transgenic mice with targeted disruptions in melanocortin signaling and human families with naturally occurring mutations in melanocortin signaling. Gene-targeting techniques have been used to generate mice with inactivating mutations of POMC, MC3-R, MC4-R and MC5-R (140-144). POMC KO and MC4-RKO mice are hyperphagic, hyperleptinemic and obese, recapitulating the characteristic

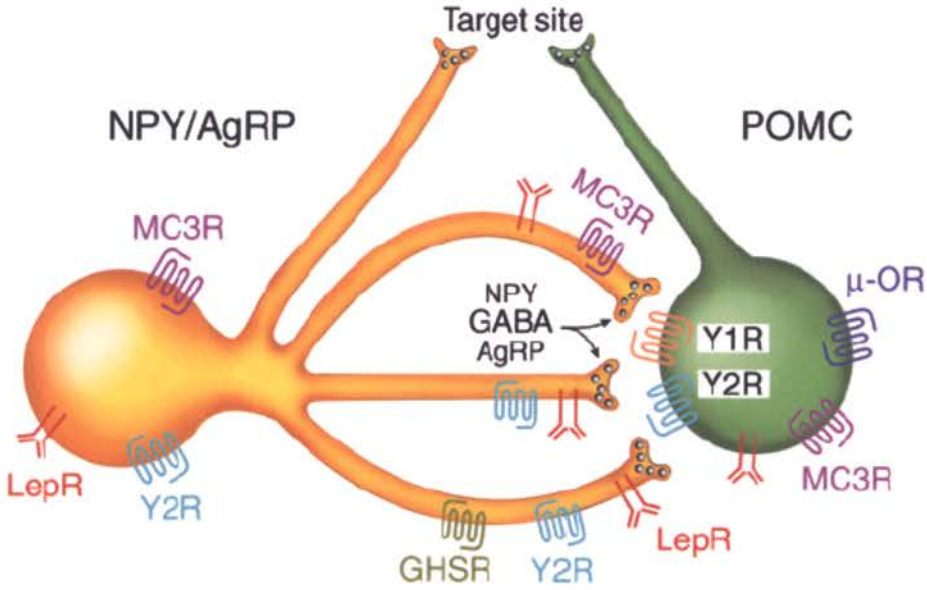

Figure 1-4. Schematic of the melanocortin system within the arcuate nucleus of the hypothalamus. NPY/AgRP and POMC neurons within the arcuate nucleus form a regulated network due to dense NPY/AgRP fiber projections to POMC cell bodies. Several receptors for the many hormones and neuropeptides known to regulate the network are indicated. Figure modified from Cowley, 2001.

features of the *agouti* obesity syndrome found in A^{Y} mice, A^{VY} mice, and transgenic AgRP overexpressing mice (130). Mice heterozygous for the null MC4-R have an intermediate phenotype suggesting a gene dosage effect of MC4-R signaling (143). MC4-RKO are resistant to the anorectic and metabolic effects of the MC3/4-R agonist MTII (145), supporting the role of MC4-R, and not MC3-R in mediating the anorectic effects of melanocortins. Indeed, although MC3-RKO mice were found to have a mild obesity phenotype, they are also hypophagic and have reduced lean body mass (142, 145). MC5-RKO mice have normal appetite and body weight arguing against this receptor having a significant role in energy homeostasis (142). The findings from these genetic studies have been corroborated by pharmacologic studies demonstrating the MTII inhibits food intake and SHU9119 (a nonselective MC3/4-R antagonist) enhances it in wild-type mice (146). Like mice, humans with mutations in either the POMC or MC4-R genes have melanocortin obesity phenotypes. Null mutations in the POMC gene are rare in humans, however patients with these mutations have been discovered and they have syndromes that include obesity, red hair and adrenal insufficiency from the lack of ACTH peptide (147). Unlike POMC mutations, MC4-R mutations are common in humans. Studies have revealed that the percentage of obese patients with mutations in the MC4-R to be between 4% and 6% (148-152). Furthermore, data from these studies also indicate that haploinsufficiency of the MC4-R gene is the most common monogenic form of childhood-onset obesity. The clinical syndrome of hyperphagia, obesity, hyperinsulinemia and increased linear growth found in patients with haploinsufficiency of the MC4-R is nearly identical to that seen in mice (21). Collectively, these data

support the central melanocortin system serving comparable roles in the regulation of energy homeostasis in both mice and humans.

8. Regulation of the Central Melanocortin System

8.1 Fasting and Leptin

The observation that leptin-induced anorexia is resisted by MC4-RKO mice (145) and blocked in wild-type mice by third ventricle administration of SHU9119 (153) suggested that the central melanocortin system had a role in mediating many of the feeding and metabolic effects of leptin. Data from a number of studies provide compelling evidence that the hypothalamic melanocortin system in particular has the primary role of mediating the feeding and metabolic effects of leptin. Both POMC and AgRP/NPY neurons express OB-Rb mRNA (154, 155). Expression of POMC mRNA in the ARC is decreased in response to fasting (156) and this decrease is reversed by leptin replacement (157, 158). Leptin administration stimulates the phosphorylation of the signal-transducer and activator of transcription 3 (STAT3) transcription factor (159), and induces the expression of c-fos immunoreactivity and suppressor-of-cytokine–signaling 3 (SOCS-3) mRNA (160) in POMC neurons. In response to leptin, POMC neurons are depolarized and increase their firing rates (135), leading to the release of mature POMC-derived peptides (161, 162). In contrast to POMC neurons, AgRP/NPY neurons are inhibited by leptin. AgRP mRNA is increased in response to fasting and this increase is reversed by leptin replacement (163). Leptin administration stimulates the expression of SOCS-3

mRNA, but not c-fos immunoreactivity in AgRP/NPY neurons. This observation suggests that the effect of leptin on AgRP/NPY neurons is inhibitory (160). Leptin decreases the basal spike frequency of AgRP/NPY neurons in fasted mice and inhibits the release of AgRP from hypothalamic explants (161).

Evidence supporting a role for the brainstem melanocortin system in mediating the feeding and metabolic effects of leptin is not as convincing as data in support of the hypothalamic melanocortin system. OB-Rb is expressed in the NTS (108, 110), but unlike ARC POMC neurons, it has never been shown definitively that NTS POMC neurons express OB-Rb. Expression of POMC mRNA in the NTS is reduced in response to fasting, however unlike ARC POMC mRNA it is not restored to fed levels with leptin replacement (164, 165). Leptin administration stimulates STAT3 phosphorylation in NTS neurons (166). However, there currently is not agreement on whether pSTAT3 is expressed in NTS POMC neurons in response to leptin. One study reported seeing co-expression (167), whereas another published nearly simultaneously reported co-expression was not apparent (164). The question of whether the brainstem melanocortin system has a role in mediating the feeding and metabolic effects of leptin remains unresolved at this time.

8.2 Insulin

Insulin is synthesized as a preprohormone by beta cells of the islets of Langerhans in the pancreas and released in response to increases in plasma glucose levels (168). Insulin

generates its intracellular effects by binding to the insulin receptor, a disulfide-bonded glycoprotein plasma membrane receptor. Insulin receptors are expressed in the ARC and NTS (169). ARC POMC neurons co-express insulin receptors and insulin infusion reverses fasting induced changes in ARC POMC mRNA and NPY mRNA expression (170, 171). Anorexia following third-ventricular administration of insulin is prevented by subthreshold doses of SHU-9119 (170). Specific studies investigating the effects of insulin on NTS POMC neurons have yet to be conducted, so at this time experimental evidence primarily supports the role of the hypothalamic melanocortin system in mediating the anorectic effects of insulin.

8.3 Cholecystokinin

Data support the brainstem melanocortin system of having a primary role in mediating the anorectic effects of cholecystokinin (CCK). CCK is a peptide that is synthesized primarily in the duodenum and jejunum of the gastrointestinal tract, although CCK expression has also been reported in the brain (172, 173). CCK is released from the duodenum and jejunum in response to the intraluminal presence of nutrient-digestive products, and has been proposed to serve a feedback function in the short-term control of food intake by reducing meal size (174, 175). The feeding inhibitory actions of CCK are mediated through their interaction with CCK-A receptors (176). In the brain, the highest expression of CCK-A receptors is in the NTS and AP, whereas expression in the hypothalamus is low (177). In response to CCK, NTS POMC neurons express c-fos (137, 178) and increase their firing rates via indirect activation by CCK-A expressing

vagal afferents (178). Inhibition of food intake in response to peripheral injections of CCK are partially attenuated by third-ventricular injection of SHU9119, but are completely attenuated by fourth-ventricle injection of SHU9119 (137) supporting the role of brainstem MC4-Rs and NTS POMC neurons in mediating the anorectic effects of CCK.

8.4 Ghrelin

Ghrelin is a recently identified gut-derived peptide that is classified as a growth hormone secretagogue [reviewed in (179)] and is an endogenous agonist for the growth hormone secretagogue receptor (GHS-R) (180). The primary site of ghrelin expression is the fundus of the stomach (180), although low level expression has been reported in the brain (181, 182) and other peripheral organs [reviewed in (183)]. GHS-R is expressed in both the central nervous system and the periphery. In the brain, GHS-R mRNA expression is highest in the hypothalamus with the ARC and PVN having the densest concentration of GHS-R mRNA. GHS-R mRNA is also expressed in all three components of the dorsal vagal complex, including the NTS, the AP, and the DMV (184). Ghrelin mRNA expression and peptide release from the stomach are increased in response to fasting (185, 186) and hypoglycemia (187) and fall rapidly after ingestion of a meal suggesting that ghrelin acts as a meal initiation factor (185). Both peripheral and central injections of ghrelin stimulate food intake (188-190), and peripheral administration of ghrelin induces the expression of c-fos primarily in the ARC (191). AgRP/NPY neurons express c-fos in response to ghrelin, but c-fos was not induced in ARC POMC neurons (192).

Both AgRP mRNA and NPY mRNA are increased in response to ghrelin administration and this is likely a direct effect as AgRP/NPY neurons co-expresss GHS-R (193). ARC POMC neurons are hyperpolarized and AgRP/NPY neurons are depolarized in response to ghrelin (181). The orexigenic effects of ghrelin are abolished in agouti (A^Y) and AgRP/NPY double knockout mice (194) supporting the hypothesis that signaling via the hypothalamic melanocortin system plays a key role in mediating the feeding effects of ghrelin. The reported anticatabolic effects of ghrelin administration in rodent models of cardiac cachexia (195) and cancer cachexia (196) may in part be due to its ability to inhibit melanocortin signaling by increasing AgRP mRNA expression, but appropriate studies to test this hypothesis have yet to be conducted.

8.5 Proinflammatory Cytokines

As described in an earlier section, the central melanocortin system plays a pivotal role in mediating the metabolic effects of leptin, an adipocyte-derived cytokine. This observation naturally raised the question of whether the central melanocortin system also had a role in mediating the metabolic effects of additional cytokines. Experiments demonstrating that neurons in both the ARC and NTS were activated in response to inflammatory cytokines and that the anorectic and metabolic effects of inflammatory cytokines were elicited when they were injected centrally supported a potential role for the central melanocortin system. Surprisingly, at the time the work in this thesis was done, this was a question that had received very little attention. For example, in an exhaustive search of the literature, with the exception of the previously described co-

expression studies with OB-Rb, I was unable to find a single study that had investigated the co-expression of POMC and AgRP/NPY neurons with cytokine receptors. However, there was sufficient data from a limited number of experiments investigating the effects of inflammation and individual cytokines on the central melanocortin system to suggest an interaction existed. In transcriptional regulation studies, ARC POMC mRNA was increased following a peripheral injections of LPS (197) and TNF-α (198). A peripheral injection of TNF-α was also shown to decrease AgRP mRNA expression (198). However, the most convincing work came from studies investigating the feeding and metabolic effects of CNTF. CNTF is a member of the cytokine family that includes IL-6, LIF, and oncostatin M and promotes anorexia and loss of LBM when injected peripherally (199-201). CNTF receptors are expressed in the hypothalamus and hindbrain and utilize the gp130 subunit for intracellular signaling when bound to CNTF (202). Peripheral injections of CNTF stimulate the expression of c-fos and SOCS-3 in the ARC (203, 204). Selective ablation of the gp130 subunit from POMC neurons using the Cre-loxP system abolished the anorectic effect of i.c.v. CNTF injections (205). These results supported the central melanocortin system having a primary role in mediating the anorectic effects of CNTF. Finally, at the time this thesis work began, it had recently been shown that MC4-RKO mice, or wild-type mice receiving SHU9119 were resistant to anorexia following administration of LPS and IL-1β (206-208). Collectively, these earlier studies provided compelling data supporting a potential role for the central melanocortin system in mediating the anorectic and metabolic effects of inflammatory cytokines. The primary goal of the neuroanatomical and functional studies that I

conducted for this thesis work was to test the hypothesis that the central melanocortin system was a target for inflammatory cytokines.

9. Additional Orexigenic/Anorexigenic Neuropeptides Regulated by Inflammation

Although the work in this thesis focused on the regulation of the central melanocortin system by inflammatory cytokines, there are additional neuropeptide systems including NPY, melanin-concentrating hormone (MCH), and CART with acknowledged roles in the regulation of energy homeostasis that may also be targeted by inflammatory cytokines and therefore warrant discussion.

9.1 Neuropeptide Y

NPY, a neuropeptide produced by neurons in many regions of the brain including the ARC is strongly supported by many studies as playing an important role in the regulation of food intake and energy homeostasis. Central injections of NPY potently stimulate feeding (209, 210) and increase liver and white adipose tissue lipogenesis (211). The biological actions of NPY are mediated by five G protein-coupled receptors (Y1-Y5) with most experimental evidence supporting the Y1 and Y5 receptors in the regulation of food intake and metabolism (212-214). The PVN contains dense Y1 and Y5 expression and injection of Y1 and Y5 specific antagonists into the PVN reduce the orexignenic effect of centrally administered NPY (215-217). Hypothalamic NPY mRNA expression

and peptide secretion is increased with fasting and decreased with leptin replacement (218-220). However, studies investigating the potential role of NPY in mediating the metabolic effects of inflammatory cytokines have provided primarily negative results. In response to peripheral LPS, hypothalamic NPY mRNA expression has been reported to be unchanged (89, 197, 221). Hypothalamic NPY mRNA expression is also reported to be unchanged (222), or slightly decreased, (90) in response to IL-1β. Hypothalamic NPY peptide secretion is unchanged in response to IL-1β (223). Interestingly, hypothalamic NPY expression is increased in anorectic, tumor-bearing rodents and NPY injections result in worsened anorexia (224, 225). Overall, these data suggest that the hypothalamic NPY system probably does not have a significant role in mediating the anorectic and metabolic effects of inflammatory cytokines.

9.2 Melanin-Concentrating Hormone

MCH is a 19-amino acid cyclic peptide produced primarily by neurons in the LHA (226) that stimulates feeding and increases body weight with chronic administration (227, 228). MCH knockout mice (MCH-KO) are hypophagic, have increased metabolic rates and decreased fat mass (229). MCH-containing fibers project to several hypothalamic nuclei including the ARC, PVN and VMH and to extra-hypothalamic areas such as the neocortex, dorsal and ventral parabrachial nuclei and the dorsal vagal complex (226, 230). MCH binds to two G protein-coupled receptors, somatostatin-like (SLC-1) or MCH-R1 (231) and MCH-R2, which is expressed in the brains of humans, but not rodents (232). Expression of MCH-R1 in the brain is widespread with dense

hypothalamic concentrations in the ARC, DMH, LHA and VMH (233). MCH-R1 knockout mice are lean, hyperactive and hypermetabolic (234). In humans, MCH-R2 is densely expressed in the ARC and VMH (235). MCH neurons express OB-Rb (234) and hypothalamic MCH mRNA expression and peptide levels are increased in *ob/ob* mice (236) and by fasting in wild-type mice (237). Increased MCH expression is normalized with leptin injections (220). Hypothalamic MCH mRNA expression is increased by peripheral LPS administration (197) and to date this remains the only study investigating the effect of inflammation on MCH mRNA expression in the brain. AgRP and SHU9119 increase MCH mRNA expression (238), whereas in hypothalamic explants, MCH has been shown to increase α-MSH secretion and inhibit AgRP secretion (239). These results suggest a degree of cross-regulation that exists between the hypothalamic melanocortin system and the LHA MCH system. The observation that MCH mRNA expression is increased with LPS administrations indicates that this system might be a target for inflammatory cytokines. Determining if the LHA MCH system has a role in mediating the anorectic and metabolic effects of inflammatory cytokines and, if it does, if it accomplishes this role independently or in collaboration with the hypothalamic melanocortin system are attractive questions for future experiments.

9.3 Cocaine and Amphetamine-Regulated Transcript

CART is a 102- (long form), or 89- (short form) amino acid peptide (240) that is involved in a number of physiological processes including food intake, body weight regulation, reward and reinforcement (241). Central injections of CART decrease food

intake and body weight indicting that CART acts as an anorexigenic neuropeptide (242). CART mRNA is robustly expressed in hypothalamic nuclei (ARC, PVN) and brainstem nuclei (NTS) known to play a role in the regulation of food intake and energy metabolism (243-245). Within the ARC, CART colocalizes with POMC, whereas in the NTS CART and POMC do not colocalize (167). CART receptor(s) have not been cloned at the time this thesis was written so our understanding of the sites and mechanisms of CART's actions is minimal. CART mRNA in the ARC is decreased with fasting and restored by leptin replacement (242). Regulation of CART mRNA in the ARC by inflammation has also been shown as peripheral injections of LPS increase CART mRNA expression (197). Regulation of CART by other inflammatory mediators has not been studied. However, the observation that virtually all ARC POMC neurons co-express CART (167, 243) coupled with data from studies presented in this thesis demonstrating that ARC POMC neurons are direct targets for cytokines suggests that CART may have a role in mediating the anorectic and metabolic effects of inflammatory cytokines.

10. Therapeutic Benefit of Targeting Melanocortin Signaling in Acute and Chronic Disease

10.1 MC4-R Antagonism and Anorexia of Acute Illness and Inflammation

In the first study that examined the effect of melanocortin blockade on cytokine-mediated anorexia, variable yellow (A^{vy}/a) obese mice displayed enhanced anorexia when administered IL-1β (246). However, increased CRF levels in the (A^{vy}/a) mice were

thought to be the primary cause for this enhanced sensitivity to IL-1β and interest in the ability of melanocortin blockade to inhibit cytokine-mediated anorexia was rekindled by studies demonstrating that the central melancortin system played a key role in mediating the anoroexic effects of leptin (247) and that blockade of melanocortin signaling with AgRP (248), or SHU9119 (153) inhibited leptin-induced anorexia. The ability of central melanocortin blockade to inhibit cytokine-mediated anorexia was first demonstrated in rats when anorexia following a central administration of LPS was attenuated by co-administration of SHU9119 (249). Interestingly, this study also revealed an antipyrectic role for melanocortins in the brain, likely due to their recognized anti-inflammatory properties (discussed below). SHU9119 has also proved effective in reversing anorexia caused by a single i.c.v. injection of IL-1β (250) and in tumor-bearing animals (251). The observation that MC4-RKO mice resist LPS and tumor-induced anorexia (207, 208) whereas MC3-RKO mice respond with heightened anorexia (207) support the role for MC4-R in transducing cytokine-mediated anorectic signals. Recently, additional support for the role of MC4-R has been provided by studies showing that small-molecule, selective MC4-R antagonists can attenuate IL-1β-induced anorexia (206). The current hypotheis regarding the hightened anorexia observed in MC3-RKO in response to inflammation will be discussed below.

10.2 MC4-R Antagonism and Cachexia of Chronic Disease

The observation that blockade of central melanocortin signaling could reverse anorexia induced by acute inflammation naturally led investigators to ask if central melanocortin

signaling also played a significant role in the pathogenesis of cachexia of chronic disease. The first study to address this question demonstrated that central administration of AgRP attenuated the development of anorexia and weight-loss in mice injected with LPS and in mice bearing a Lewis lung carcinoma (208). Shortly after the publication of this first study, it was reported by a second group that intracerebroventricular injection of SHU9119 into rats bearing a prostate adenocarcinoma produced comparable anorexia-sparing effects (251). Importantly, both studies reported that tumor growth in the experiments utilizing tumor-bearing animals was identical between treatment and vehicle-treated groups. This observation supported the argument that metabolic derangement due to tumor growth was mediated by central melanocortin receptor activation. Had the tumors been acting as simple metabolic sinks, it would have been anticipated that increased nutrient intake observed in the AgRP and SHU-9119 animals would have resulted in increased tumor growth (208, 251).

Evidence supporting a primary role of MC4-R antagonism in producing anticachectic effects has come from genetic and pharmacologic studies that selectively targeted MC4-R signaling. MC4-RKO mice have been shown to resist the development of cachexia in models of LPS sepsis (208), cancer (207, 208), renal failure (252) and cystic fibrosis (253). Selective antagonism of MC4-R signaling using small-molecule, selective MC4-R antagonists has also proved effective in reducing anorexia and loss of lean body mass (254), or loss of lean body mass alone (255) in tumor-bearing rodents. In contrast to the MC4-R, antagonism of the MC3-R produces enhanced anorexia and weight loss in animal models of cachexia. MC3-RKO suffer more severe cachectic phenotypes

compared to wild-type mice following LPS administration and with tumor growth (207). Two leading hypothesis have been proposed to explain the observed detrimental effect of MC3-R-deletion on the cachectic syndrome. First, data supports the role of MC3-R as an inhibitory autoreceptor expressed by POMC neurons in the ARC that diminishes POMC neuronal activity, leading to a reduction in α-MSH release onto MC4-R (135). Loss of inhibitory MC3-R tone could lead to increased α-MSH release in response to stimulatory signals. Second, MC3-R is expressed on macrophages and has anti-inflammatory effects by suppressing cytokine release (256); therefore a lack of MC3-R tone may worsen cachexia by facilitating increased cytokine release with inflammation. Collectively, these observations strongly argue that selective antagonism of the MC4-R, but not the MC3-R, may represent an effective therapy for cachexia of chronic disease.

10.3 Anti-Inflammatory Role of Melanocortins

In addition to its demonstrated role in the regulation of energy homeostasis, melanocortins have also been shown to possess anti-inflammatory and immunomodulatory properties. Binding of α-MSH to MC1-R and MC3-R on macrophages and lymphocytes decreases the expression of proinflammatory cytokines including IL-1β, IL-6, TNF-α and interferon-γ (IFN-γ) (257, 258) and increases the expression of the proinflammatory cytokine synthesis inhibitor interleukin-10 (IL-10) (258). At the molecular level, the anti-inflammatory effects of α-MSH are mediated by its ability to increase the expression of IκBα (259, 260), the endogenous inhibitor of NF-κB, a transcription factor that regulates multiple immediate-early gene expressions

involved in immune and inflammatory responses (261). Central injections of α-MSH attenuates pyrexia following administrations of LPS (249) and IL-1β (250), but potentiates the observed anorexia demonstrating the divergent roles of melanocortins in regulating the metabolic and anti-inflammatory response of the CNS to inflammation. In the periphery, data from a number of studies support the hypothesis that the anti-inflammatory properties of melanocortins have an important physiologic role. Melanocortin receptors are expressed in the cardiovascular system (262, 263) and stimulation of melanocortin signaling with α-MSH decreases cardiac injury in a murine model of ischemia/reperfusion acute myocardial infarction (264). Activation of MC3-R on resident macrophages is hypothesized to mediate this effect as the cardioprotective effect of α-MSH is blocked by SHU9119, but not the MC4-R selective antagonist HS204 (264, 265). MC1-R activation, in addition to its role in melanogenesis, has been demonstrated to mediate the potent anti-inflammatory effects of α-MSH in the epithelial-lined organs of the body including the skin (266), lungs (267), and gut (268). The anti-inflammatory properties of melancortins may prove a key barrier to the potential use of exogenous antagonists of melanocortin receptors to attenuate anorexia and cachexia of acute and chronic disease due to the role of melanocortins as anti-inflammatory molecules.

Hypothesis and Specific Aims of this Thesis

The overall goals of the research presented in this thesis were to test the following hypotheses: 1) The central melanocortin system is a key target for the actions of proinflammatory cytokines and the activity of this system is regulated by cytokines produced during inflammatory states, and 2) Persistent increased activation of the central melancortin system plays a key role in the pathogenesis of cachexia of chronic disease and blockade of melanocortin signaling can attenuate the development of cachexia . The specific aims of this research were as follows:

1. Determine if POMC and AgRP neurons can be directly targeted by proinflammatory cytokines by examining if these neurons co-express receptors for the cytokines IL-1β and LIF.
2. Examine the effect on POMC and AgRP transcriptional activity in response to exposure to the individual cytokines IL-1β and LIF, and models of acute or chronic inflammation.
3. Examine the effect of IL-1β on regulating the *in vitro* release of α-MSH and AgRP from hypothalamic explants.
4. Determine if IL-1β-mediated changes in ARC POMC and AgRP neuronal activity are dependent upon the synthesis of prostaglandins by cyclooxygenase enzymes.
5. Determine if genetic, or pharmacologic blockade of central melanocortin signaling could successfully attenuate the development of cardiac cachexia in two independent rodent models of chronic heart failure.

CHAPTER 2-Manuscript #1

Regulation of central melanocortin signaling by interleukin-1β

Jarrad M. Scarlett[1], Erin E. Jobst[3,4,5], Pablo J. Enriori[3,5], Darren D. Bowe[1,5], Ayesha K. Batra[1], Wilmon F. Grant[1], Michael A. Cowley[3] and Daniel L. Marks[1,2]

[1]Center for the Study of Weight Regulation and Associated Disorders, Oregon Health and Science University, Portland, Oregon 97239

[2]Department of Pediatrics, Oregon Health and Science University CDRCP, Portland, Oregon 97239

[3]Division of Neuroscience, Oregon National Primate Research Center, Oregon Health and Science University, Beaverton, Oregon 97006

[4]School of Physical Therapy, Pacific University, Hillsboro, Oregon 97123

[5]These authors contributed equally to this work

Chapter 2 is a manuscript as it appears in the original paper published in the journal *Endocrinology*.

Regulation of central melanocortin signaling by interleukin-1 beta. *Endocrinology*. 2007 Sep;148(9):4217-25. Epub 2007 May 24.

Abstract

Anorexia and involuntary weight loss are common and debilitating complications of a number of chronic diseases and inflammatory states. Proinflammatory cytokines, including interleukin-1β (IL-1β), are hypothesized to mediate these responses through direct actions on the central nervous system. However, the neural circuits through which proinflammatory cytokines regulate food intake and energy balance remain to be characterized. Here we report that IL-1β activates the central melanocortin system, a key neuronal circuit in the regulation of energy homeostasis. Proopiomelanocortin (POMC) neurons in the arcuate nucleus of the hypothalamus (ARC) were found to express the type I interleukin-1 receptor. Intracerebroventricular injection of IL-1β induced the expression of Fos protein in ARC POMC neurons, but not in POMC neurons in the commissural nucleus of the tractus solitarius (NTS). We further show that IL-1β increases the frequency of action potentials of ARC POMC neurons and stimulates the release of α-melanocyte-stimulating hormone (α-MSH) from hypothalamic explants in a dose-dependent fashion. Collectively, our data support a model in which IL-1β increases central melanocortin signaling by activating a subpopulation of hypothalamic POMC neurons and stimulating their release of α-MSH.

Introduction

Activation of the host immune system in response to tissue injury or infection triggers the release of proinflammatory cytokines that mediate a number of metabolic and behavioral responses including anorexia, pyrexia and malaise (8, 269). This illness behavior is hypothesized to be elicited by cytokines exerting their actions on the central nervous system (CNS) (100, 270). Acutely, these responses represent an adaptive response that promotes survival of the host (271), but may become harmful if sustained. For example, short-term anorexia appears to promote survival as increased mortality occurs with forced feeding of animals suffering from illness (272). In contrast, prolonged anorexia, as occurs in animals with cachexia, or disease-associated wasting, promotes increased morbidity and mortality (273). However, the means by which cytokines alter energy regulation and the relationship of cytokine signaling to neural systems previously shown to be involved in the regulation of energy homeostasis remains largely unknown.

The central melanocortin system plays a critical role in the regulation of food intake and energy homeostasis. This occurs principally via the action of melanocortin peptides derived from proopiomelanocortin (POMC) with a family of five G protein-coupled melanocortin receptors (MC1R through MC5R), and the endogenous melanocortin receptor antagonist agouti-related protein (AgRP) (1). In the mammalian brain, the central melanocortin system is comprised of adjacent populations of POMC and AgRP/neuropeptide Y (NPY) co-expressing neurons in the arcuate nucleus of the hypothalamus (ARC) and a caudal brainstem population of POMC neurons in the commissural nucleus of the tractus solitarius (NTS) (45, 274). Two melanocortin receptor

subtypes, the melanocortin-3 (MC3R) and melanocortin-4 (MC4R) receptors, are expressed in the brain and are thought to be the primary mediators of the behavioral and metabolic effects of melanocortin peptides (1, 143). The ability of POMC and AgRP/NPY neurons to recognize and respond to a number of circulating signals of energy balance including leptin, insulin, and ghrelin strongly supports this system having a critical role in the regulation of energy homeostasis (181, 275, 276). Leptin, a 16-kDa protein resembling the structure of 4-α-helical bundle cytokines (277), acts through leptin receptors present on ARC POMC and AgRP/NPY neurons (154, 278) to suppress food intake and increase energy expenditure by increasing the release of α-melanocyte-stimulating hormone (α-MSH) from POMC neurons and decreasing the release of NPY and AgRP (275). The responsiveness of the central melanocortin system to leptin raises the possibility that it may play a role in mediating the anorectic effects of additional cytokines.

The proinflammatory cytokine interleukin-1β (IL-1β) is secreted by activated immune cells and plays a critical role in mediating the inflammatory response of the host against infection and tissue injury (95, 279, 280). Administration of IL-1β, peripherally or centrally, induces anorexia, fever, and activation of the hypothalamo-pituitary-adrenal (HPA) axis (279-281). Intracerebroventricular (i.c.v.) administration of the IL-1 receptor antagonist (IL-1ra) attenuates the anorexic effects of peripheral IL-1β and lipopolysaccharide (LPS) administration (96). The effects of IL-1β in the brain are mediated by the type I IL-1 receptor (IL-1R) (282). Low to moderate levels of IL-1R mRNA are expressed by neurons in regions of the brain associated with energy homeostasis, including the ARC and brainstem (87). In previous work, IL-1β given

intravenously to rats was shown to induce Fos protein in POMC mRNA-expressing neurons in the ARC, suggesting that the central melanocortin system may be a target for IL-1β signaling and have a role in mediating the behavioral effects of IL-1β (100). This hypothesis is strengthened by the observation that the anorexic effects of IL-1β can be blocked by central administration of a nonspecific melanocortin receptor antagonist (250).

In the present study, we report that IL-1β activates a subpopulation of POMC neurons in the ARC, but not in the NTS and stimulates the release of α-MSH from hypothalamic explants in a dose-dependent manner. Our data also show that POMC neurons in the ARC express IL-1R mRNA. Collectively, our data support a model in which IL-1β increases central melanocortin signaling by activating a subpopulation of hypothalamic POMC neurons and stimulating them to release α-MSH.

Materials and methods

Animals and Surgical Procedures

Male Sprague-Dawley rats (300-350g; Charles River Laboratories), wild-type C57BL/6J mice (4-5 weeks of age; Jackson Laboratory), and transgenic C57BL/6J POMC-EGFP mice (6-8 weeks of age; genotyping and breeding of mice were as described previously(135)) were maintained on a normal 12:12 light/dark cycle with *ad libitum* access to food (Purina rodent diet 5001; Purina Mills) and water. Experiments were conducted in accordance with the NIH Guide for the Care and Use of Laboratory

Animals and approved by the Animal Care and Use Committees of Oregon Health and Science University and the Oregon National Primate Research Center.

i.c.v. cannulation and injections

Male POMC-EGFP mice were anesthetized with a ketamine cocktail and placed in a stereotaxic apparatus (Cartesian Instruments). A sterile guide cannula with obdurator stylet was stereotaxically implanted into the lateral ventricle (1.0 mm posterior to bregma, 0.5 mm lateral to midline, and 2.3 mm below the surface of the skull). The cannula was then fixed in place with dental cement. The animals were individually housed after surgery for a minimum of 1 week and were handled and administered 1μl i.c.v. injections of commercial artificial cerebrospinal fluid (Harvard Apparatus) daily. On the day of the experiment, mice were treated at 0900 with 40 mg/kg intraperitoneal ketorolac (K1136, Sigma-Aldrich) dissolved in sterile saline, or sterile saline. At 1000 h mice received i.c.v. injections of 10 or 100 ng murine IL-1β (R&D Systems, Inc.) dissolved in aCSF, or aCSF alone. Ninety minutes after treatment, mice were deeply anesthetized and perfused transcardially with 0.9% saline followed by ice-cold 4% paraformaldehyde in 0.01 M phosphate buffered saline (PBS). Brains were post-fixed for 2 h in fixative and then stored overnight in 20% sucrose in PBS as a cryoprotectant before being frozen at –80°C until use. The positions of the cannulae were verified at the end of the experiment by histological analysis.

Implantation of osmotic minipumps

ALZET micro-osmotic pumps (Model 1007D, DURECT Corporation) were filled with ketorolac (K1136, Sigma-Aldrich) dissolved in sterile saline (n = 12) or sterile saline (n =18). Ketorolac-filled pumps were calibrated to deliver a constant infusion of 1.0 mg/kg every six hours. Male C57BL/6J mice were anesthetized with a ketamine cocktail and the pumps were implanted subcutaneously on the dorsal surface of each mouse. Mice were allowed two days of recovery prior to use in hypothalamic peptide secretion studies.

Immunohistochemistry for c-Fos and EGFP

Dual-immunofluoresence histochemistry was performed as previously described(167). Briefly, free-floating sections were cut at 30 μm from perfused brains using a sliding microtome. Three sets of sections were generated from the hypothalamus and hindbrain of each brain. Hypothalamic sections were collected from the diagonal band of Broca (Bregma 1.0 mm) caudally through the mammillary bodies (Bregma –3.00 mm). Hindbrain sections were collected from the facial nucleus (Bregma –5.75 mm) caudally through the spinal cord (283). The sections were incubated for 1 h at room temperature in blocking reagent (5% normal donkey serum in 0.01 M PBS and 0.3% Triton X-100). After the initial blocking step, the sections were incubated in rabbit anti-c-Fos antibody (PC38, EMD Biosciences, Inc.) diluted 1:75,000 in blocking reagent for 48 h at 4 C, followed by incubation in 1:500 donkey anti-rabbit Alexa 594 (Molecular Probes, Inc.) for 1 h at room temperature. Hindbrain sections were then incubated in rabbit anti-GFP antibody directly conjugated to Alexa 488 (Molecular Probes, Inc.) diluted 1:4000 in

blocking reagent for 1 h at room temperature. Hypothalamic sections did not require this step. Between each stage the sections were washed thoroughly with 0.01 M PBS. Incubating the sections in the absence of primary antisera was used to ensure specificity of the secondary antibodies. Sections were mounted onto gelatin-coated slides, coverslipped using Vectashield mounting media (Vector Laboratories) and viewed under a fluorescence microscope (Leica 4000 DM; Leica Microsystems)

Cell Counting

The number of c-Fos immunoreactive cells and double-labeled cells was counted by eye in sections representing the ARC and the NTS by investigators blinded to the treatments. Results were expressed as the number of cells per section as well as the percentage double-labeled. Each set of ARC sections contained 7-9 sections expressing immunopositive cells and each set of caudal brainstem sections contained 5-7 caudal brainstem sections expressing immunopositive cells. A cell was determined to be single-labeled when visible only under the fluorescence filter corresponding to the emission wavelength of the primary/secondary antibody complex used (e.g. 594nm and not 488nm for c-Fos). Cells were examined at multiple focal planes within the section and at multiple magnifications to ensure that the cell was indeed representative of a single-labeled cell. When the cell was visible at both 594- and 488-nm filters, it was deemed to be double-labeled. Double-labeled cells were examined at multiple focal planes within the section and at multiple magnifications to ensure that the cell was indeed representative of a single cell labeled with both antibody complexes and not two single-

labeled cells in close proximity within different levels of the optical section. The cells were also examined under a third wavelength (350nm) not corresponding to the emission wavelength of either of the secondary antibodies to ensure that the immunoreactivity was specific.

Electrophysiology

Standard electrophysiological techniques were used, as previously described(135). Briefly, 8 week-old male POMC-EGFP mice were anesthetized with isoflurane and killed quickly by decapitation. Coronal hypothalamic slices containing the ARC were cut at 185μm with a vibrating slicer (Leica VT1000S) under ice-cold aCSF solution of the following composition (in mM): 126 NaCl, 2.5 KCl, 1.2 $MgCl_2/6H_2O$, 2.4 $CaCl_2/2H_2O$, 1.2 NaH_2PO_4/H_2O, 21.4 $NaHCO_3$ and 11.1 glucose (saturated with 95% O_2/5% CO_2). Slices were stored for at least 1 h in a holding chamber with aCSF at room temperature and continuously bubbled with 95% O_2/5% CO_2. Individual slices were submerged in a recording chamber and superfused continuously with carbogenated ACSF at 35°C (3-5 mL/min). All recordings were made from ARC POMC neurons, identified by bright green fluorescence(135). Electrode resistances were 2-4 MΩ when filled with an intracellular solution of the following composition, in mM: 128 K- gluconate, 10 HEPES, 1 EGTA, 10 KCl, 1 $MgCl_2$, 0.3 $CaCl_2$, 5 (Mg)ATP, 0.3 (Na)GTP. Current- clamp recordings were performed in whole-cell configuration with an Axopatch 200B amplifier (Axon Instruments). Data were filtered at 2 kHz and then sampled at 50-100 kHz by pClamp 8.2 software (Axon Instruments). Data were stored on a hard disk for analysis

using Mini Analysis (Synaptosoft, Inc.). Only neurons with stable holding currents not exceeding 100 pA for the ten minute baseline were studied. Approximately ten minutes of baseline data were recorded for each arcuate neuron prior to drug application. Murine IL-1β (R&D Systems, Inc.) was applied at specified concentrations to the superfusion medium by gravity perfusion for approximately three minutes and data were recorded for approximately fifteen minutes after drug was discontinued. All data are presented as mean ± SEM. Differences in drug effects were tested by either a one sample Student's t test with a hypothetical mean of 0 mV (membrane potential) or with Student's t test (firing rate). For drug-induced changes in firing rate, changes are normalized to the five minute period immediately prior to drug application. Only cells with a minimum average of five action potentials/20 sec bin during baseline were included in the analysis to avoid the potential of overestimating changes in firing rate with extremely low-firing cells.

Hypothalamic peptide secretion

Male C57BL/6J mice (n = 30) were anesthetized with isoflurane and killed quickly by decapitation. The brain was removed (with care taken to ensure that there was no contamination of the hypothalamic portion with residual pituitary) and a 2 mm slice was prepared using a vibrating microtome (Leica VS 1000) to include the paraventricular and arcuate nuclei. Individual hypothalami received a 1 h equilibration period with aCSF (aCSF; NaCl 126 mM, Na_2HPO 0.09 mM, KCl 6 mM, $CaCl_2$ 4 mM, $MgSO_4$ 0.09 mM, $NaHCO_3$ 20 mM, glucose 8 mM, ascorbic acid 0.18 mg/ml, 0.6 TIU aprotinin/ml) at 37°C. Hypothalami were then incubated for 45 min at 37°C in 700 µl aCSF (basal

period) before being challenged with a single concentration of murine IL-1β (R&D Systems, Inc.) (0.0001 nM to 1.0 nM) in 700 µl aCSF for 45 min at 37°C. Tissue viability was verified by a 45 min exposure to 700 µl aCSF containing 56 mM KCl. Treatments were performed in quadruplicate. At the end of each treatment period, supernatants were removed and frozen at –80°C until assayed by radioimmunoassay. Hypothalamic explants that failed to show peptide release 3X above that of basal in response to aCSF containing 56 mM KCl were excluded from data analysis.

Hypothalamic peptide secretion following ketorolac treatment

Male C57BL/6J mice that had been implanted with ketorolac-filled (n = 12) or saline-filled osmotic pumps (n = 18) were divided into five groups of six animals each. Mice from all groups were anesthetized with isoflurane and killed quickly by decapitation. Brains were removed and processed on a vibrating microtome as described above. Individual hypothalami received a 1 h equilibration period with aCSF at 37°C. A single group of hypothalami from mice that received saline pumps (n = 6) were incubated for 45 min at 37°C in 700 µl aCSF + ketorolac (121 µM) (basal period) before being challenged with 0.1 nM murine IL-1β in 700 µl aCSF + ketorolac (121 µM) for 45 min at 37°C. Hypothalami from the remaining four groups were incubated for 45 min at 37°C in 700 µl aCSF (basal period) before being challenged with either 0.05 nM (n =6 for saline and ketorolac-treated mice) or 0.1 nM (n =6 for saline and ketorolac-treated mice) murine IL-1β in 700 µl aCSF for 45 min at 37°C. Tissue viability was verified by a 45 min exposure to 700 µl aCSF containing 56 mM KCl. Treatments were performed in

quadruplicate. At the end of each treatment period, supernatants were removed and frozen at –80°C until assayed by radioimmunoassay. Hypothalamic explants that failed to show peptide release 3X above that of basal in response to aCSF containing 56 mM KCl were excluded from data analysis.

α-MSH radioimmunoassay

α-MSH immunoreactivity was measured with a rabbit anti-α-MSH specific for α-MSH (Phoenix Pharmaceuticals, Inc.). The antibody cross-reacts fully with the mature α-MSH [N-acetylated α-MSH], and partially (46%) with desacetylated α-MSH, but not with NPY or AgRP. ^{125}I-labeled α-MSH was prepared by the iodogen method and purified by high-pressure liquid chromatography (University of Mississippi Peptide Radioiodination Service Center, University, MS). All samples were assayed in duplicate. The assay was performed in a total volume of 350 µl of 0.06 M phosphate buffer, pH 7.3, containing 1% BSA. The sample was incubated for three days at 4°C before the separation of free and antibody-bound label by goat anti-rabbit IgG serum (Phoenix Pharmaceuticals, Inc). One hundred microliters of supernatant was assayed. The lowest detectable level that could be distinguished from the zero standard was 0.30 fmol/tube. The intra-assay variation (CV%) was determined by replicate analysis (n=10) of two samples at α-MSH concentrations of 2 and 10 fmol/tube, and the results were 7.8% and 7.5% respectively. The inter assay variation (CV%) was 10.7% and 12.1% for the range of values measured.

Double-label in situ hybridization histochemistry

Simultaneous visualization of POMC and IL-1R mRNA in the rat brain (n = 3) was performed as previously reported (284), with slight modifications. Coronal sections (20 μm) were cut on a cryostat and thaw-mounted onto Superfrost Plus slides (VWR Scientific, West Chester, PA). Hypothalamic sections were collected in a 1:6 series from the diagonal band of Broca (Bregma 0.50 mm) caudally through the mammillary bodies (Bregma –5.00 mm). Hindbrain sections were collected in a 1:6 series from the facial nucleus (Bregma –10.00 mm) caudally through the spinal cord (285). Antisense ^{33}P-labeled rat IL-1R riboprobe (corresponding to bases 207-930 of rat interleukin-1 receptor type I; GenBank accession number M95578) (0.2 pmol/ml) and antisense digoxigenin-labeled rat POMC riboprobe (corresponding to bases 49-644 of rat proopiomelanocortin; GenBank accession number AF510391) (concentration determined empirically) were denatured, dissolved in hybridization buffer along with tRNA (1.7 mg/ml), and applied to slides. Controls used to establish the specificity of the IL-1R riboprobe included slides incubated with an equivalent concentration of radiolabeled sense IL-1R riboprobe, or radiolabeled antisense probe in the presence of excess (1,000×) unlabeled antisense probe. Slides were covered with glass coverslips, placed in a humid chamber, and incubated overnight at 55°C. The following day, slides were treated with RNase A and washed under conditions of increasing stringency. The sections were incubated in blocking buffer and then in Tris buffer containing antidigoxigenin fragments conjugated to alkaline phosphatase (Roche Molecular Biochemicals), diluted 1:250, 3 h at room temperature. POMC cells were visualized with Vector Red substrate (SK-5100; Vector Laboratories) according to the manufacturer's protocol. Slides were dipped in 100%

ethanol, air dried, and then dipped in NTB-2 liquid emulsion (Eastman Kodak Co.). Slides were developed 13 days later and coverslipped. Determination of cells expressing both IL-1R and POMC mRNA was performed using criteria previously described(284). Briefly, POMC-mRNA-containing cells were identified under fluorescent illumination, and custom-designed software was used to count the silver grains (corresponding to radiolabeled IL-1R mRNA) over each cell. Signal-to-background ratios (SBRs) for individual cells were calculated; an individual cell was considered to be double-labeled if it had an SBR of 2.5 or more. For each animal, the amount of double-labeling was calculated as a percentage of the total number of POMC-mRNA-expressing cells and then averaged across animals to produce mean ± SEM.

Statistical analysis

Data are expressed as mean $\pm$ SEM for each group. Statistical analysis was performed using SPSS (v. 14.0) and Prism (v. 3.03) software. All data were analyzed with either a one-sample t test (electrophysiology data), an unpaired t test (immunohistochemistry data), one-way ANOVA followed by a post hoc analysis using a Bonferroni corrected t test (c-Fos with ketorolac data), or a two-way ANOVA followed by a one-way ANOVA with post hoc analysis using a Bonferroni multiple comparison test (secretion study with ketorolac). For all analyses, significance was assigned at the $p < 0.05$ level.

Results

IL-1β selectively activates c-Fos expression in ARC POMC-EGFP neurons

To test whether IL-1β activates ARC and NTS POMC-EGFP neurons, we examined the expression of c-Fos in POMC-EGFP neurons following i.c.v. injection of IL-1β. In agreement with the literature, i.c.v. administration of IL-1β (10ng) induced c-Fos-immunoreactivity (c-Fos-IR) in the ARC (aCSF, 21 ± 2 cells per section, n=4; IL-1β, 79 ± 2 cells per section, n=5; $p < 0.0001$) (**Fig. 1b,e,h,j**) and NTS (aCSF, 3 ± 1 cells per section, n=4; IL-1β, 49 ± 5 cells per section, n=4; $p < 0.0001$) (**Fig. 2b,e,j**). In the ARC, few POMC-EGFP neurons expressed c-Fos in aCSF treated animals (7% ± 2% co-expression) (**Fig. 1c,k**). IL-1β increased the c-Fos expression in ARC POMC-EGFP neurons by ~ 4-fold (31% ± 2% co-expression; $p < 0.0001$) (**Fig. 1f,i,k**). No additional increase in the number of POMC-EGFP neurons activated by IL-1β was observed when higher doses (100ng) of IL-1β were administered (data not shown). In contrast to the arcuate POMC-EGFP neurons, NTS POMC-EGFP neurons were unresponsive to IL-1β. Expression of c-Fos by NTS POMC-EGFP neurons was very low in aCSF-treated animals (2% ± 0.5% co-expression) (**Fig. 2f,k**), and remained low after IL-1β treatment (3% ± 0.5% co-expression; $p > 0.05$) (**Fig. 2f,i,k**).

Activation of ARC POMC-EGFP neurons by IL-1β is decreased by inhibition of cyclooxygenase activity

To determine if the synthesis of prostaglandin intermediates is necessary for the activation of ARC POMC neurons by IL-1β, we examined the expression of c-Fos in ARC POMC-EGFP neurons from mice that had received an intraperitoneal (i.p.) injection of ketorolac (40 mg/kg) or saline one hour prior to receiving an i.c.v. injection of IL-1β (10ng) or aCSF. The overall expression of c-Fos-IR in the ARC of mice that received IL-1β was significantly reduced in animals that had received i.p. ketorolac compared to animals that had received an i.p. injection of saline (saline, 45 ± 2 cells per section, n=4; ketorolac, 25 ± 1 cells per section, n=6; $p < 0.001$), but was still significantly increased compared to animals that had received ketorolac and an i.c.v. injection of aCSF (18 ± 1 cells per section, n=4; $p < 0.01$) (**Fig. 3a**). As before, the expression of c-Fos in ARC POMC-EGFP neurons was increased by i.c.v. IL-1β in animals that had received i.p. saline injections (aCSF, 10% ± 1% co-expression, n=4; IL-1β, 23% ± 1% co-expression, n=4; $p < 0.001$) (**Fig. 3b**). Pretreatment with ketorolac reduced the expression of c-Fos in ARC POMC-EGFP neurons following IL-1β treatment (ketorolac, 16% ± 1% co-expression, n=6; saline, 23% ± 1% co-expression, n=4; $p < 0.01$), but failed to completely attenuate activation compared to animals that had received i.p saline and i.c.v. aCSF ($p > 0.05$) (**Fig. 3b**).

IL-1β increases the firing rate of ARC POMC-EGFP neurons

Using EGFP-labeled cells in ARC slices from male POMC-EGFP mouse brains, we observed that bath-applied IL-1β (1 nM) depolarized 11 of 15 (73%) POMC-EGFP neurons tested (2.5 ± 0.9 mV; $p< 0.05$, one-sample Student's *t* test). In 4 of 15 (27%)

POMC-EGFP neurons tested, IL1β induced a small hyperpolarization (1.2 ± 0.1 mV; $p < 0.05$, one-sample Student's *t* test).

Of the spontaneously firing POMC-EGFP neurons (12 of 15 tested), IL1β (1 nM) increased the firing frequency of 10 cells (83%) (**Fig. 4a**). To avoid overestimation of drug-induced increases in firing rate that occurs if extremely low-firing cells are assessed, 2 cells were excluded from analysis. IL-1β increased the firing rate 78.8 ± 12.1% from baseline to the ten-minute washout period ($n=8$; $p < 0.0001$) (**Fig. 4b**). During its peak effect during the first 250 seconds after IL1β addition to the bath (**Fig. 4b**), IL1β increased POMC-EFGP neuronal activity by 87.4 ± 15.4% above baseline ($p < 0.0001$).

IL-1β stimulates the release of α-MSH from murine hypothalamic explants

To investigate the effect of IL-1β on α-MSH release in vitro, hypothalamic explants harvested from male C57BL/6 mice were incubated with IL-1β (0.01 nM, 0.1 nM, 1.0 nM, 3.0 nM, and 30.0 nM; $n=4$ per IL-1β dose). These doses were chosen based on previous work estimating basal IL-1β concentration in the hypothalamus at 0.01-0.02 nM and increasing approximately 10-fold during pathological conditions(286). IL-1β significantly increased the release of α-MSH from hypothalamic explants with a calculated $EC_{50} = 5.9 \times 10^{-11}$ M (**Fig. 5**). These results demonstrate that *in vivo* hypothalamic concentrations of IL-1β that are produced during pathological conditions are able to potently stimulate the *in vitro* release of α-MSH from hypothalamic explants.

Ketorolac treatment does not block IL-1β-stimulated release of α-MSH from murine hypothalamic explants

To determine if inhibition of prostaglandin synthesis would reduce the IL-1β-stimulated release of α-MSH from hypothalamic explants we repeated our explant studies using two doses of IL-1β (0.05 nM and 0.1 nM) in the presence of ketorolac. We observed that acutely blocking prostaglandin synthesis by incubating the explants in aCSF containing ketorolac (121 μM) did not alter either basal, or IL-1β-stimulated α-MSH release ($p<0.01$ vs. aCSF) (**Fig. 6**). To investigate the effects of chronic blockade of prostaglandin synthesis on IL-1β-stimulated α-MSH release we implanted osmotic pumps containing either ketorolac or saline two days prior to the explant study. Both doses of IL-1β stimulated α-MSH release from hypothalamic explants from mice that had received saline-filled pumps, though only the higher dose of 0.1 nM reached significance ($p<0.001$ vs. aCSF) (**Fig. 6**). Mice with ketorolac-filled pumps had reduced α-MSH release in response to both doses of IL-1β used compared to mice with saline pumps. However, this reduction did not achieve statistical significance for either dose of IL-1β ($p>0.05$ vs. saline pump groups) and α-MSH release was still significantly increased in animals that had received ketorolac pumps at the high dose of IL-1β ($p<0.05$ vs. aCSF) (**Fig. 6**). No significant interaction was found between method of infusion and dose of IL-1β by two-way ANOVA.

POMC mRNA co-expression with IL-1R mRNA in the hypothalamus

Hypothalamic sections from rat brains were processed for double-label *in situ* hybridization for POMC and IL-1R. The pattern of silver grain clusters representing cells in the ARC expressing IL-1R mRNA was similar to that previously reported with a radiolabeled probe(87) (**Fig. 7a**). Including excess unlabeled antisense probe with radiolabeled antisense probe abolished all specific signal, and no signal was seen with application of radiolabeled sense probes. A number of POMC mRNA-expressing neurons in the ARC, represented by cell bodies filled with fluorescent red precipitate, had overlying clusters of silver grains, signifying co-expression of IL-1R mRNA (**Fig 7b**). Semiquantitative image analysis revealed that with a signal to background ratio of 2.5 set as the threshold for neurons to be considered double-labeled, 35% $\pm$ 7% of the digoxigenin-labeled POMC neurons co-expressed IL-1R mRNA. Technical limitations in obtaining consistent labeling of POMC neurons in the NTS using digoxigenin-labeled riboprobes prevented a thorough repetition of these studies in the NTS. However, in instances in which POMC neurons in the NTS were successfully labeled using digoxigenin-labeled riboprobes, no co-expression with IL-1R mRNA was observed (not shown).

Discussion

Both obesity and cachexia of chronic disease are known to be associated with increases in the circulating levels of proinflammatory cytokines (287, 288). Therefore, understanding how these cytokines interact with and regulate central feeding circuits is critical to our overall understanding of these disorders of energy balance. Data from a number of

previous studies strongly suggested that the central melanocortin system might play a significant role in mediating the anorexic effects of IL-1β. Elevated cellular activity in ARC POMC neurons, as indicated by an increase in c-Fos expression, has been shown to occur in rats following IL-1β administration(100). Furthermore, the anorexic effects of IL-1β can be attenuated by central administration of either a mixed MC3R/MC4R antagonist (SHU9119) (250), or a MC4R-selective small molecule antagonist (206). However, a comprehensive investigation of the sensitivity of the entire central melanocortin system to IL-1β and a characterization of the role of IL-1β in the biosynthesis and release of α-MSH from POMC neurons is lacking. In the present study, we report that ARC POMC neurons express IL-1R and that IL-1β selectively activates ARC POMC neurons. We further demonstrate that in acute hypothalamic slices, IL-1β depolarizes and increases the frequency of action potentials of ARC POMC neurons. In hypothalamic explants, IL-1β stimulates the release of α-MSH in a dose-dependent fashion. These findings suggest that IL-1β increases signaling at melanocortin receptors by targeting ARC POMC neurons and stimulating the release of α-MSH.

Our data suggest that ARC POMC neurons are distinct from NTS POMC neurons, in that arcuate POMC neurons are responsive to IL-1β as measured by the expression of c-Fos. One explanation for our inability to observe activation of NTS POMC neurons might be due our central injections of IL-1β not stimulating vagal nerve afferents to the NTS. This possibility is reinforced by data that support a role for viscerosensory afferents of the vagus nerve mediating the responsiveness of NTS neurons to peripheral administration of compounds, including IL-1β (289). Indeed, cholecystokinin-sensitive vagal afferents have been shown to directly activate NTS POMC-EGFP neurons (137).

However, neurons in the brains of vagotomized animals retain sensitivity to central injections of IL-1β (290), indicating that the absence of IL-1β-mediated vagal signaling is an unlikely explanation for our observed lack of POMC neuron activation in the NTS.

The expression of IL-1R mRNA by a subset of ARC POMC neurons indicates that these neurons may be direct targets for the actions of IL-1β. Our observation that some, but not all ARC POMC neurons express IL-1R suggests that only a distinct subset of neurons participate in IL-1β-mediated signaling. This hypothesis is supported by our observation that only 31% ± 2% of POMC neurons express c-Fos in response to IL-1β. However, recordings from ARC POMC neurons also revealed that IL-1β induces a small hyperpolarization in 27% of POMC neurons tested. Although the physiological relevance of this hyperpolarization is unknown, it suggests that the population of POMC neurons that express c-Fos following IL-1β administration may only represent a fraction of the total ARC POMC population that participates in IL-1β-mediated signaling. In addition, the expression of IL-1R mRNA by ARC POMC neurons does not conclusively demonstrate that IL-1β acts directly upon ARC POMC neurons. Indirect mechanisms of IL-1β-mediated regulation of ARC POMC neuronal activity remain a strong possibility. We observed that ARC POMC neurons represented a minority population of cells that expressed IL-1R mRNA in the ARC. However, ARC POMC neurons not expressing IL-1R mRNA frequently had IL-1R mRNA-expressing cells of unknown phenotype directly adjacent to them. Data from previous studies suggest that many of the neural responses to IL-1β are mediated by the synthesis of endogenous prostaglandins. Blockade of prostaglandin synthesis with cyclooxygenase inhibitors or deletion of the *Ptges* gene that encodes for microsomal prostaglandin E synthase-1 (mPGES-1), the inducible terminal

enzyme in thePGE2 synthesizing pathway, attenuates important components of the IL-1β-induced systemic response including HPA activation (291) and anorexia (292). Indeed, IL-1β-mediated depolarization of magnocellular neurons in the paraventricular nucleus occurs indirectly through the synthesis and secretion of prostaglandin (PG) E_2 (PGE2) (293). Our results demonstrating that activation of c-Fos in ARC POMC neurons and increased release of α-MSH from hypothalamic explants in response to IL-1β, is decreased, but not completely blocked in the presence of a cyclooxygenase inhibitor suggest that activation of these neurons can occur via prostaglandin-independent mechanisms. IL-1β has also been shown to alter the membrane potential and firing rates of neurons in the anterior hypothalamus via PGE2-independent regulation of γ-amino butyric acid (GABA) neurons that project onto these neurons (294). Future studies will be necessary to determine the potential role that these indirect mechanisms may play in mediating the observed effects of IL-1β on the membrane potential and firing rates of ARC POMC neurons.

Conflicting data exist concerning the role of the ARC in mediating IL-1β-induced anorexia. One group previously demonstrated that destruction of the ARC, by neonatal monosodium glutamate (MSG) treatment, or knife cut disruption of vertical projections from the ARC to the paraventricular nucleus resulted in augmented anorexia in response to IL-1β (100). Although data from these experiments do not support our model of increased hypothalamic melanocortin signaling mediating IL-1β-induced anorexia, it is important to highlight important caveats of these two paradigms in the context of our results. First, both experimental paradigms would result in substantial disruption of numerous ARC neuropeptide systems. Of particular significance are AgRP neurons,

which co-express NPY and make synaptic contact with POMC neurons, forming a complex neural network whose interplay produces both anorectic and orexigenic effects (295). ARC AgRP/NPY neurons express c-Fos in response to peripheral IL-1β administration(100), and central injections of both NPY and AgRP have been shown to reverse IL-1β-induced anorexia (206, 296). Second, as discussed by the manuscript's authors, ablation of the ARC by MSG failed to completely eliminate all IL-1β sensitive POMC-expressing neurons in the hypothalamus. The combined ability of these neurons to be activated by IL-1β coupled with an impaired or absent compensatory AgRP/NPY response could allow sufficient MC4R activation to drive the observed heightened anorexia. Further characterization of the response of ARC AgRP/NPY neurons to IL-1β may prove essential in resolving this apparent conflict and elucidating the integrated effect of IL-1β on the POMC-AgRP/NPY neural network.

In summary, our results suggest that the hypothalamic melanocortin system is an important target for IL-1β signaling in the brain. The data presented here argue that IL-1β has a predominately stimulatory effect on the activity of the hypothalamic melanocortin system and that increased hypothalamic melanocortin signaling may play a key role in mediating the acute behavioral effects of IL-1β. The observation that IL-1 R knockout mice are obese(69) indicates that this system may also play a tonic role in body weight regulation and also provide a mechanism for anorexia and weight loss in both acute and chronic disease states.

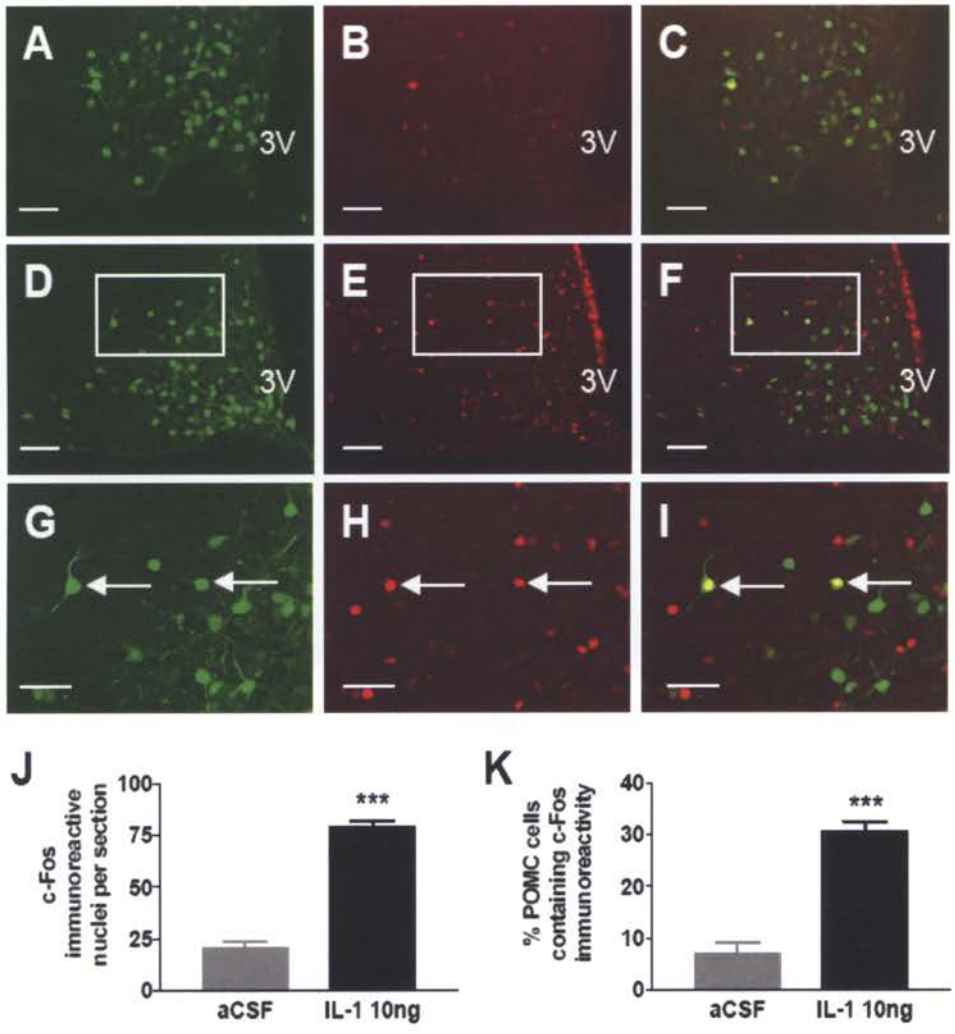

Figure 2-1. IL-1β activates POMC-EGFP neurons in the hypothalamus. (**a,d,g**) Expression of EGFP in the hypothalamus of POMC-EGFP mice. (**b**) Expression of c-Fos (red) in aCSF-treated animals (i.c.v., n=4) is low. (**c**) Few POMC neurons express c-Fos following aCSF treatment. (**e,h**) Expression of c-Fos in IL-1β-treated animals (10ng, i.c.v., n=5) is increased. (**f,i**) IL-1β activates c-Fos in POMC neurons. (**g,h,i**) Panels g-i represent an enlargement of panels d-f shown for clarity. White boxes denote regions of enlargement. (**j**) IL-1β increases the expression of c-Fos in the ARC by ~3.5 fold (two-tailed Student's t-test, ***p<0.0001 vs. aCSF). (**k**) ~30% of POMC neurons are activated by i.c.v. IL-1β (10ng, two-tailed Student's t-test, ***p<0.0001 vs. aCSF). Scale bars = 65μm (**a-f**) and 60 μm (**g-i**).. 3V = third ventricle.

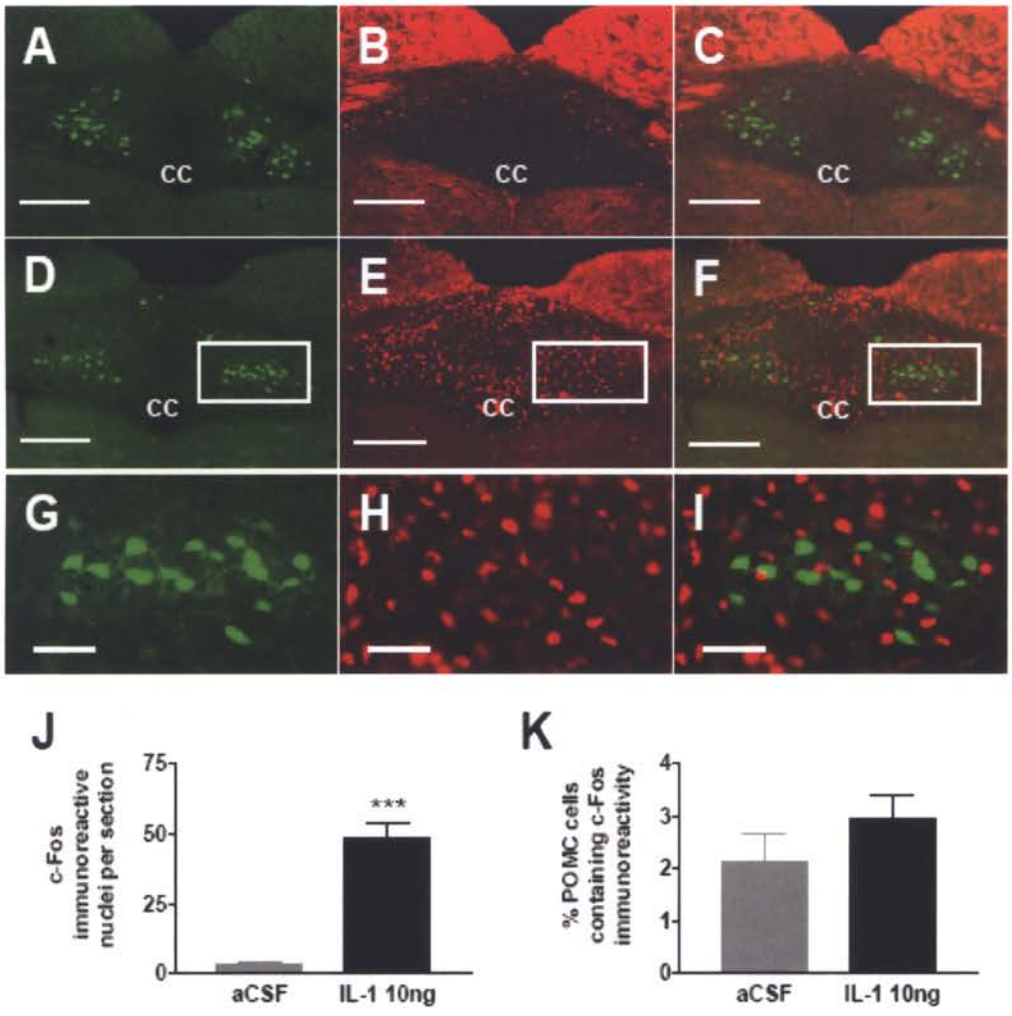

Figure 2-2. IL-1β does not activate POMC-EGFP neurons in the NTS. (**a,d,g**) Expression of EGFP in the NTS of POMC-EGFP mice. (**b**) Expression of c-Fos (red) in aCSF-treated animals (i.c.v., n=4) is very low. (**f**) Few POMC neurons express c-Fos following aCSF treatment. (**e,h**) Expression of c-Fos in IL-1β-treated animals (10ng, i.c.v., n=4) is increased. (**f,i**) IL-1β does not activate c-Fos in POMC neurons. (**g,h,i**) Panels g-i represent an enlargement of panels d-f shown for clarity. White boxes denote regions of enlargement. (**j**) IL-1β increases the expression of c-Fos in the NTS by ~16 fold (two-tailed Student's t-test, ***$p<0.0001$ vs. aCSF). (**k**) IL-1β does not increase the number POMC neurons activated in the NTS (two-tailed Student's t-test, p = ns vs. aCSF). Scale bars = 100μm (**a-f**) and 60 μm (**g-i**). CC = central canal.

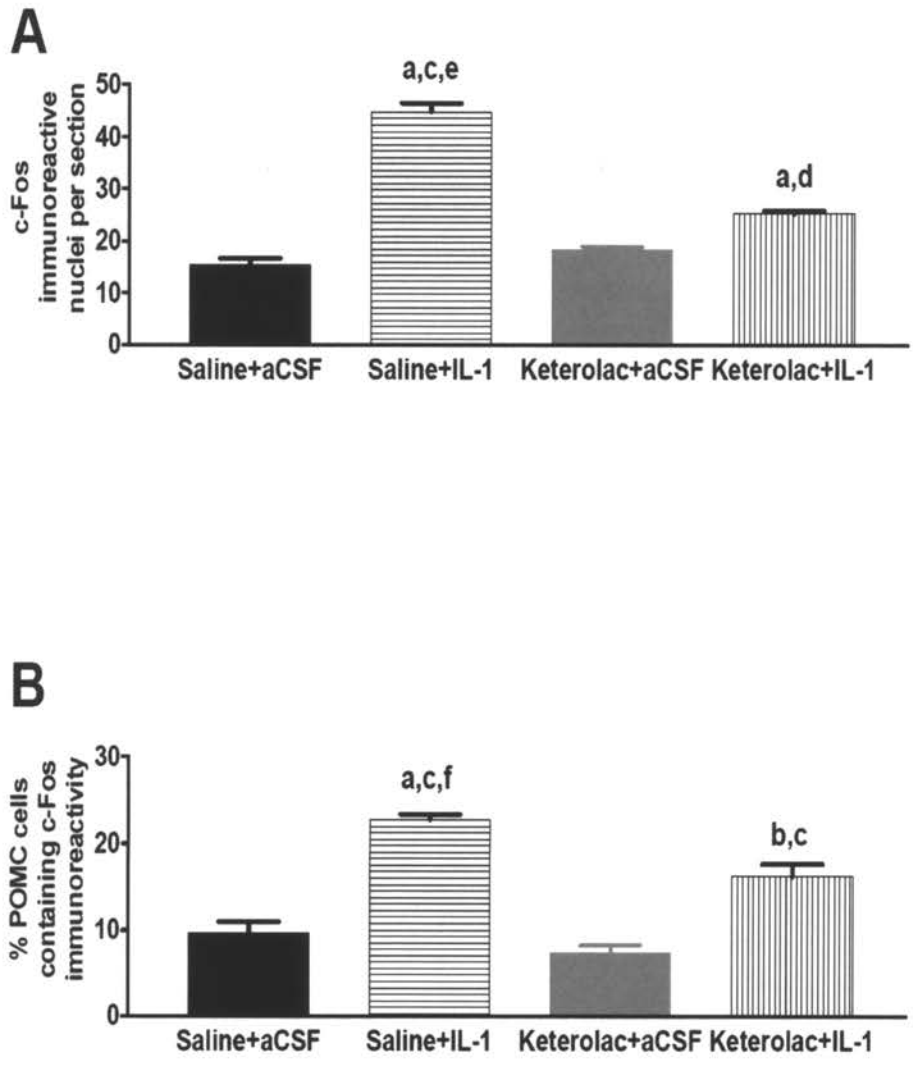

Figure 2-3. Ketorolac reduces IL-1β activation of POMC-EGFP neurons in the hypothalamus. (**a**) Expression of c-Fos in the ARC of POMC-EGFP mice receiving i.p. ketorolac (40 mg/kg) or saline followed by i.c.v injection of IL-1β (10ng) or aCSF 1 hr later (saline + aCSF, n =4; saline + IL-1β, n = 4; ketorlac + aCSF, n = 4; ketorolac + IL-1β, n = 6). (**b**) Reduced expression of c-Fos in ARC POMC-EGFP neurons in mice receiving i.p. ketorolac (40 mg/kg) or saline followed by i.c.v injection of IL-1β (10ng) or aCSF 1 hr later (saline + aCSF, n =4; saline + IL-1β, n = 4; ketorlac + aCSF, n = 4; ketorolac + IL-1β, n = 6). Data is expressed as mean ± SEM, statistics by one-way ANOVA followed by a post hoc analysis using a Bonferroni corrected t test; $^{a}p<0.001$ vs Saline+aCSF, $^{b}p<0.01$ vs Saline+aCSF, $^{c}p<0.001$ vs Ketorolac+aCSF, $^{d}p<0.01$ vs Ketorolac+aCSF, $^{e}p<0.001$ vs Ketorolac+IL-1, $^{f}p<0.01$ vs Ketorolac+IL-1.

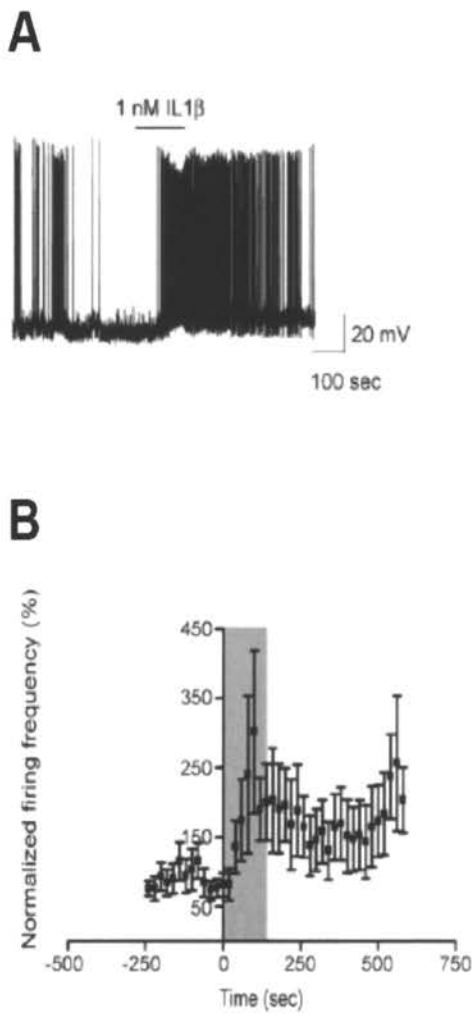

Figure 2-4. IL-1β increases the firing rate of ARC POMC-EGFP neurons. (**a**) Example of raw data (15 minute trace) showing bath application of IL-1β (1 nM). IL1 β depolarized and increased spontaneous activity of a single ARC POMC-EGFP neuron. Mean of membrane potential five minutes prior to IL1 β application = - 54.5 mV; during application (2.32 min) = - 51.4 mV; mean peak depolarization (from 1.5 min after start of drug application to 3.5 min into washout) = - 45.6 mV. Mean firing frequency five minutes prior to IL1β application = 0.52 Hz; during application = 1.86 Hz; five minutes into washout period = 1.48 Hz. (**b**) IL-1β (1 nM) increases the firing rate of ARC POMC-EGFP neurons ($n = 8$; $p < 0.0001$, baseline compared with washout). Shaded region corresponds to time of IL1 β addition to bath. Error bars represent SEM.

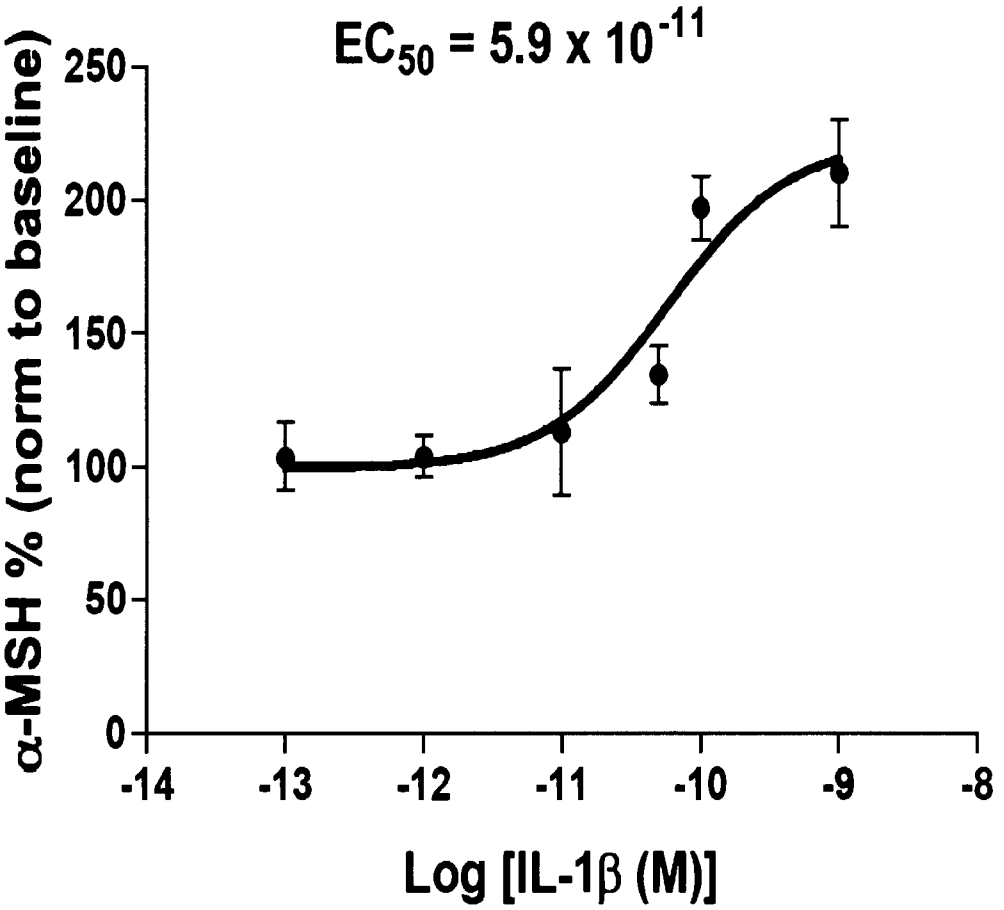

Figure 2-5. IL-1β stimulates *in vitro* release of α-MSH from murine hypothalamic explants in dose-dependent manner with a calculated $EC_{50} = 5.9 \times 10^{-11}$ M. Values are means ± SEM (n = 4 for each dose).

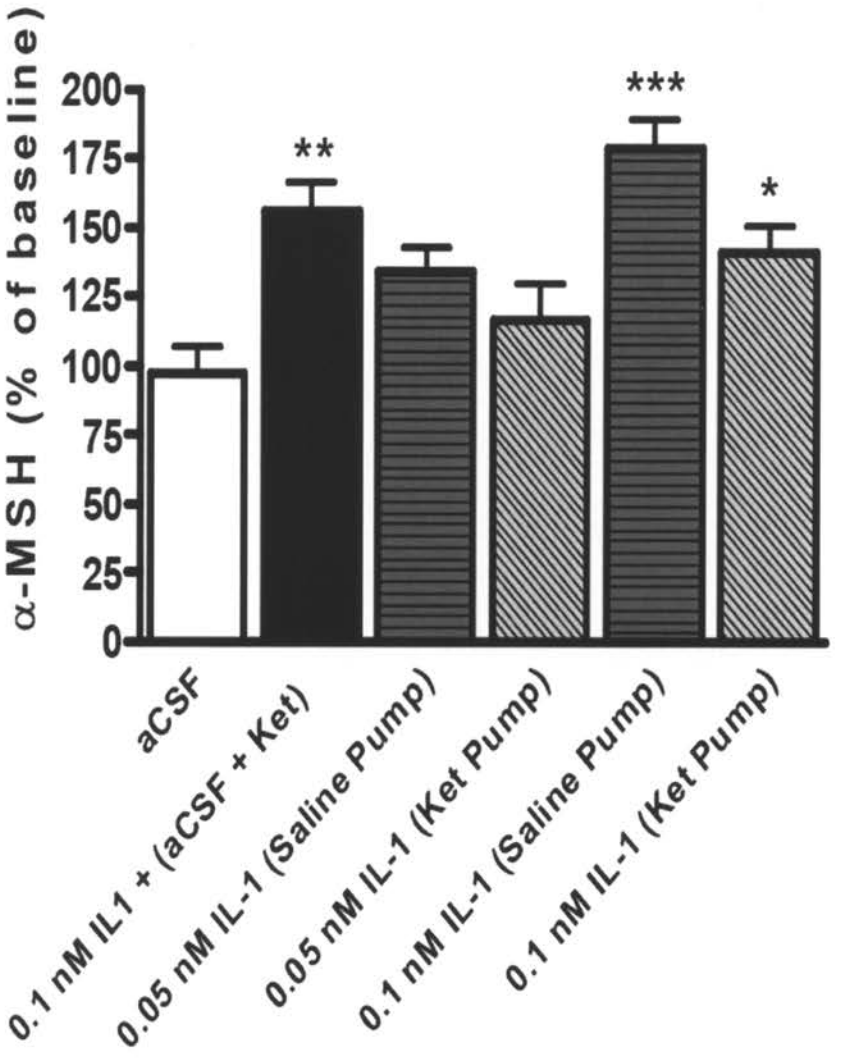

Figure 2-6. Acute and chronic ketorolac treatment does not reverse IL-1β-stimulated *in vitro* release of α-MSH from murine hypothalamic explants. Data is expressed as mean ± SEM (n = 6 for each dose), statistics by one-way ANOVA followed by a post hoc analysis using a Bonferroni multiple comparison test; *p<0.05 vs. aCSF, **p<0.01 vs. aCSF, ***p<0.001 vs. aCSF.

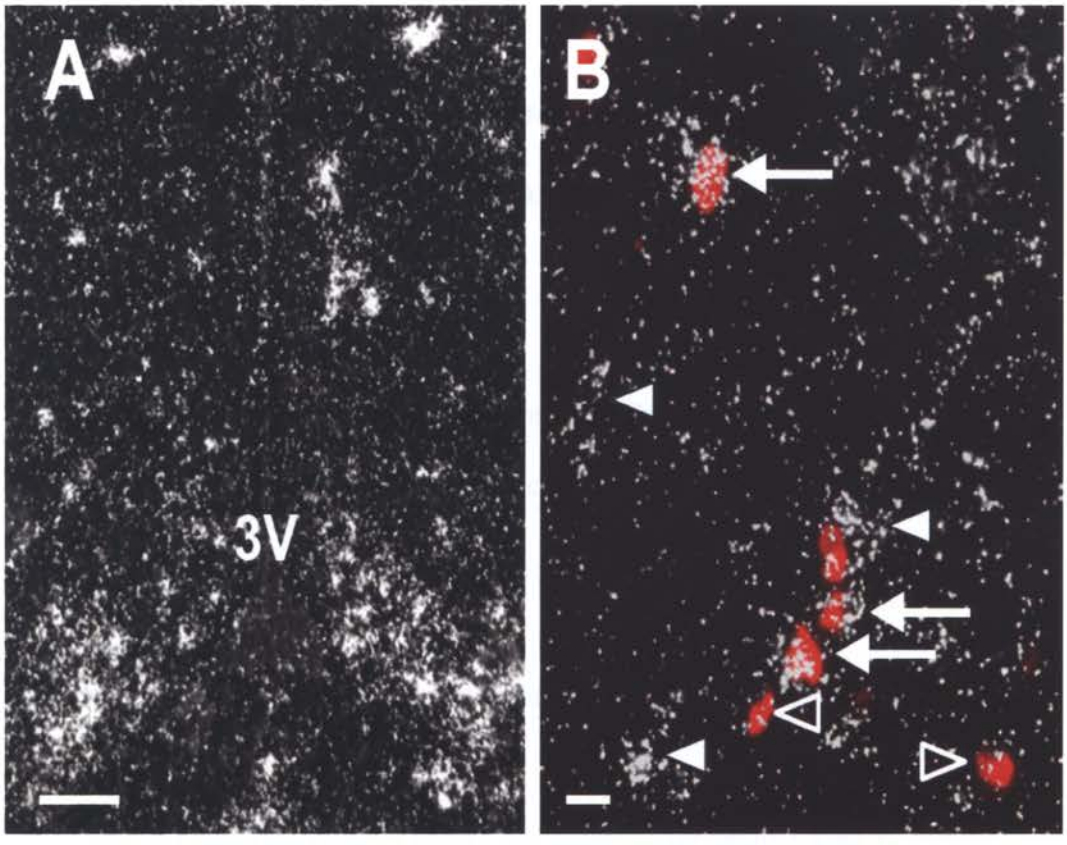

Figure 2-7. Co-expression of POMC mRNA and IL-1R mRNA in the hypothalamus. (**a**) Representative darkfield photomicrograph showing distribution of IL-1R mRNA (white silver grain clusters) in the ARC of wild-type rats. (**b**) Double-label ISH revealed clusters of silver grains representing IL-1R mRNA-expressing cells overlying ARC POMC mRNA-expressing neurons (red precipitate). *Arrows* point to POMC neurons that co-expresses IL-1R mRNA. *Open arrowheads* represent POMC neurons that do not co-express IL-1R mRNA. *Arrowheads* represent silver grain clusters not overlying POMC neurons. Scale bars = 300 μm (a) and 70 μm (b). 3V = third ventricle.

CHAPTER 3-Manuscript #2

Regulation of AgRP mRNA transcription and peptide secretion by acute and chronic inflammation

Jarrad M. Scarlett[1], Xinxia Zhu[1], Pablo J. Enriori[3], Darren D. Bowe[1], Ayesha K. Batra[1], Peter R. Levasseur[1], Wilmon F. Grant[1], Michael M. Meguid[4], Michael A. Cowley[3] and Daniel L. Marks[1,2,]

[1]Center for the Study of Weight Regulation and Associated Disorders, Oregon Health and Science University, Portland, Oregon 97239

[2]Department of Pediatrics, Oregon Health and Science University CDRCP, Portland, Oregon 97239

[3]Division of Neuroscience, Oregon National Primate Research Center, Oregon Health and Science University, Beaverton, Oregon 97006

[4]Surgical Metabolism and Nutrition Laboratory, Department Surgery, State University of New York Upstate Medical University, Syracuse, New York 13210

Chapter 3 is a manuscript as it has been prepared for submission to the journal *Endocrinology*.

Abstract

Agouti-related protein (AgRP) is an orexigenic neuropeptide produced by neurons in the hypothalamic arcuate nucleus (ARC) that is a key component of central neural circuits that control food intake and energy expenditure. Disorders in energy homeostasis, characterized by hypophagia and increased metabolic rate, frequently develop in animals with either acute or chronic diseases. Recently, studies have demonstrated that proopiomelanocortin (POMC)-expressing neurons in the ARC are activated by the proinflammatory cytokine interleukin-1β (IL-1β). In the current study, we sought to determine if inflammatory processes regulate the expression of AgRP mRNA and to characterize the response of AgRP neurons to IL-1β. Here we show by real-time RT-PCR and *in situ* hybridization analysis that AgRP mRNA expression in rodents is increased in models of acute and chronic inflammation. AgRP neurons were found to express the type I interleukin-1 receptor and the percentage of expression was significantly increased following a peripheral administration of lipopolysaccaride. Furthermore, we demonstrate that IL-1β inhibits the release of AgRP from hypothalamic explants. Collectively, these data indicate that proinflammatory signals decrease the secretion of AgRP while increasing the transcription of the AgRP gene. These observations suggest that AgRP neurons may participate with ARC POMC neurons in mediating the anorexic and metabolic responses to acute and chronic disease processes.

Introduction

Disorders in the regulation of energy intake and energy expenditure are frequent occurrences during acute and chronic diseases (4, 8). Recent studies suggest that the synthesis and release of proinflammatory cytokines, including interleukin-1β (IL-1β), interleukin-6 (IL-6), tumor necrosis factor-α (TNF-α) and leukemia inhibitory factor (LIF) in response to pathophysiological processes induce anorexia and increased metabolic rate by acting upon centers of the brain that are known to control energy homeostasis (8, 32, 280, 297). One region in the brain that is a candidate target for the actions of inflammatory cytokines is the arcuate nucleus of the hypothalamus (ARC). The ARC is a key site that integrates peripheral signals of energy balance and regulates energy homeostasis by transducing signals that modulate eating behavior and metabolism (42, 135, 298). Within the ARC, there are a number of neuropeptide-expressing neurons that play important roles in the regulation of energy homeostasis by providing either anorexigenic or orexigenic signals (298). One key population of neurons in the ARC that provides orexigenic drive are neurons that express the neuropeptide agouti-related protein (AgRP).

AgRP is an endogenous antagonist of the anorexigenic neuropeptide alpha-melanocyte-stimulating hormone [α-MSH; derived from the proopiomelanocortin (POMC) precursor] (130, 299). AgRP promotes food intake and positive energy balance via inhibition of α-MSH-stimulated signaling and inverse agonism at the type 3 and type 4 central melanocortin receptors (MC3-R and MC4-R) (130, 300, 301). In the CNS, AgRP is produced exclusively by neurons in the ARC where it is colocalized with

neuropeptide Y (NPY) (132) and the inhibitory neurotransmitter GABA (131). Central infusion of AgRP(302), or overexpression of AgRP in transgenic mice(303) induces hyperphagia and obesity. AgRP neurons recognize and respond to a number of peripheral signals of energy balance, including insulin and the adipose-derived hormone leptin(163).

Leptin is a 16-kDa protein that has a fundamental role in the regulation of feeding behavior, metabolism and neuroendocrine function(304, 305). The functional long form of the leptin receptor is a member of the class-I cytokine receptor family(306) and it is expressed by neurons in the hypothalamus associated with energy homeostasis, including AgRP(307) and POMC-expressing neurons(154). AgRP mRNA expression is increased during fasting and can be returned to pre-fasting levels with leptin replacement(163). Leptin has also been shown to inhibit the *in vitro* release of AgRP from hypothalamic explants harvested from both rats (308) and mice (161). The responsiveness of AgRP neurons to leptin raises the possibility that additional cytokines that are synthesized and released during inflammatory states may also be involved in the regulation of AgRP neuronal activity. Indeed, it has been reported that AgRP mRNA expression in mice is decreased six hours after receiving a peripheral administration of TNF-α (198).

IL-1β is a proinflammatory cytokine that is rapidly released in response to infection and tissue injury and can elicit a number of behavioral and metabolic responses including anorexia, pyrexia and increased basal metabolic rate (279-281, 309). In rodents, anorexia can be reliably induced by both peripheral and central administrations of recombinant IL-1β(100, 280). The effects of IL-1β in the brain are mediated by the type I IL-1 receptor (IL-1R) and these receptors are expressed by neurons in regions of the brain associated

with energy homeostasis, including the ARC (87). In previous work, IL-1β given intravenously to rats was shown to induce Fos protein in NPY mRNA-expressing neurons in the ARC(100). Recently, our lab has shown that IL-1β specifically activates a subpopulation of ARC POMC neurons and potently stimulates the release of α-MSH from hypothalamic explants (310). In the current study, we tested the hypothesis that AgRP-expressing neurons in the ARC are targets for IL-1β's action in the regulation of food intake and metabolism. Specifically, we investigated whether: (1) AgRP gene transcription is regulated by IL-1β given as a single injection or as a result of induced acute and chronic inflammatory states; (2) AgRP peptide secretion from *ex vivo* hypothalamic explants is regulated by IL-1β and if prostaglandin synthesis is a required step; (3) AgRP neurons are direct targets for the action of IL-1β by identifying AgRP neurons in the Arc that co-express IL-1R mRNA.

Materials and Methods

Animals

Male Sprague-Dawley rats (300-350g; Taconic Farms), F344/NTacfBR rats (200-250g; Taconic Farms), IL-1R KO mice (5-8 weeks of age; Jackson Laboratory) and C57BL/6J mice (5-8 weeks of age; Jackson Laboratory) were maintained on a normal 12:12 light/dark cycle with *ad libitum* access to food (Purina rodent diet 5001; Purina Mills) and water. Experiments were conducted in accordance with the NIH Guide for the Care and Use of Laboratory Animals and approved by the Animal Care and Use Committees

of Oregon Health and Science University and the Oregon National Primate Research Center.

Implantation of lateral ventricle cannulae

Male Sprague-Dawley rats and C57BL/6J mice were anesthetized with a ketamine cocktail and placed in a stereotaxic apparatus (Cartesian Instruments). A sterile guide cannula with obdurator stylet was stereotaxically implanted into the lateral ventricle. For rats, the coordinates used were: 1.0 mm posterior to bregma, 1.25 mm lateral to midline, and 4.0 mm below the surface of the skull. For mice, the coordinates used were: 1.0 mm posterior to bregma, 0.5 mm lateral to midline, and 2.3 mm below the surface of the skull (283, 285). The cannula was then fixed in place with dental cement. The animals were individually housed after surgery for a minimum of 1 week and were handled and administered 5µl (rats) or 1µl (mice) i.c.v. injections of commercial artificial cerebrospinal fluid (Harvard Apparatus) daily.

Central IL-1β injection in rats for AgRP mRNA and c-fos mRNA double-label study

On the day of the experiment at 0900, rats received i.c.v. injections of 10 ng rat IL-1β (R&D Systems, Inc.) dissolved in 5µl aCSF, or aCSF alone. Ninety minutes after treatment, rats were anesthetized with isoflurane and killed by decapitation. The brains were immediately removed from the calvaria and frozen on dry ice. Brains were stored at –80°C until sectioned on a cryostat.

Central IL-1β injection in mice for AgRP mRNA expression study

On the day of the experiment at 0900, mice received i.c.v. injections of 10 ng murine IL-1β (R&D Systems, Inc.) dissolved in 1μl aCSF, or aCSF alone and were placed in clean cages without food. Eight hours after treatment, mice were anesthetized with isoflurane and killed by decapitation. The brains were immediately removed from the calvaria and a hypothalamic block was dissected out, preserved in RNAlater solution (Ambion, Inc.) and stored at –80°C until RNA extraction and RT-PCR analysis.

Rat tumor model

Male F344/NTacfBR rats were individually housed and divided into three groups: Sham-operated controls, tumor-bearing, and sham-operated rats that were pair-fed with the tumor-bearing group such that they were given a quantity of food each day equal to the average amount eaten by the tumor-bearing rats from the previous day. On day 0, the animals were anesthetized with a ketamine cocktail and fresh tumor tissue (0.2 – 0.3g) from a rat donor was implanted subcutaneously into the flank of the rat as previously described (311). The tumor is a methylcholanthrene induced sarcoma that does not metastasize. Its characteristic growth curve vs. time is curvilinear and was previously documented (312). On day 13 after tumor implantation, tumor growth had fallen within the predetermined endpoints of the study, according to OHSU IACUC Policy on Tumor Burden and the animals were sacrificed. The brains were immediately removed from the

calvaria and a hypothalamic block was dissected out, preserved in RNAlater solution (Ambion, Inc.) and stored at –80°C until RNA extraction and RT-PCR analysis.

Subtotal nephrectomy procedure

Chronic renal failure was induced in male F344/NTacfBR rats using a two-stage, five-sixth nephrectomy procedure. In the first stage of the procedure, animals were anesthetized with a ketamine cocktail and a left flank incision was made to allow visualization of the left kidney. Surgical ablation of two poles of the left kidney resulted in an approximate two-thirds reduction of the total left renal mass. Sham-operated control rats underwent left renal decapsulation during this stage. Animals were allowed nine days of recovery prior to the second stage of the nephrectomy procedure. In the second stage of the procedure, animals were anesthetized with a ketamine cocktail and a right flank incision was made to allow visualization and surgical resection of the right kidney. Sham-operated control rats underwent right renal decapsulation during this stage. Two doses of buprenorphine (0.05 mg/kg) were administered before incision and post- operation in each stage. After the second surgery, animals were housed in individual cages and body weight and food intake were measured daily. Animals were sacrificed 14 days after the second surgery. Blood was collected for BUN and plasma creatinine assays. Brains were collected and a hypothalamic block was dissected out, preserved in RNAlater solution (Ambion, Inc.) and stored at –80°C until RNA extraction and RT-PCR analysis.

Implantation of osmotic minipumps

ALZET micro-osmotic pumps (Model 1007D, DURECT Corporation) were filled with ketorolac (K1136, Sigma-Aldrich) dissolved in sterile saline, or sterile saline. Ketorolac-filled pumps were calibrated to deliver a constant infusion of 1.0 mg/kg every six hours. Male C57BL/6J mice were anesthetized with a ketamine cocktail and the pumps were implanted subcutaneously on the dorsal surface of each mouse. Mice were allowed two days of recovery prior to use in studies.

Hypothalamic peptide secretion

Male C57BL/6J mice (n = 30) were anesthetized with isoflurane and killed quickly by decapitation. The brain was removed (with care taken to ensure that there was no contamination of the hypothalamic portion with residual pituitary) and a 2 mm slice was prepared using a vibrating microtome (Leica VS 1000) to include the paraventricular and arcuate nuclei. Individual hypothalami received a 1 h equilibration period with aCSF (aCSF; NaCl 126 mM, Na_2HPO 0.09 mM, KCl 6 mM, $CaCl_2$ 4 mM, $MgSO_4$ 0.09 mM, $NaHCO_3$ 20 mM, glucose 8 mM, ascorbic acid 0.18 mg/ml, 0.6 TIU aprotinin/ml) at 37°C. Hypothalami were then incubated for 45 min at 37°C in 700 µl aCSF (basal period) before being challenged with a single concentration of murine IL-1β (R&D Systems, Inc.) (0.0001 nM to 1.0 nM) in 700 µl aCSF for 45 min at 37°C. Tissue viability was verified by a 45 min exposure to 700 µl aCSF containing 56 mM KCl. Treatments were performed in quadruplicate. At the end of each treatment period,

supernatants were removed and frozen at –80°C until assayed by radioimmunoassay. Hypothalamic explants that failed to show peptide release 3X above that of basal release in response to aCSF containing 56 mM KCl were excluded from data analysis.

Hypothalamic peptide secretion following ketorolac treatment

Male C57BL/6J mice that had been implanted with ketorolac-filled (n = 6) or saline-filled osmotic pumps (n = 12) were divided into three groups of six animals each. Mice from all groups were anesthetized with isoflurane and killed quickly by decapitation. Brains were removed and processed on a vibrating microtome as described above. Individual hypothalami received a 1 h equilibration period with aCSF at 37°C. A single group of hypothalami from mice that received saline pumps (n = 6) were incubated for 45 min at 37°C in 700 µl aCSF + ketorolac (121 µM) (basal period) before being challenged with 0.1 nM murine IL-1β in 700 µl aCSF + ketorolac (121 µM) for 45 min at 37°C. Hypothalami from the remaining two groups were incubated for 45 min at 37°C in 700 µl aCSF (basal period) before being challenged with 0.1 nM (n =6 for saline and ketorolac-treated mice) murine IL-1β in 700 µl aCSF for 45 min at 37°C. Tissue viability was verified by a 45 min exposure to 700 µl aCSF containing 56 mM KCl. Treatments were performed in quadruplicate. At the end of each treatment period, supernatants were removed and frozen at –80°C until assayed by radioimmunoassay. Hypothalamic explants that failed to show peptide release 3X above that of basal releasein response to aCSF containing 56 mM KCl were excluded from data analysis.

AgRP radioimmunoassay

AgRP immunoreactivity was measured with a rabbit anti-α-AgRP (Phoenix Pharmaceuticals, Inc.). The antibody cross-reacts fully with the mature AgRP. ^{125}I-labeled AgRP was prepared by the iodogen method and purified by high-pressure liquid chromatography (University of Mississippi Peptide Radioiodination Service Center, University, MS). All samples were assayed in duplicate. The assay was performed in a total volume of 350 µl of 0.06 M phosphate buffer, pH 7.3, containing 1% BSA. The sample was incubated for three days at 4°C before the separation of free and antibody-bound label by goat anti-rabbit IgG serum (Phoenix Pharmaceuticals, Inc). One hundred microliters of supernatant was assayed. The lowest detectable level that could be distinguished from the zero standard was 0.30 fmol/tube. The intra-assay variation (CV%) was determined by replicate analysis (n=10) of two samples at AgRP concentrations of 2 and 10 fmol/tube, and the results were 7.8% and 7.5% respectively. The inter-assay variation (CV%) was 10.7% and 12.1% for the range of values measured.

RNA preparation and RT-PCR

Total RNA was extracted from hypothalamic blocks using Qiagen RNeasy kits (Qiagen, Inc., Valencia, CA). Hypothalamic blocks were dissected by making coronal cuts at the rostral extent of the optic chiasm and caudal to the mammillary bodies; sagittal cuts were made along the optic tracts. Cortex was then removed at the level of the corpus callosom. DNA was removed from total RNA using RNase-Free DNase (Qiagen Inc., Valencia,

CA). RT reactions were prepared using a TaqMan Reverse Transcription Kit (Applied Biosystems, Inc., Foster City, CA). For each reaction cDNA synthesis was prepared using 500ng of RNA in a reaction containing 4µl 10X RT Buffer, 9µl 25mM $MgCl_2$, 8µl 10mM dNTPs, 1.5µl 50µM Random Hexamers, 1µl RNase Inhibitor, 1.5µl MultiScribe Reverse Transcriptase, q.s. to 40µl with nuclease-free water. RT reactions were performed on an Eppendorf Mastercycler (Eppendorf AG, Hamburg, Germany) programmed for 25°C for 10 min, 37°C for 1 hr, and 95°C for 5 min. Samples were diluted with 40µl nuclease-free water and stored at 4°C until RT-PCR was performed.

Real-Time RT-PCR was performed on an ABI 7300 Real Time PCR System using rat-specific primer probe sets obtained from Applied Biosystems, Foster City, CA. Each RT-PCR reaction contained 10µl TaqMan Universal PCR Master Mix, 1µl Assays-on-demand Gene Expression Assay Mix, 4µl nuclease-free water, and 5µl cDNA. Samples and endogenous controls (eukaryotic 18s rRNA) were run in duplicate to assure repeatability. Auto Ct values were calculated using 7300 RQ Study Software v.1.3 and verified.

Single-label *in situ* hybridization

Single-label in situ hybridization to identify cells expressing AgRP mRNA in rat brains was performed as previously described (284). Coronal sections (20 µm) were cut on a cryostat and thaw-mounted onto Superfrost Plus slides (VWR Scientific, West Chester, PA). Hypothalamic sections were collected in a 1:6 series from the diagonal band of

Broca (Bregma 0.50 mm) caudally through the mammillary bodies (Bregma –5.00 mm). Antisense ^{33}P-labeled rat AgRP riboprobe (corresponding to bases 14-383 of rat AgRP; GenBank accession number AF206017) was denatured, dissolved in hybridization buffer at a concentration of 0.05 pmol/ml along with tRNA (1.7 mg/ml), and applied to slides. Slides were covered with glass coverslips, placed in a humid chamber, and incubated overnight at 55°C. The following day, slides were treated with RNase A and washed under conditions of increasing stringency. The tissue was dehydrated in 100% ethanol, air dried, and then dipped in NTB-2 liquid emulsion (Eastman Kodak Co.) diluted 1:1 with distilled water. Slides were developed 5 days later and coverslipped.

Single-label *in situ* hybridization image analysis

All slides were assigned a random three-letter code, alphabetized, and read unilaterally under dark-field illumination with custom software designed to count the total number of cells and the number of silver grains (corresponding to radiolabeled AgRP mRNA) over each cell. Cells with a signal to background ratio (SBR) of at least 2 or greater were considered to express AgRP mRNA. Data are expressed as the total number of identifiable cells and grains/cell (a semiquantitative index of mRNA content/cell).

Double-label *in situ* hybridization

Simultaneous visualization of AgRP mRNA with either IL-1R mRNA or c-fos mRNA in the rat brain was performed as previously reported (284), with slight modifications.

Coronal brain sections (20 μm) were cut on a cryostat and thaw-mounted onto Superfrost Plus slides (VWR Scientific, West Chester, PA). Hypothalamic sections were collected in a 1:6 series from the diagonal band of Broca (Bregma 0.50 mm) caudally through the mammillary bodies (Bregma –5.00 mm). Hindbrain sections were collected in a 1:6 series from the facial nucleus (Bregma –10.00 mm) caudally through the spinal cord(285). Antisense ^{33}P-labeled rat IL-1R riboprobe (corresponding to bases 207-930 of rat interleukin-1 receptor type I; GenBank accession number M95578) (0.2 pmol/ml), or ^{33}P-labeled rat c-fos riboprobe (corresponding to bases 210-479 of rat proto-oncogene c-FOS gene; GenBank accession numbers AY780201 and AY780202) (0.1 pmol/ml) and antisense digoxigenin-labeled rat AgRP riboprobe (concentration determined empirically) were denatured, dissolved in hybridization buffer along with tRNA (1.7 mg/ml), and applied to slides. Slides were covered with glass coverslips, placed in a humid chamber, and incubated overnight at 55°C. The following day, slides were treated with RNase A and washed under conditions of increasing stringency. The sections were incubated in blocking buffer and then in Tris buffer containing antidigoxigenin fragments conjugated to alkaline phosphatase (Roche Molecular Biochemicals) diluted 1:250 for 3 h at room temperature. AgRP cells were visualized with Vector Red substrate (SK-5100; Vector Laboratories) according to the manufacturer's protocol. Slides were dipped in 100% ethanol, air dried, and then dipped in NTB-2 liquid emulsion (Eastman Kodak Co.) diluted 1:1 with distilled water. Slides were developed 6 days (c-fos), or 11 days (IL-1R) later and coverslipped. Determination of cells expressing both AgRP mRNA and c-fos mRNA, or IL-1R mRNA was performed using criteria previously described(284). Briefly, AgRP mRNA-containing cells were identified under fluorescent illumination,

and custom-designed software was used to count the silver grains (corresponding to radiolabeled c-fos mRNA or IL-1R mRNA) over each cell. Signal-to-background ratios (SBRs) for individual cells were calculated; an individual cell was considered to be double-labeled if it had an SBR of 2.5 or more. For each animal, the amount of double-labeling was calculated as a percentage of the total number of AgRP mRNA-expressing cells and then averaged across animals to produce mean ± SEM.

Statistical analysis

Data are expressed as mean ± SEM for each group. Statistical analysis was performed using SPSS (v. 14.0) and Prism (v. 3.03) software. All data were analyzed with either an unpaired t test, one-way ANOVA followed by a post hoc analysis using a Bonferroni corrected t test, or a two-way ANOVA followed by a one-way ANOVA with post hoc analysis using a Bonferroni multiple comparison test (secretion study with ketorolac). For all analyses, significance was assigned at the $p < 0.05$ level.

Results

Acute inflammation increases AgRP mRNA expression

To determine if AgRP expression is increased during periods of acute inflammation, we measured AgRP mRNA expression in two independent rodent models of acute inflammation. In our first study, we administered i.p. injections of lipopolysaccaride

(100 μg/kg), or saline to rats at 0800 and sacrificed the animals eight hours later. Cells expressing AgRP mRNA were readily identifiable in the ARC of all animals by single-label *in situ* hybridization (**Fig. 1**). Data analysis revealed that the number of identifiable AgRP-expressing neurons and the cellular content of AgRP mRNA (as reflected by silver grains per cell) were both significantly higher in rats that had received LPS compared to saline treated rats ($P < 0.05$ for both measures) (**Fig. 2**). In our second study, we administered i.c.v. injections of murine IL-1β (10 ng), or aCSF to mice at 0800 and sacrificed the animals eight hours later. IL-1β treatment did not increase AgRP expression compared to aCSF treatment in mice (AgRP: relative quantity [RQ]; aCSF 0.96 ± 0.32, n=4, vs. IL-1β 0.95 ± 0.20, n=7; p = 0.64) (**Fig. 3A**), or rats (RQ; = aCSF 1.18 ± 0.10, n=5, vs. IL-1β 1.16 ± 0.08, n=10; p = 0.81) (**Fig. 3B**).

Chronic inflammation increases AgRP mRNA expression

To extend our findings that AgRP mRNA expression is increased in the setting of acute inflammation, we investigated AgRP mRNA expression in two models of chronic inflammation. In our first model, we observed that AgRP mRNA expression was significantly increased in tumor-bearing rats compared to sham-operated, *ad libitum* fed rats (AgRP: relative quantity [RQ]; tumor-bearing 2.31 ± 0.60, n=10, vs. sham-operated, *ad libitum* fed 0.92 ± 0.25, n=10; p < 0.001) (**Fig. 4A**). AgRP mRNA expression was also elevated in sham-operated, pair-fed rats (RQ = 1.76 ± 0.26, n=9) compared to sham-operated, *ad libitum* fed rats (p < 0.001) (**Fig. 4A**), but was still significantly lower than tumor-bearing rats (p < 0.05) (**Fig. 4A**). In our second model of chronic inflammation,

rats that had received a two-stage, five-sixth nephrectomy procedure had significantly elevated BUN and plasma creatinine levels 14 days after the procedure compared to sham-operated rats (data not shown) thus confirming the effectiveness of the procedure in inducing a state of renal failure. AgRP mRNA expression was significantly elevated in rats with renal failure compared to sham-operated rats (RQ; nephrectomy 0.94 ± 0.34, n=16, vs. sham-operated 0.62 ± 0.15, n=10; $p < 0.01$) (**Fig. 4B**).

AgRP neurons express c-fos mRNA following i.c.v. IL-1β administration

In a previous study, it was reported that an intravenous injection of IL-1β induced Fos immunoreactivity in ARC neurons and that 23% of these Fos-immunoreactive neurons also expressed NPY mRNA (100). To both confirm and extend upon these findings, we performed double-label *in-situ* hybridization for AgRP mRNA and Fos mRNA on brains from rats that had been given i.c.v. injections of IL-1β (10 ng; n = 4) or aCSF (n = 4) and sacrificed 90 minutes later. IL-1β treatment significantly increased the number of identifiable c-fos mRNA-expressing cells in the ARC (aCSF, 16 ± 5 cells per animal, n=4; IL-1β, 133 ± 20 cells per animal; $p < 0.01$) (**Fig. 5A**). Co-expression of AgRP mRNA and c-fos mRNA was very low in aCSF treated animals ($2\% \pm 0.5\%$) and was significantly increased by IL-1β treatment ($13.3\% \pm 1.7\%$; $p < 0.001$) (**Fig 5B**).

AgRP mRNA co-expression with IL-1R mRNA

IL-1R mRNA is densely expressed in the hypothalamus, suggesting that this site is responsive to IL-1β-mediated signaling. Indeed, RT-PCR analysis revealed that in the mouse hypothalamus the abundance of IL-1R mRNA (Relative quantity [RQ] = 2.284 ± 0.186, n=7) is more than two-fold higher than OB-Rb mRNA (1.001 ± 0.60, n=7 $p < 0.0001$) and MC4-R mRNA (1.016 ± 0.084, n=7 $p < 0.0001$). To determine if AgRP mRNA-expressing cells co-express IL-1R mRNA we performed double-label *in-situ* hybridization on brains from rats that had been administered i.p. injections of saline (n = 6). Additionally, a second group of rats in the same study received i.p. injections of LPS (100 μg/kg, n = 5) to measure potential changes in co-expression in the setting of acute inflammation. Both group of rats were injected at 0800 and sacrificed 8 hours later. In both groups of rats, a significant number of AgRP mRNA-expressing neurons in the ARC, represented by cell bodies filled with fluorescent red precipitate, had overlying clusters of silver grains, signifying co-expression of IL-1R. Semiquantitative image analysis revealed that with a signal to background ratio of 2.5 set as the threshold for neurons to be considered double-labeled, 25.0% ± 2.4% of the digoxigenin-labeled AgRP neurons in saline treated rats co-expressed IL-1R mRNA (**Fig. 6A,B**). LPS treatment caused a significant increase in the number of AgRP mRNA-expressing cells co-expressing IL-1R mRNA (34.6% ± 2.5%) compared to saline treated animals ($p < 0.05$). Co-expression of IL-1R mRNA by ARC POMC mRNA-expressing cells was not affected by LPS treatment (data not shown).

IL-1β decreases AgRP release from murine hypothalamic explants

To investigate the effect of IL-1β on AgRP release *in vitro*, hypothalamic explants harvested from male C57BL/6 mice were incubated with IL-1β (0.01 nM, 0.1 nM, 1.0 nM, 3.0 nM, and 30.0 nM; n=4 per IL-1β dose). These doses were chosen based on previous work estimating basal IL-1β concentration in the hypothalamus at 0.01-0.02 nM and increasing approximately 10-fold during pathological conditions(286). IL-1β significantly decreased the release of AgRP from hypothalamic explants with a calculated $EC_{50} = 1.3 \times 10^{-11}$ M (**Fig. 7**). These results demonstrate that *in vivo* hypothalamic concentrations of IL-1β that are produced during pathological conditions are able to potently inhibit the *in vitro* release of AgRP from hypothalamic explants.

Ketorolac treatment does not prevent IL-1β-mediated inhibition of AgRP secretion from murine hypothalamic explants

To determine if inhibition of prostaglandin synthesis would prevent the IL-1β-mediated inhibition of AgRP secretion from hypothalamic explants, we repeated our explant studies in the presence of ketorolac. We observed that acutely blocking prostaglandin synthesis by incubating the explants in aCSF containing ketorolac (121 μM) did not alter IL-1β-mediated inhibition of AgRP release ($p<0.05$ vs. aCSF) (**Fig. 8**). To investigate the effect of chronic blockade of prostaglandin synthesis on IL-1β-mediated inhibition of AgRP release, we implanted mini-osmotic pumps containing either ketorolac or saline two days prior to conducting the explant study. IL-1β (1.0 nM) inhibited AgRP release from hypothalamic explants from mice that had received saline-filled pumps ($p<0.01$ vs. aCSF) (**Fig. 8**). Mice with ketorolac-filled pumps had decreased AgRP release in

response to IL-1β ($p<0.05$ vs. aCSF) that was not significantly different compared to mice with saline pumps ($p>0.05$ vs. saline pump groups) (**Fig. 8**). No significant interaction was found between method of infusion and dose of IL-1β by two-way ANOVA.

Discussion

The findings of the present study demonstrate that the transcriptional and secretory activity of AgRP neurons is regulated by inflammatory signals. AgRP mRNA expression was increased in models of both acute and chronic inflammation. AgRP neurons were found to co-express IL-1R mRNA, and inflammation following a peripheral dose of LPS increased the number of AgRP neurons that co-expressed IL-1R mRNA. Finally, the secretion of AgRP from hypothalamic explants was inhibited by IL-1β and blockade of prostaglandin synthesis failed to attenuate this observed inhibition.

AgRP mRNA expression is increased during periods of fasting. This process is hypothesized to be primarily a leptin-dependent process as leptin replacement can reverse fasting-induced increases in AgRP mRNA expression (132, 313, 314). In the context of these findings, one could hypothesize that decreased circulating levels of leptin as a result of illness-induced anorexia and weight loss could explain our observation that AgRP mRNA expression was increased in response to acute and chronic inflammatory states. However, arguing against this hypothesis are numerous studies showing that in many acute and chronic inflammatory settings, leptin levels are paradoxically elevated despite significant decreases in food intake and body weight (252, 315-319). An alternative

hypothesis is that cytokines derived from the immune responses may be responsible for overriding classical responses of orexigenic pathways to changes in energy balance. Support for this alternative hypothesis can be found from studies examining the response of the hypothalamic NPY system to inflammation. NPY activity is potently increased in states of non-inflammatory negative energy balance including starvation and dietary restriction (320-322). However, this strong NPY activation is not observed in many states of illness-induced anorexia and weight loss including acute cytokine administration (223, 323) and in tumor-bearing rats (324).

Previously, it had been reported that NPY mRNA-expressing neurons in the hypothalamus express Fos-IR in response to a peripheral injection of IL-1β (100). As the majority of ARC NPY neurons co-express AgRP (132), we hypothesized that IL-1β might play an important role in regulating the activity of AgRP neurons. Using double-label *in situ* hybridization, we demonstrated that AgRP neurons might by directly targeted by IL-1β as 25.0% ± 2.4% of AgRP neurons in the rat ARC were found to co-express IL-1R mRNA. Interestingly, we observed a significant increase in the number of AgRP neurons co-expressing IL-1R mRNA following a peripheral injection of LPS, suggesting that the sensitivity of this orexigenic system to cytokine signaling may be enhanced during an inflammatory state. AgRP peptide secretion from hypothalamic explants was potently decreased by IL-1β administration and this effect was not attenuated by blockade of prostaglandin synthesis. These secretion results suggest that IL-1β has a predominant inhibitory effect on the population of AgRP neurons. This hypothesis is supported by our observation that very few AgRP neurons (13.3% ± 1.7%) co-express c-fos mRNA in response to IL-1β. We did not observe an increase in AgRP

mRNA expression in mice or rats eight hours after they had received a central injection of IL-1β. One explanation for this observation is that we chose a time point that was either too early or too late to measure changes in AgRP mRNA expression that might have occurred. However, it is also possible that IL-1β may act principally to regulate the secretory activity of AgRP neurons, and does not have a role in regulating AgRP transcriptional activity. Indeed, we were also unable to detect changes in POMC mRNA expression in mice and rats eight hours after they had received a central injection of IL-1β (data not shown), but have clearly shown in previous experiments that IL-1β activates ARC POMC neurons leading to the increased release of α-MSH (310).

Currently, there exists conflicting data in the literature regarding the role of the ARC in mediating IL-1β-induced anorexia that results from this study may help to reconcile. In an earlier study, it was shown that destruction of the ARC, by neonatal monosodium glutamate (MSG) treatment, or knife cut disruption of vertical projections from the ARC to the paraventricular nucleus resulted in augmented anorexia in response to IL-1β (100). From these results, the authors concluded that the apparent role of the ARC was not to promote, but rather to restrain IL-1β-induced anorexia. However, these data and the authors' conclusion appear to be at odds with recently published data from our lab demonstrating that IL-1β activates ARC POMC neurons and potently stimulates the release of the anorexigenic neuropeptide α-MSH from hypothalamic explants (310). An important caveat to the MSG ablation studies is that IL-1β sensitive POMC-expressing neurons in the lateral hypothalamus were left intact. Previously, in studies comparing the effects of MSG vs. gold thioglucose (GTG) in mice it had been noted that the lateral POMC-expressing neurons (largely spared by MSG) may be more important in the

control of body weight and feeding than the medial POMC-expressing neurons (325). These observations, when coupled with results from another study showing that AgRP cell body and fiber staining is virtually eliminated following MSG treatment (44) may explain why more pronounced anorexia is observed in MSG-treated animals treated with IL-1β.

In an intact setting, IL-1β-mediated activation of ARC POMC neurons (causing increased α-MSH release) and inhibition of AgRP neurons (causing decreased AgRP release) produces a strong anorexigenic effect via increased MC4-R signaling. Single injections of AgRP have been shown to induce hyperphagia for as long as one week in the rat (302). The long duration of the orexigenic effect of AgRP suggests that during periods of illness the release of AgRP acts as a balancing orexigenic signal that regulates the severity of anorexia and provides a mechanism for a period of rebound hyperphagia when the illness is resolved. Teleologically, an initial period of hypophagia with an acute illness may be beneficial as energy that would otherwise be spent in the acquisition and digestion of food is shunted to systems combating the illness. Hyperphagia following resolution of the illness would allow recovery of energy that had been utilized during the period of illness. However, lesions of the ARC that ablate both POMC and NPY/AgRP neurons in the ARC, but spare IL-1β-sensitive extra-arcuate POMC neurons in the hypothalamus disrupt the normal competition that occurs at MC4 receptors between α-MSH and AgRP. Worsened anorexia in response to IL-1β might then occur due to a complete loss of AgRP competition at MC4 receptors that are being activated by α-MSH coming from the remaining IL-1β-sensitive extra-arcuate POMC neurons. Our observations that AgRP secretion is decreased in response to IL-1β, but that the

biosynthetic capacity for AgRP neurons to produce AgRP is increased in response to inflammation support this hypothesized model.

In summary, we have shown that the expression of AgRP mRNA is increased in models of both acute and chronic inflammation and that the secretion of AgRP from hypothalamic explants is decreased in response to IL-1β. Combined with previous work demonstrating that α-MSH secretion is increased in response to IL-1β, our data support a role for increased hypothalamic melanocortin signaling in mediating cytokine-induced anorexia during acute and chronic inflammatory states.

Acknowledgments

We thank Erin Jobst, Maria Glavas, Pushpa Sinnayah, Aaron Eusterbrock and Autumn Fletcher for technical assistance and Dr. Stephanie Krasnow for helpful comments. This work was supported by NIH DK 70333.

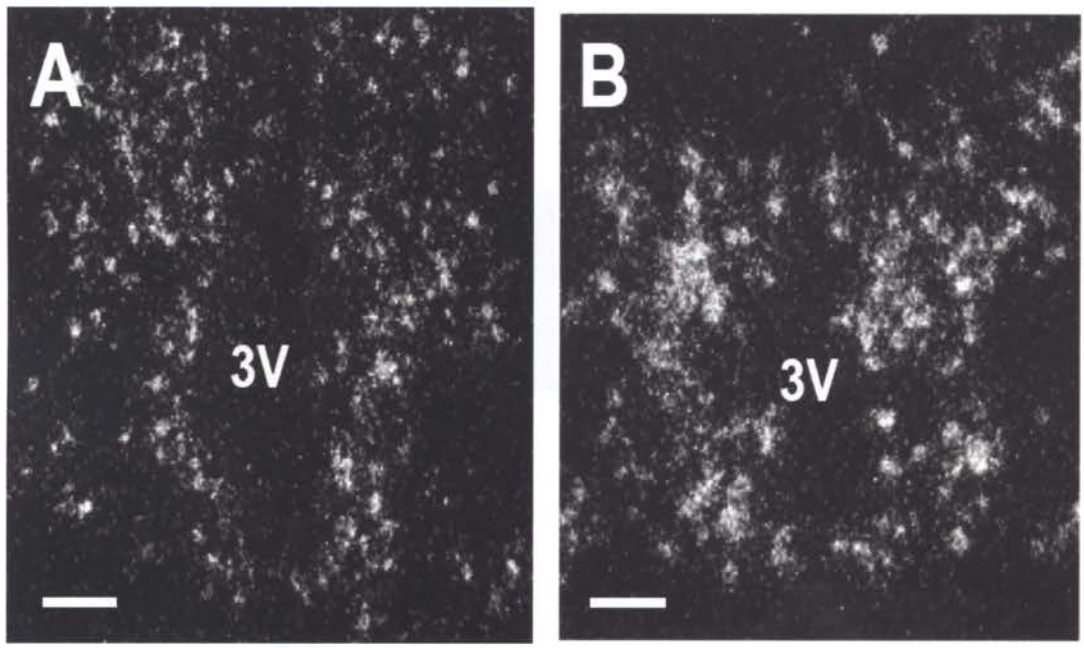

Figure 3-1. Dark-field photomicrographs showing AgRP mRNA-expressing cells (as reflected by the presence of clusters of white silver grains) in the arcuate nucleus of (A) saline-treated and (B) LPS-treated rats. Scale bars = 300μm. 3V = third ventricle.

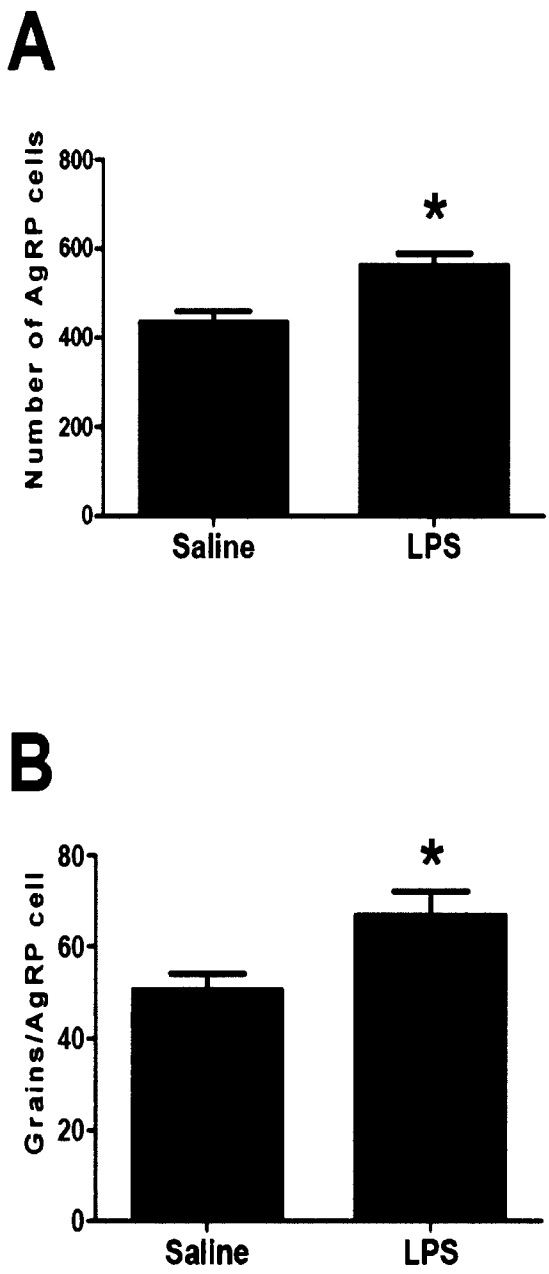

Figure 3-2. LPS treatment increased the number of (A) identifiable AgRP mRNA-containing cells and (B) grains per AgRP cell compared to saline-treated controls. Values are presented as the mean $\pm$ SEM. * $p < 0.05$.

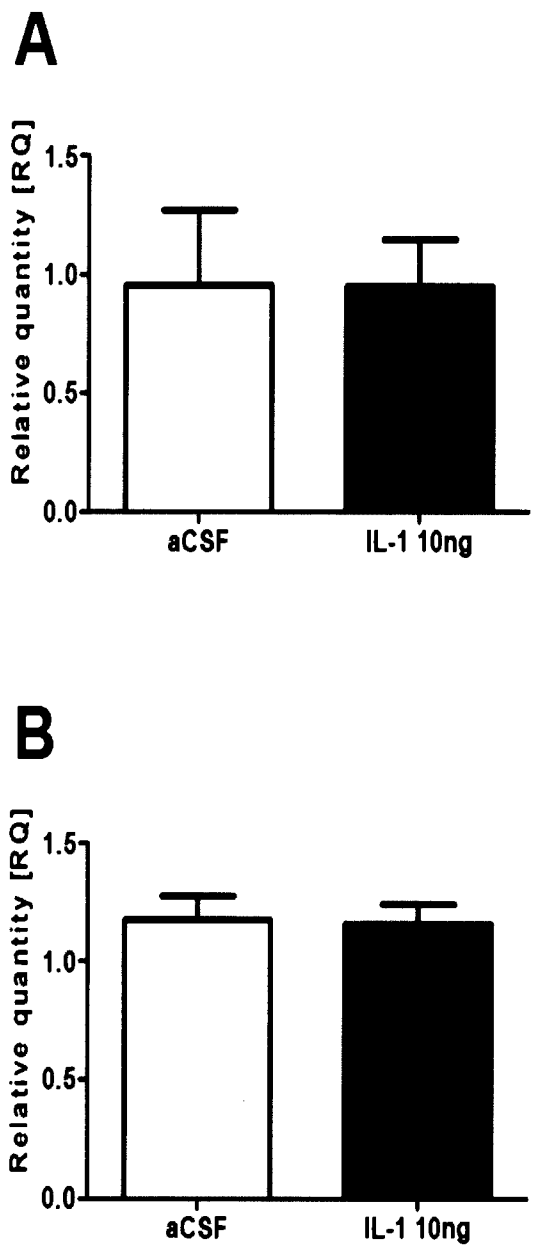

Figure 3-3. AgRP mRNA expression is not increased in mice and rats eight hours after a single injection of IL-1β (10ng) as determined by real-time RT-PCR. (A) AgRP mRNA expression in mice. (B) AgRP mRNA expression in rats. $p>0.05$ for both groups.

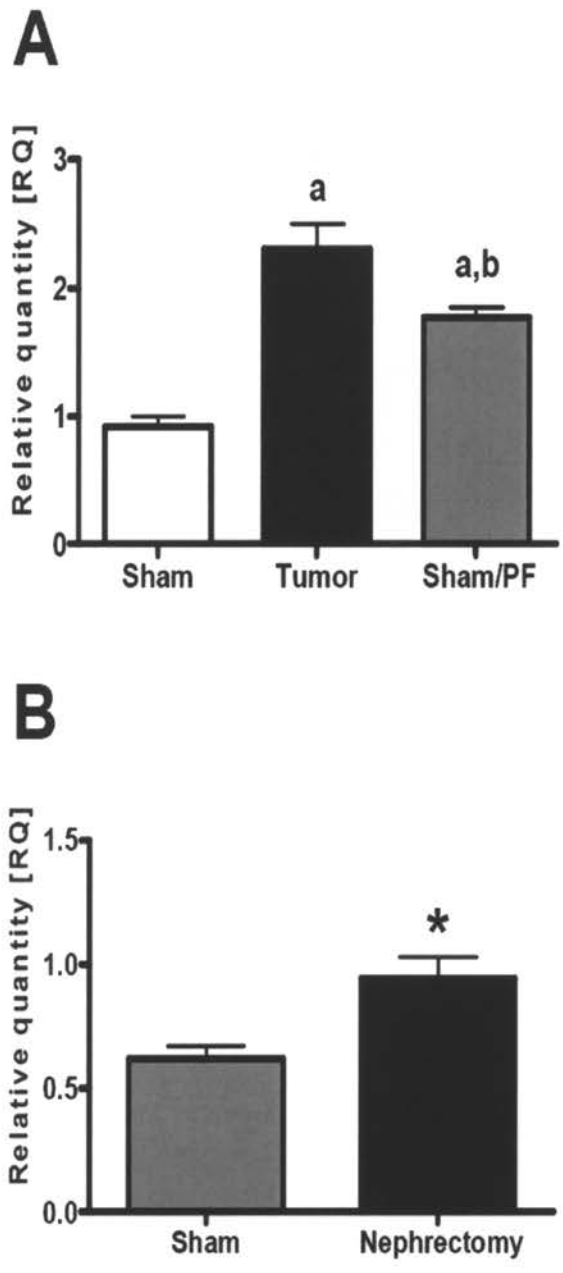

Figure 3-4. AgRP mRNA expression is increased in rat models of chronic inflammation as determined by real-time RT-PCR. (A) Treatment groups: Sham (sham-operated, *ad libitum fed*), Tumor (tumor-bearing) and Sham/PF (sham-operated, pair-fed). [a]$p<0.001$ vs Sham, [b]$p<0.05$ vs Tumor. (B) Treatment groups: Sham (sham-operated) and Nephrectromy (renal failure). * $p < 0.05$. Values are presented as the mean $\pm$ SEM.

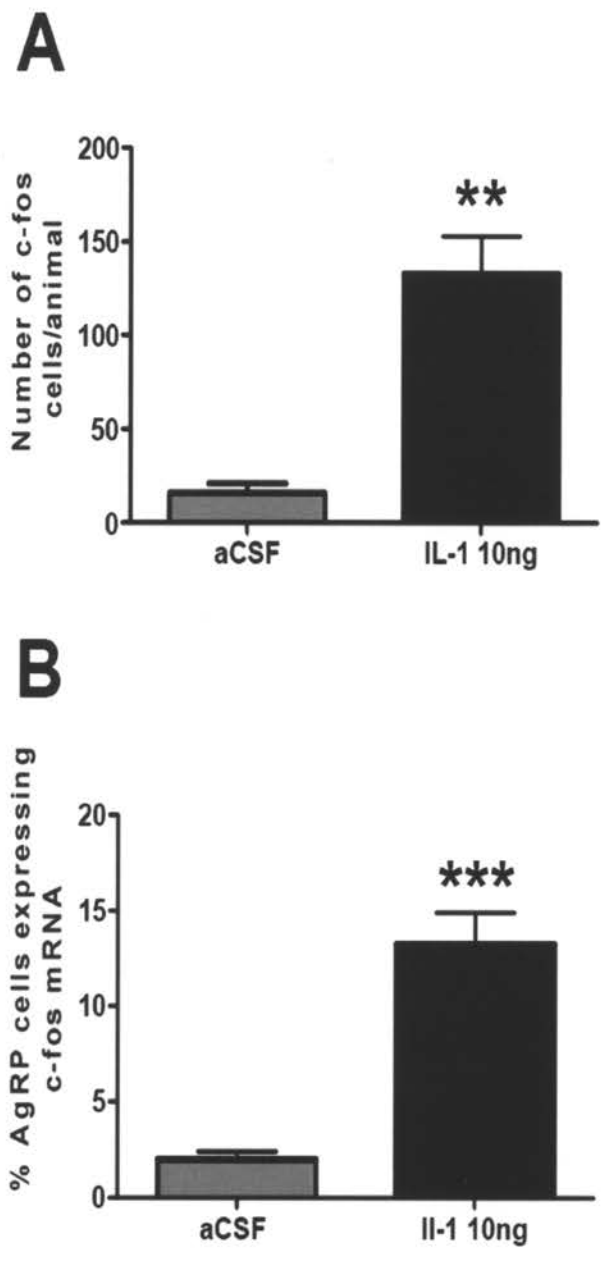

Figure 3-5. IL-1β activates AgRP mRNA-expressing neurons in the ARC. (A) The number of identifiable c-fos mRNA cells per animal after treatment with aCSF or IL-1β (10ng). (B) The percentage of AgRP mRNA-expressing cells that co-express c-fos mRNA after treatment with aCSF or IL-1β (10ng). **$p<0.001$ vs. aCSF, ***$p<0.0001$ vs. aCSF. Values are presented as the mean $\pm$ SEM.

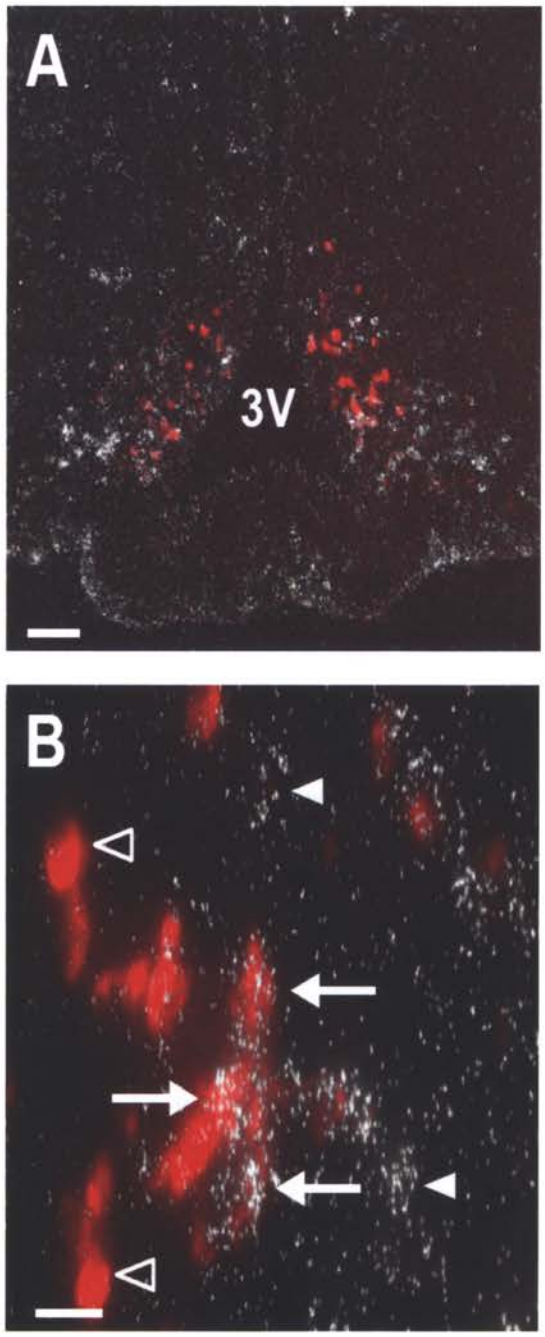

Figure 3-6. Representative photomicrographs showing co-expression of AgRP mRNA and IL-1R mRNA in the hypothalamus. (A) Photomicrograph showing distribution of IL-1R mRNA (white silver grain clusters) in relation to AgRP mRNA (red flourescent cells) in the ARC of rats. (B) Double-label *in situ* hybridization revealed clusters of silver grains overlying ARC AgRP mRNA-expressing neurons. *Arrows* point to AgRP neurons that co-express IL-1R mRNA. *Open arrowheads* represent AgRP neurons that do not co-express IL-1R mRNA. *Arrowheads* represent silver grain clusters not overlying AgRP neurons. Scale bars = 100 μm (A) and 25 μm (B). 3V = third ventricle.

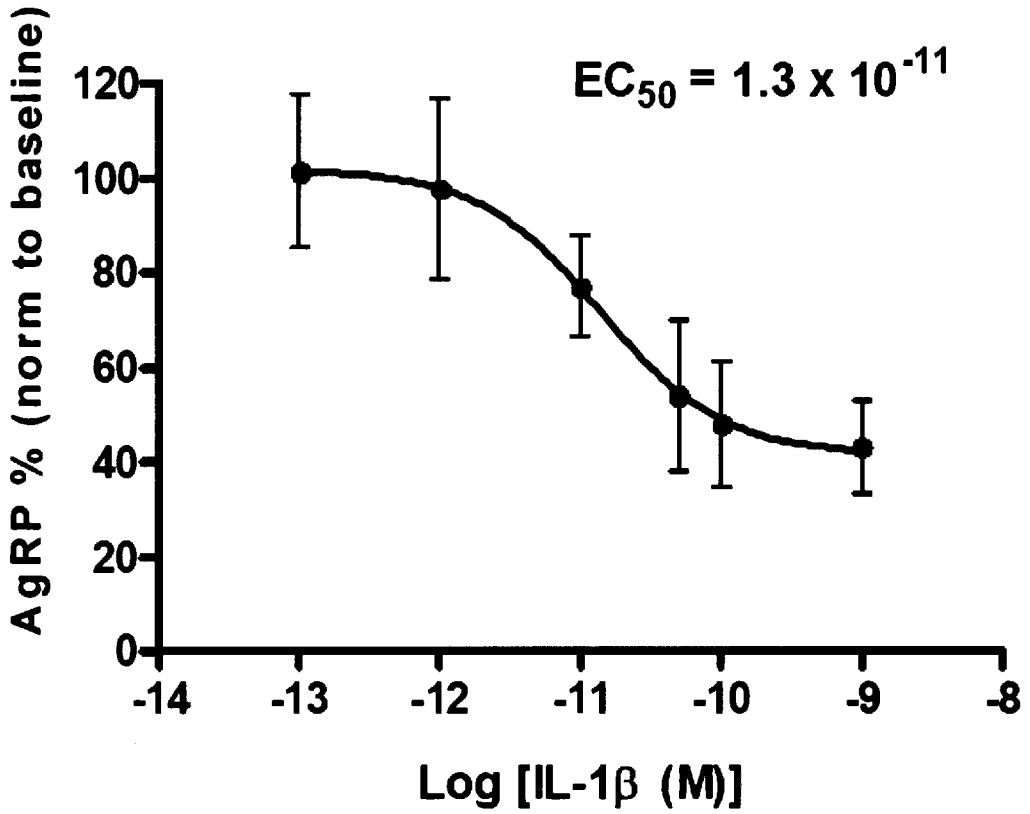

Figure 3-7. IL-1β decreases the *in vitro* release of AgRP from murine hypothalamic explants in a dose-dependent manner with a calculated $EC_{50} = 1.3 \times 10^{-11}$ M. Values are means ± SEM (n = 4 for each dose).

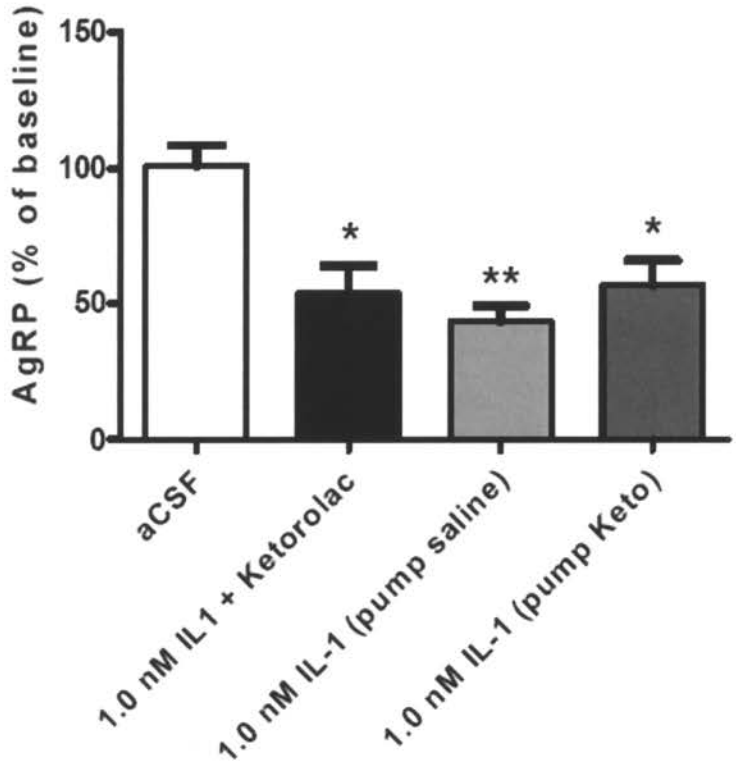

Figure 3-8. Acute and chronic ketorolac treatment does not attenuate IL-1β-mediated decreases in *in vitro* release of AgRP from murine hypothalamic explants. Data are expressed as mean ± SEM (n = 6 for each dose), and were analyzed by one-way ANOVA followed by a post hoc analysis using a Bonferroni multiple comparison test; *$p<0.05$ vs. aCSF, **$p<0.01$ vs. aCSF.

CHAPTER 4-Manuscript #3

Genetic and pharmacologic blockade of central melanocortin signaling attenuates development of cardiac cachexia in rodent models of chronic heart failure

Jarrad M. Scarlett[1], Darren D. Bowe[1,3], Xinxia Zhu[1], Ayesha K. Batra[1], Wilmon F. Grant [1] and Daniel L. Marks[1,2,*]

[1]Center for the Study of Weight Regulation and Associated Disorders, Oregon Health and Science University, Portland, Oregon 97239

[2]Department of Pediatrics, Oregon Health and Science University CDRCP, Portland, Oregon 97239

Chapter 3 is a manuscript as it has been prepared for submission to the journal, *Journal of Clincial Investigation.*

Abstract

Cardiac cachexia is a catabolic syndrome characterized by increased metabolism of lean body mass (LBM) and fat mass that frequently develops in patients with chronic heart failure (CHF). CHF patients who develop cardiac cachexia have a poorer prognosis, as this syndrome is an independent risk factor for increased morbidity and mortality. Experimental evidence suggests a role for the production and signaling of proinflammatory cytokines in the pathogenesis of cardiac cachexia, but the systems involved in transducing these signals have yet to be fully characterized. Here we report that genetic and pharmacologic blockade of the central melanocortin system, a key neuronal circuit in the regulation of energy homeostasis, significantly increased the accumulation of LBM and fat mass and decreased organ hypotrophy in two independent rodent models of CHF. Collectively, our data support a role for the central melanocortin system in the pathogenesis of cardiac cachexia and suggests that blockade of central melanocortin singnaling represents a potential therapeutic target for the treatment of cardiac cachexia.

Introduction

The growing prevalence of chronic heart failure (CHF) is a major health problem in developing countries. Cardiac cachexia, a syndrome of anorexia and wasting of fat and lean body mass (LBM), is a debilitating complication that frequently develops in patients with CHF(4, 326). The prognosis of patients with CHF who develop cardiac cachexia is worse than that of CHF patients with similar degrees of left ventricular dysfunction who do not develop cardiac cachexia(327, 328). In one study, the mortality at 18 months in patients with CHF that had been diagnosed with cardiac cachexia was as high as 50% compared to 17% in patients with CHF that did not develop cardiac cachexia(327). There is evidence to suggest that immune and neurohumoral mechanisms may play a critical role in the pathogenesis of cardiac cachexia. Increased circulating levels of the proinflammatory cytokines TNF-α, interleukin-1β (IL-1β) and interleukin-6 (IL-6) have been measured in CHF patients with cardiac cachexia (28, 329, 330). Administration of these cytokines, either peripherally or centrally, induces anorexia, weight loss and activation of the hypothalamic-pituitary-adrenal (HPA) axis (331, 332). The metabolic and behavioral responses elicited by inflammatory cytokines are hypothesized to occur via their interaction with circuits in the central nervous system (CNS) that regulate metabolism and food intake (100, 333).

A candidate target for inflammatory cytokines in the brain is the central melanocortin system. The central melanocortin system plays a critical role in the regulation of feeding behavior, linear growth and metabolic rate (42, 275). This occurs principally via the

action of α-melanocyte stimulating hormone (α-MSH), a peptide derived from the proopiomelanocortin (POMC)-expressing neurons in the hypothalamus and brainstem(1). The feeding and metabolic effects of α-MSH are mediated by the melanocortin-4 receptor (MC4-R), a G protein-coupled receptor expressed predominately in the brain(1). Acute and chronic stimulation of MC4-R produces anorexia, weight loss and increased metabolic rate(146, 334) whereas genetic deletion, or antagonism of MC4-R by agouti-related protein (AgRP), an endogenous melanocortin receptor antagonist, promotes food intake and weight gain(130, 206).

Data from a number of studies support a critical role for the central melanocortin system in the pathogenesis of cachexia of chronic disease. The secretion of α-MSH is potently increased from hypothalamic explants in response to IL-1β(310). Mice with impaired central melanocortin signaling due to targeted deletion of the MC4-R (MC4-RKO) are resistant to the development of cachexia in models of LPS sepsis (208), cancer (207, 208), and renal failure (252). Pharmacologic blockade of MC4-R signaling with AgRP has been shown to attenuate cachexia in a murine model of cancer cachexia (335). Ghrelin, a gut-derived peptide agonist for the growth hormone secretagogue receptor (GHS-R), attenuates the development of cachexia in rat of models of CHF(195) and cancer-cachexia(196). The anti-cachectic effect of ghrelin may in part be explained by its ability to decrease central melanocortin signaling by increasing AgRP mRNA expression(336) and hyperpolarizing POMC neurons in the hypothalamus(181). Collectively, these data support blockade of central melanocortin signaling as a potential therapy for cardiac cachexia.

In the present paper, we investigated the effect of genetic and pharmacologic blockade of central melanocortin signaling on the accumulation and retention of LBM and fat mass in murine and rat models of CHF. To our knowledge, these are the first studies demonstrating a potential role for the central melanocortin system in the pathogenesis of cardiac cachexia.

Materials and Methods

Animals

Male wild-type (WT) C57BL/6J mice (6-8 months of age; Jackson Laboratory), MC4-RKO mice (6-8 months of age; raised in C57BL/6J background), and male Wistar rats (40-50g; Charles River Laboratories) were maintained on a normal 12:12 light/dark cycle with *ad libitum* access to food (Purina rodent diet 5001; Purina Mills) and water. Prior to surgeries, mice were divided into four groups: wild-type sham-operated (WT-Sham), wild-type myocardial infarcted (WT-MI), MC4-RKO sham-operated (MC4-sham), and MC4-RKO myocardial infarcted (MC4-MI). The rats were initially divided into two groups after their first surgery: sham-operated (Sham) and aortic-banded (Band) and after receiving a second surgery to implant lateral ventricle cannulas they were divided into four groups: sham-operated, aCSF-treated (Sham-aCSF), sham-operated, AgRP treated (Sham-AgRP), banded, aCSF treated (Band-aCSF) and banded, AgRP-treated (Band-AgRP). Experiments were conducted in accordance with the NIH Guide for the Care and

Use of Laboratory Animals and approved by the Animal Care and Use Committees of Oregon Health and Science University.

Murine myocardial infarction surgeries

Permanent myocardial infarcts were produced in wild-type and MC4R-KO mice by ligation of the anterior descending branch of the left coronary artery (CAL). Briefly, mice were anesthetized with intraperitoneal pentobarbital sodium (4 mg/ml, 14 μl/g body wt, Nembutal, Abbott Laboratories; North Chicago, IL), placed in a supine position, and intubated. Mice were ventilated with a mixture of 100% oxygen and room air with a mechanical rodent Mini-Vent ventilator (100 cycles/min, Harvard Apparatus; Holliston, MA). Ventilator stroke volume was adjusted to fully inflate but not overexpand the lungs. A lateral sternotomy was performed, exposing the anterior surface of the heart. The anterior descending branch of the left main coronary artery (LAD) was ligated at a position ~1mm from the tip of the normally positioned left auricle with a 7-0 polypropylene monofilament suture (Prolene, Ethicon; Somerville, NJ). The ligature was not removed after placement. Sham operations were created by passing the suture under the coronary artery at the position used for ligation without ever constricting the artery. After chest closure, mice were recovered in a sternal position, warmed, and provided with 100% oxygen by nose cone. Analgesia was extended with subcutaneous 2.5 mg/kg buprenorphine HCl (Buprenex, Reckitt and Colman Pharmaceuticals; Richmond, VA). Mice must have survived 8 weeks after surgery to be included in the study.

Murine body composition

Body composition was determined before infarction surgeries and the end of the experiment by dual energy x-ray absorptiometry (DEXA, PIXImus mouse densitometer, MEC Lunar Corp., Minster, OH). The instrument was calibrated at the start of each recording session with a murine calibration standard. All animals were fasted for 12 h before DEXA analysis to minimize the effect of ingested food on the DEXA analysis. Individual organ weights (including heart, liver, lung, and spleen) were measured at necropsy at the end of the final DEXA scan.

Murine indirect calorimetry

Oxygen consumption (VO_2) was determined by indirect calorimetry (Oxymax, Columbus Instruments, Columbus, OH). Mice were housed in separate chambers at 24 ± 1 C. Mice were first acclimatized to the chambers for 2 d. Measurements were recorded for 4–8 h during the middle of the light cycle (1100–1600 h). Samples were recorded every 3 min with the room air reference taken every 30 min and the air flow to chambers 500 ml/min. Basal oxygen consumption was determined for individual curves as the average of the lowest plateau regions corresponding to resting periods. Total oxygen consumption was the result of all samples recorded corresponding to periods of movement as well as inactivity.

Rat aortic banding surgeries

Male Wistar rats were anesthetized by intraperitoneal injection of pentobarbital sodium (60 mg/kg body wt). Rats were ventilated with a mixture of 100% oxygen and room air by mechanical ventilation at a tidal volume of 320 uL and a frequency of 120 bpm (MiniVent, Harvard Apparatus). The aortic stenosis was induced via a left thoracic incision by banding the ascending aorta with titanium clips (Weck Atrauclip, 0.6-mm internal diameter) as previously described (337). The Sham group consisted of sham-operated rats prepared by a similar surgical treatment without placement of the clip. After chest closure, rats were recovered in a sternal position, warmed, and provided with 100% oxygen by nose cone. Analgesia was extended with subcutaneous 2.5 mg/kg buprenorphine HCl (Buprenex, Reckitt and Colman Pharmaceuticals; Richmond, VA). The rats were group housed until the sham-operated rats reached an average weight of 200g at which time both sham-operated and banded rats were separated into individual cages for food intake and body weight measurement studies.

Rat intracerebroventricular (i.c.v.) cannulation and injections

Cannulation implantation was performed when the average weight of the sham-operated rats reached 300g. Sham and aortic-banded rats were anesthetized as described above and placed in a stereotaxic apparatus (Cartesian Research, Inc.). A sterile guide cannula with obdurator stylet was implanted 1mm lateral to bregma, 1.5mm posterior to bregma, and 3.6mm below the surface of the skull. The cannula was then fixed in place with

dental cement. After surgery, the rats remained individually housed and allowed 5 days to recover before receiving their first DEXA scan and beginning the treatment period. During recovery, the rats were handled daily and administered 5µl i.c.v. injections of commercial artificial cerebrospinal fluid (aCSF) (Harvard Apparatus) daily. During the two-week treatment period, animals received 5 µl injections of either aCSF or 1nmol AGRP (Phoenix Pharmaceuticals) dissolved in 5 µl aCSF once every 48 hours for a total of eight injections.

Rat body composition

Body composition was determined before and after the two-week AGRP or aCSF treatment period by DEXA (Hologic QDR Discovery A Densitometer) at the OHSU General Clinical Research Center Body Composition core. All animals were fasted for 12 h before DEXA analysis to minimize the effect of ingested food on the DEXA analysis. Individual organ weights were measured at necropsy at the end of the final DEXA scan. The ratio of LBM to total body water was determined using quantitative magnetic resonance (QMR, EchoMRI, Houston, TX) by the Cincinnati Mouse Metabolic Phenotyping Center as previously described (338).

Tissue parameters.

A macroscopic necropsy was done for each animal at the time of sacrifice. The heart was removed, the atria and great vessels were removed, and the combined weight of the

ventricles and septum was weighed. The liver and kidneys were also removed and weighed. Rat brains were removed and hypothalamic blocks were dissected out and stored in RNAlater (Ambion, Inc.) at –80°C.

RNA preparation and RT-PCR

Total RNA was extracted from mice and rat hypothalamic blocks and rat calf muscle using Qiagen RNeasy kits (Qiagen, Inc., Valencia, CA). Hypothalamic blocks were dissected by making coronal cuts at the rostral extent of the optic chiasm and caudal to the mammillary bodies; sagital cuts were made along the optic tracks. Cortex was then removed at the level of the corpus callosom. DNA was removed from total RNA using RNase-Free DNase (Qiagen Inc., Valencia, CA). RT reactions were prepared using a TaqMan Reverse Transcription Kit (AppliedBiosystems, Inc., Foster City, CA). For each reaction cDNA synthesis was prepared using 500ng of RNA in a reaction containing 4µl 10X RT Buffer, 9µl 25mM $MgCl_2$, 8µl 10mM DNTPs, 1.5µl 50µM Random Hexamers, 1µl RNase Inhibitor, 1.5µl MulitScribe Reverse Transcriptase, q.s. to 40µl with nuclease-free water. RT reactions were performed on an Eppendorf Mastercycler (Eppendorf AG, Hamburg, Germany) programmed for 25°C for 10 min, 37°C for 1 hr, and 95°C for 5 min. Samples were diluted with 40µl nuclease-free water stored at 4°C until RT-PCR was performed.

Real-Time RT-PCR was performed on an ABI 7300 Real Time PCR System using rat-specific primer probe sets obtained from Applied Biosystems, Foster City, CA. Each RT-

PCR reaction contained 10μl TaqMan Universal PCR Master Mix, 1μl Assays-on-demand Gene Expression Assay Mix, 4μl nuclease-free water, and 5μl cDNA. Samples and Endogenous controls (Eukaryotic 18s rRNA) were run in duplicate to assure repeatability. Auto Ct values were calculated using 7300 RQ Study Software v.1.3 and verified.

Statistical Analysis

Data are expressed as mean ± SEM for each group. Statistical analysis was performed using SPSS (v. 14.0) and Prism (v. 5.0) software. Comparisons of data between the four groups were made with one-way ANOVA followed by a post hoc analysis using a Bonferroni multiple comparison test. Changes during treatment were analyzed with a two-way ANOVA for repeated measures followed by a Bonferroni test. Comparisons between 2 groups were made by unpaired Student's *t* test. For all analyses, significance was assigned at the $P < 0.05$ level.

Results

Wild-type mice develop cardiac cachexia following myocardial infarction

Eight weeks after surgery, the heart weights of WT-MI mice were significantly increased compared to WT-Sham mice (WT-Sham 0.16 ± 0.01 g *vs* WT-MI 0.32 ± 0.01 g, $P < 0.001$; Table 1). The hearts of WT-Sham mice had normal histological architecture, whereas ligation of the LAD in WT-MI mice produced large infarctions and scarring of

the ventricle wall that was visible when stained with Masson's trichrome stain (Figure 1). WT-Sham mice gained a significant amount of weight in the period after surgery (Table 1, $P < 0.001$), but WT-MI mice failed to gain weight and at the end of the study their weight had decreased compared to baseline (Table 1, P = ns). Significant accumulation of LBM and fat mass after surgery occurred in WT-Sham mice, but not WT-MI mice after surgery (Table 1). The percent increase in LBM per animal over the course of the study was significantly higher for WT-Sham mice compared to WT-MI mice (WT-Sham 11.24% $\pm$ 1.11% *vs* WT-MI 1.73% $\pm$ 1.27%, $P < 0.001$; Figure 2). Kidney and liver weights were higher in WT-Sham mice compared to WT-MI mice (Table 1) with the difference in kidney weights being significant (WT-Sham 0.24 $\pm$ 0.01 g *vs* WT-MI 0.20 $\pm$ 0.01 g, $P < 0.01$). Resting metabolic rate was significantly higher in WT-MI mice (2826 $\pm$ 78 mL/kg/hr) compared to WT-Sham mice (2371 $\pm$ 59 mL/kg/hr; P <0.001; Figure 3).

MC4-RKO mice resist cardiac cachexia following myocardial infarction

To test the role of the MC4-R in the pathogenesis of cardiac cachexia, we performed sham (MC4-Sham) and myocardial infarction (MC4-MI) surgeries in MC4-RKO mice. Eight weeks after surgery, the heart weights of MC4-MI mice were significantly increased compared to MC4-Sham mice (MC4-Sham 0.18 $\pm$ 0.01 g *vs* MC4-MI 0.32 $\pm$ 0.01 g, $P < 0.001$; Table 1) and these values not different compared to their respective WT-Sham and WT-MI groups (P = ns; Table 1). Weight gain, LBM and fat mass accumulation, kidney weights and liver weights were comparable between MC4-Sham and MC4-MI mice (Table 1). There was no difference in the percent increase in LBM per animal over the course of the study for MC4-Sham mice compared to MC4-MI mice

(MC4-Sham 14.45% ± 1.12% *vs* MC4-MI 14.26% ± 1.47%, P = ns; Figure 2) and both groups were significantly higher compared to WT-Sham mice (Figure 2). There was no difference in the resting metabolic rate of WT-MI mice (2826 ± 78 mL/kg/hr) compared to WT-Sham mice (2371 ± 59 mL/kg/hr; P <0.001; Figure 3).

AGRP administration reverses cardiac cachexia in rats with CHF

We next examined the effect of i.c.v. AgRP administration for two weeks to reverse cardiac cachexia in a rat model of CHF induced by aortic banding. Prior to being divided into aCSF and AgRP treatment groups, rats receiving sham operations (n = 14) were significantly larger than their banded (n = 15) littermates (Sham 294.5 + 3.27 g *vs* Band 266.6 + 5.03 g; $P < 0.001$; Table 2) and had higher daily food intake (Sham 25.50 + 0.52 g *vs* Band 19.67 + 0.82 g; $P < 0.001$; Table 2). Sham-aCSF, Sham-AgRP and Band-AgRP rats gained significant amounts of body weight over the two-week treatment period, but Band-aCSF rats failed to significantly gain weight (Table 2). Weight gain, LBM and fat mass accumulation, kidney weights and liver weights were significantly increased by AgRP treatment in banded rats (Band-aCSF *vs* Band-AgRP; Table 2). The percent increase in LBM per animal over the course of the study was higher in Sham-aCSF rats compared to Band-aCSF rats (Sham-aCSF 11.62% ± 2.04% *vs* Band-aCSF 3.39% ± 2.50%, $P < 0.05$; Figure 4). AgRP treatment significantly increased LBM per animal in banded rats when expressed both as a percent of baseline (Band-aCSF 3.39% ± 2.50% *vs* Band-AgRP 17.90% ± 2.29%, $P < 0.001$; Figure 4) and when expressed as absolute grams of tissue (Band-aCSF 7.12 ± 5.57g *vs* Band-AgRP 52.34 ± 5.96g; $P <$ 0.0001). Band-aCSF rats had kidney and liver weights that were significantly decreased

compared to Sham-aCSF rats (Table 2). AgRP treatment significantly reversed organ hypotrophy in banded rats (Band-aCSF *vs* Band-AgRP; Table2) and the final kidney and liver weights of Band-AgRP rats were not different compared to Sham-aCSF rats (Table 2). No significant differences in the hypothalamic mRNA expression of POMC, AgRP, neuropeptide Y (NPY), IL-1β, IL-1R, prohormone convertase 1 (PC1) and prohormone convertase 2 (PC2) was found between Sham and Banded rats (Table 3).

Discussion

Cardiac cachexia is a catabolic state characterized by anorexia and significant wasting of fat and LBM (326, 327, 339). Increased proinflammatory cytokine activation and a lack of metabolic compensation for decreased food intake that results in the catabolic/anabolic imbalance observed in patients with cardiac cachexia (27, 28). Recent studies have shown that the central melanocortin system is activated by proinflammatory cytokines(310) and that blockade of melanocortin signaling can acutely correct the body composition and abnormal metabolic responses seen in murine models of cachexia (207, 252). These observations suggested that the central melanocortin system might play a key role in the pathogenesis of cardiac cachexia and that blockade of melanocortin signaling may ameliorate the body composition and metabolic derangements observed in this syndrome.

In our first series of experiments, we demonstrated that eight weeks after receiving surgeries WT-MI mice became cachectic and experienced weight loss, reduced LBM and fat mass accumulation, and organ hypotrophy compared to WT-Sham mice (Table 1).

Mice with impaired melanocortin signaling (due to genetic deletion of the MC4-R) that received MI surgeries did not become cachectic and experienced normal weight, LBM and fat mass accumulation and comparable organ weights compared to MC4-Sham mice (Table 1). Our observation that the ending heart weights for sham operated mice (WT-Sham *vs* MC4-Sham) and MI mice (WT-MI *vs* MC4-MI) were not different from each other argues against a difference in the sensitivity of the hearts of WT *vs* MC4-RKO mice to the effects of the MI procedure contributing to our results (Table 1). These data strongly suggest a specific role for the MC4-R in transducing the cachectic signals that are produced during a state of CHF.

Activation of centrally expressed MC4-R is hypothesized to mediated the anorectic and metabolic effects of melanocortin peptides (1). However, expression of MC4-R has also been demonstrated in the musculoskeletal and cardiorespiratory systems, including the heart(263) raising the possibility that peripheral mechanisms might contribute to the prevention of cardiac cachexia with global blockade of MC4-R signaling. To test the ability of specific blockade of central melanocortin signaling to attenuate cardiac cachexia, we used a pharmacological approach by administering central injections of AgRP to rats that had developed CHF after undergoing aortic banding surgeries. At the beginning of the treatment period, banded rats were hypophagic, and had reduced body weights, LBM and fat mass accumulation compared to sham-operated rats (Table 2). Banded rats treated with aCSF over the two-week treatment period exhibited no improvements in their body composition parameters (Table 2). AgRP treatment in banded rats significantly increased food intake, weight gain, LBM and fat mass accumulation (Table 2). NMR analysis revealed no significant differences in the ratio of

LBM to body water between all four groups of rats suggesting that the observed differences in LBM accumulation were no due to differences in body water content between sham and banded rats due to heart failure (Figure 5). Organ weights of Band-AgRP rats were significantly heavier than Band-aCSF rats indicating that AgRP treatment had prevented/reversed organ hypotrophy over the treatment period (Table 2). However, AgRP treatment did not affect heart size as the ending heart weights for sham operated rats (Sham-aCSF *vs* Sham-AgRP) and banded rats (Band-aCSF *vs* Band-AgRP) were not different from each other (Table 2) demonstrating that central AgRP treatment neither promoted, nor inhibited cardiac hypertrophy. Band-AgRP rats experienced the largest amount of LBM accumulation (Table 2) and the highest percent increase in LBM per animal of all the groups (Figure 4). Although our current study was not designed to measure the effect of AgRP treatment on morbidity in CHF rats, we observed that during the treatment period that Band-AgRP rats were more active and better groomed compared to Band-aCSF rats. Future studies will be designed to measure changes in these activity patterns in response to AgRP in CHF rats. Collectively, these results suggest that blockade of central melanocortin signaling with AgRP was successful in attenuating cardiac cachexia in the aortic banded rat model of CHF.

A consistent observation in our studies was that the blockade of central melanocortin signaling resulted in increased adiposity in both our sham-operated and CHF-model animals. Hyperphagia and obesity are well-known characteristics of MC4-RKO mice (143) and rats and mice that receive repeated injections of AgRP (340), however this is the first study that shows that these results also occur in rodents with CHF. Although increased adiposity is a risk factor for cardiovascular disease and the subsequent

development of CHF (341, 342), data suggests that once CHF has developed that overweight and obese patients paradoxically have better prognosis and lower mortality risks than lean patients (328, 343). Band-AgRP rats had significantly more fat mass than Sham-aCSF rats (Table 2), but unlike MC4-RKO mice where the increased adiposity has the adverse outcome of pronounced liver steatosis(344), we did not observe liver steatosis in the Band-AgRP rats. The ability of ghrelin to increase body weight and LBM in patients with CHF(345) may in part be due to its ability to inhibit central melanocortin signaling by increasing AgRP expression(336). However, ghrelin did not significantly increase fat mass in this study, likely due to the anti-adiposity effects of ghrelin-induced growth hormone secretion.

In summary, our data suggests that the central melanocortin system, a neural integrator of hormone and cytokine signaling that regulates feeding behavior, linear growth and metabolic rate, may play a key role in the pathogenesis of cardiac cachexia. The ability of genetic and pharmacologic blockade of melanocortin signaling to increase both LBM and fat mass in rodent models of CHF suggests that compounds that selectively antagonize central melanocortin signaling may have important pharmacotherapeutic benefit for cachectic CHF patients.

TABLE 1. Characterization of Wild-Type vs MC4-RKO mice

	WT-Sham	WT-MI	MC4-Sham	MC4-MI
Number	19	15	17	11
Body weight, g				
Baseline	30.82 ± 0.78	30.44 ± 0.92	43.02 ± 1.20*	42.75 ± 1.55*
After Treatment	39.93 ± 1.37^{+}	29.77 ± 1.02	51.68 ± 1.09*$^{,+}$	52.26 ± 1.24*$^{,+}$
Heart Weight, g	0.16 ± 0.01	0.32 ± 0.01$^{\#}$	0.18 ± 0.01	0.32 ± 0.01$^{\#}$
Kidney, g	0.24 ± 0.01	0.20 ± 0.01$^{\#}$	0.25 ± 0.01*	0.23 ± 0.01*
Liver, g	1.39 ± 0.06	1.08 ± 0.03	3.38 ± 0.20*	2.92 ± 0.19*
Lean Body Mass, g				
Baseline	22.58 ± 0.26	22.96 ± 0.39	27.06 ± 0.46*	26.95 ± 0.78*
After Treatment	25.14 ± 0.45^{+}	23.37 ± 0.49	30.95 ± 0.52*$^{,+}$	30.70 ± 0.57*$^{,+}$
Fat Mass, g				
Baseline	8.27 ± 0.58	7.35 ± 0.56	16.30 ± 0.82*	16.37 ± 1.08*
After Treatment	14.56 ± 0.99^{+}	8.11 ± 0.98$^{\#}$	20.76 ± 0.68*$^{,+}$	21.81 ± 0.99*$^{,+}$

Data expressed as means ± SEM; WT = wild-type mice, MC4 = MC4-RKO mice, Sham = sham-operated, MI = myocardial infarction. *$p<0.05$ vs respective WT group; $^{\#}p<0.05$ vs respective Sham group; $^{+}p<0.05$ vs baseline.

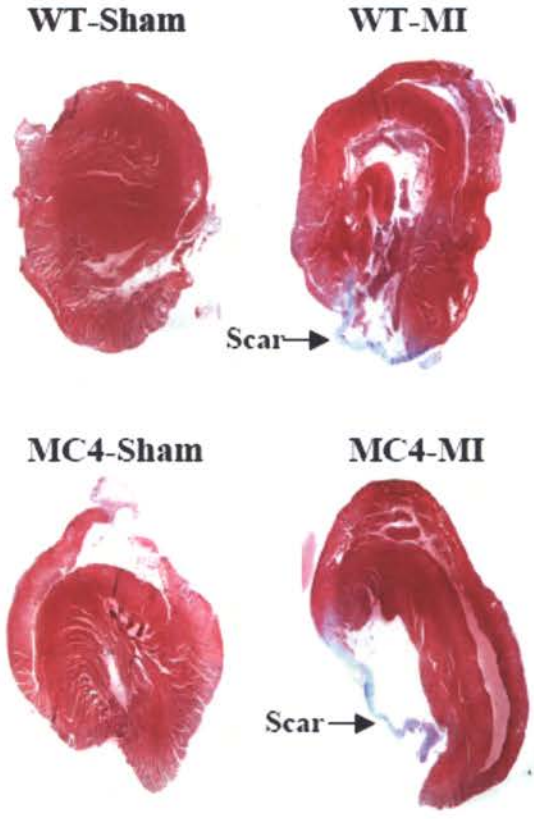

Figure 4-1. Transverse sections from the hearts of wild-type (WT; *top*) and MC4-RKO (MC4; *bottom*) mice stained with Masson's trichrome stain. Scaring of the left ventricular myocardium, as denoted by blue-green tissue staining, is evident in WT-MI and MC4-MI hearts, but absent in WT-Sham and MC4-Sham hearts.

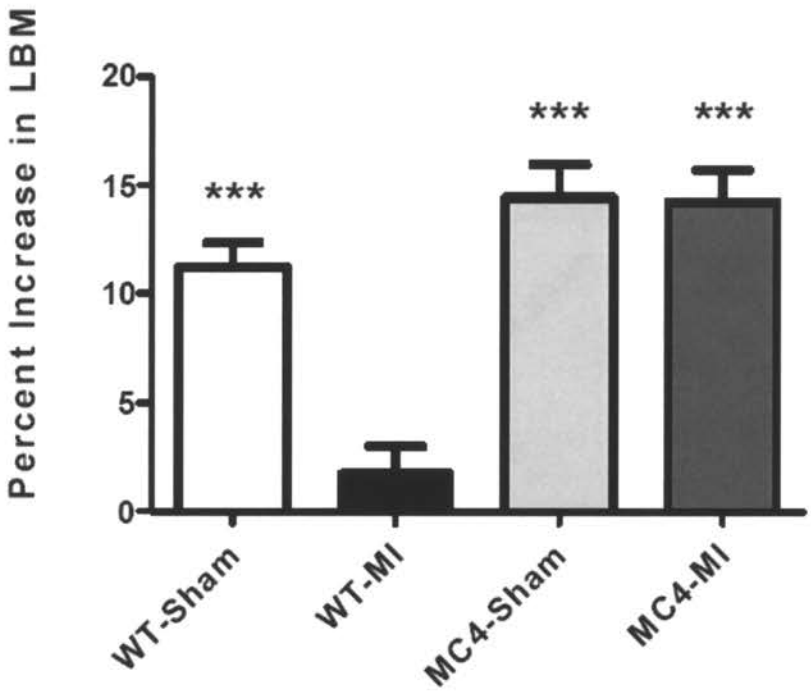

Figure 4-2. MC4-RKO mice resist cardiac cachexia and increase LBM accumulation after myocardial infarction. Data are mean ± SEM. *** $P < 0.001$ *vs* WT-MI.

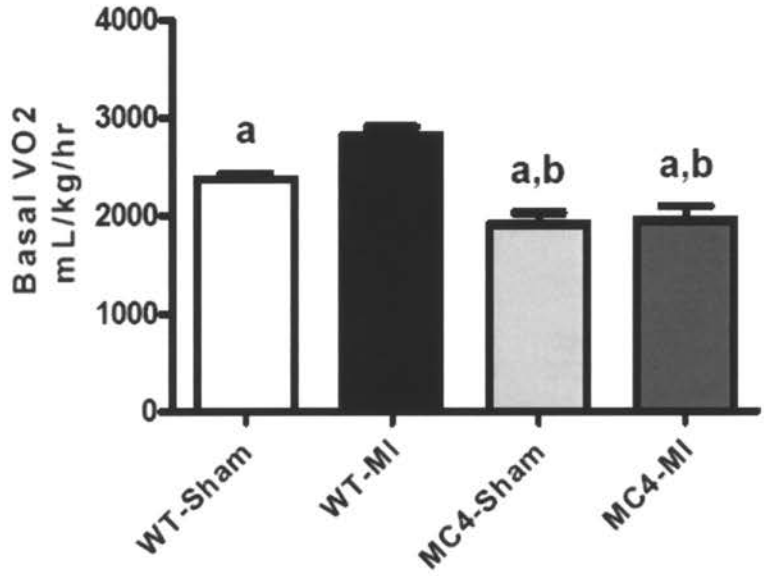

Figure 4-3. MC4-RKO resist an increase in energy expenditure in response to CHF. Basal oxygen consumption during the light phase (0900-1700) is increased in WT-MI mice (n=15) compared to WT-Sham mice (n=19). Basal oxygen consumption is not increased in MC4-MI mice (n=8) compared to MC4-Sham mice (n=10). Data are mean $\pm$ sem. $^{a}p<0.001$ vs WT-MI, $^{b}p<0.05$ vs WT-Sham.

TABLE 2. Characterization of Sham vs. Banded Rats

	Sham-aCSF	Sham-AgRP	Band-aCSF	Band-AgRP
Number	6	8	7	8
Body weight, g				
Baseline	295.0 ± 5.9	294.1 ± 3.8	264.5 ± 8.7*	268.8 ± 5.8*
After Treatment	331.3 ± 5.1†	367.5 ± 12.0†	272.8 ± 10.2*	343.3 ± 5.9*,†
Food Intake, g				
Baseline	26.12 ± 0.53	24.87 ± 0.86	18.85 ± 1.32*	20.61 ± 0.89*
During Treatment	26.73 ± 0.99	33.25 ± 2.61*,†	22.26 ± 0.69	34.64 ± 1.66*,†
Heart Weight, g	0.849 ± 0.02	0.873 ± 0.03	1.438 ± 0.02*	1.469 ± 0.08*
Kidney, g	1.321 ± 0.04	1.285± 0.04	1.049 ± 0.03*	1.230 ± 0.07*
Liver, g	12.15 ± 0.50	11.72 ± 0.53	9.07 ± 0.47*	12.48 ± 0.78*
Lean Body Mass, g				
Baseline	265.7 ± 3.35	261.0 ± 4.99	243.2 ± 7.12*	248.0 ± 5.08
After Treatment	298.6 ± 4.91†	300.4 ± 9.67†	251.2 ± 8.80*	298.9 ± 8.82*,†
Fat Mass, g				
Baseline	25.52 ± 1.18	24.30 ± 2.94	18.17 ± 1.68	17.94 ± 1.27
After Treatment	26.91 ± 1.13	58.95 ± 7.72*,†	18.46 ± 2.50	44.04 ± 3.61*,†

Data expressed as means ± SEM; Sham = sham-operated, Band = aortic banded, aCSF = i.c.v. aCSF treatment, AgRP = i.c.v. AgRP treatment. *$p<0.05$ vs respective sham group; $^{*}p<0.05$ vs respective aCSF group; $^{\dagger}p<0.05$ vs baseline.

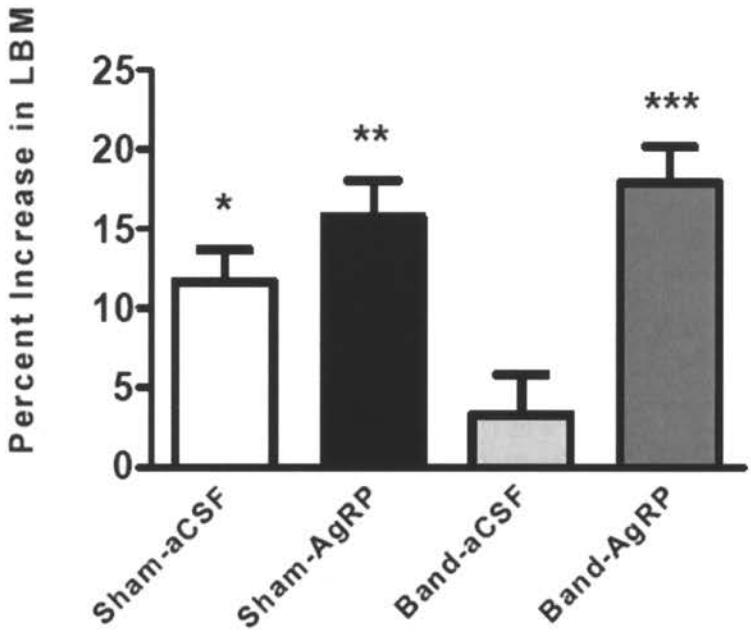

Figure 4-4. Effect of AgRP *vs* aCSF administration on the accumulation of LBM in Sham-operated and aortic-banded rats. Data are mean ± SEM. * $P < 0.05$ *vs* Band-aCSF; ** $P < 0.01$ *vs* Band-aCSF; *** $P < 0.001$ *vs* Band-aCSF.

Table 3. Hypothalamic Gene Expression (RT-PCR)

	Sham	Band	Student's *t*-Test
POMC	0.99 ± 0.16	0.94 ± 0.09	NS
AgRP	1.80 ± 0.20	1.33 ± 0.14	NS
NPY	1.26 ± 0.20	1.08 ± 0.06	NS
IL-1β	1.37 ± 0.72	3.29 ± 2.6	NS
IL-1R	1.19 ± 0.05	1.48 ± 0.22	NS
PC1	1.12 ± 0.07	1.01 ± 0.06	NS
PC2	1.20 ± 0.10	1.09 ± 0.05	NS

Data expressed as means ± SEM for avg. RQ. Sham = sham-operated. Band = aortic banded.

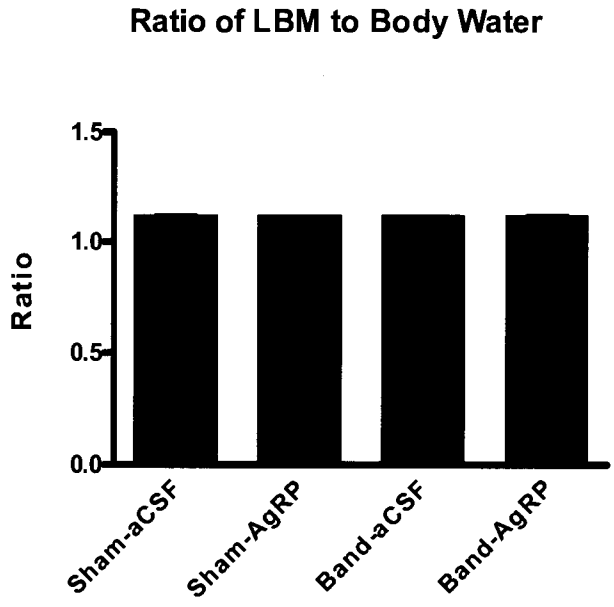

Figure 4-5. Comparison of the ratio of LBM to total body water between sham-operated and aortic-banded rats. Data are mean $\pm$ SEM.

CHAPTER 5

SUMMARY AND CONCLUSIONS

In this thesis work, our observations that IL-1β and LIF selectively activate ARC POMC neurons, but not NTS POMC neurons (Chapter 2 and Appendix), suggest that the feeding and metabolic effects of inflammatory cytokines are primarily mediated by the hypothalamic melanocortin system. These findings are similar to those reported with leptin. In the ARC, POMC mRNA expression and POMC-derived peptide synthesis is decreased with fasting and normalized with leptin replacement. In the NTS, POMC mRNA expression is also decreased with fasting. However, leptin replacement does not normalize these fasting-induced changes POMC mRNA expression in the NTS (165).

However, it is important to disclose that our experiments do not allow us to exclude a role for the brainstem melanocortin system in mediating the feeding metabolic effects of cytokines. A possible explanation for our inability to see activation of NTS POMC neurons in response to IL-1β and LIF is that these compounds were injected i.c.v. and activation might require a systemic route of administration. The NTS is a primary site of innervation by vagal afferents from the gut (346). NTS POMC neurons are directly activated by vagal afferents and activation of NTS POMC neurons by CCK occurs indirectly via activation of CCK-A expressing visceral afferents. Vagal sensory neurons also express IL-1R and LIF-R and are activated by systemic injections of IL-1β (289, 347). Indeed, differential expression of c-fos mRNA is observed between the hypothalamus and NTS in response to central and peripheral injections of IL-1β. Both routes of administration result in comparable induction of c-fos mRNA in the ARC and

PVN, whereas c-fos mRNA expression is 3-4 times greater in the NTS following a systemic injection compared to a central injection (348). Arguing against the site of injection explaining our lack of observed activation of NTS POMC neurons by cytokines are two pieces of evidence. First, neurons in the brains of vagotomized animals retain sensitivity to central injections of IL-1β (290), indicating that the absence of IL-1β-mediated vagal signaling is an unlikely explanation for our observed lack of POMC neuron activation in the NTS. Second, in an experiment conducted by a collaborating investigator, IL-1β applied to horizontal brain-slice preparations from POMC-EGFP mice that contained the solitary tract and NTS failed to activate NTS POMC-EGFP neurons (personal communication with Dr. Suzanne Appleyard). These findings support the hypothalamic melanocortin system as being the primary mediator of the feeding the metabolic effects of cytokines, including leptin, and raise the question: why would inflammatory cytokines and leptin specifically target the hypothalamic melanocortin system, but not the brainstem melanocortin system?

The potential answer to this question might be due to a key anatomical difference between the hypothalamic melanocortin system and the brainstem melanocortin system. AgRP mRNA-expressing neurons are found in the hypothalamus and most regions of the brain that contain AgRP-immunoreactive fibers also receive projections from α-MSH-immunoreactive fibers from ARC POMC neurons. However, in the brainstem there are few, if any AgRP mRNA-expressing neurons and the brainstem receives limited AgRP immunoreactive fiber projections from the ARC (134). We have demonstrated AgRP mRNA expression is increased in models of acute and chronic inflammation and that

AgRP secretion is reduced in response to IL-1β (Chapter 3). These results suggest that cytokine-mediated changes in AgRP signaling may be required to regulate the severity and duration of anorexia and hypermetabolism that are produced due to cytokine-mediated increases in α-MSH release. In contrast, cytokine-mediated increases in brainstem melanocortin signaling could be pathological in the absence of simultaneous increases in cytokine-mediated AgRP signaling.

Although the studies in this thesis were limited to studying the effects of inflammatory cytokines on the central melanocortin system, inflammatory processes result in the production of a number of additional inflammatory signaling molecules including chemokines, arachidonic acid metabolites, and nitric oxide that may also play important roles in regulating the central melancortin response to inflammation (349, 350). Indeed, our observation that ketorolac causes a small, but significant decrease in the induction of c-Fos in ARC POMC neurons in response to IL-1β (Chapter 2) indicates that prostaglandins can activate ARC POMC neurons, though the physiological relevance of this activation remains unknown. Chemokines, a family of small (8-12 kDa) proteins found in the brain and the periphery that act primarily as paracrine signaling molecules that regulate inflammatory cell recruitment and intercellular communication (350), are attractive targets for future studies. In the CNS, chemokines and their G protein-coupled receptors are constitutively expressed by microglial cells, astrocytes and neurons, and their expression is increased in response to inflammatory signals (351, 352). Expression of chemokine receptors by neurons in the hypothalamus and brainstem has been reported, though the phenotypes of the neurons that express these receptors is largely unknown

(350, 352, 353). Central injections of chemokines induce anorexia (354, 355) in rodents and mice deficient for the CCR2 chemokine receptor resist the development of obesity and insulin resistance when fed high-fat diets (356). Future studies investigating the potential interaction of these inflammatory signals with the central melanocortin system may further advance our understanding of how central melanocortin signaling is regulated during inflammatory events.

We have demonstrated that acute administration of cytokines can potently increase central melanocortin signaling (Chapter 2) and that in rodent models of chronic inflammation that AgRP mRNA expression is increased (208, 252, 254) (Chapter 3). These results, combined with an increasing number of studies demonstrating that blockade of melanocortin signaling attenuates cachexia in rodent models of chronic disease (208, 252, 254) (Chapter 4) suggest that central melanocortin signaling is increased during chronic disease. Altered secretion of α-MSH and AgRP in response to a constant cytokine stimulus could potentially account for this hypothesized increase in melanocortin signaling. However, this model would be overly simplistic and fail to account for potential perturbations that are likely induced by chronic inflammatory tone in either basal POMC or AgRP/NPY neuronal activity, or downstream signaling pathways that are engaged in by melanocortin peptides. Indeed, recent studies have demonstrated that both of these parameters are altered in response to chronic increases in leptin signaling. In response to being fed high-fat diets, mice and rats become obese and develop central leptin resistance (161, 357-359). Disruptions in signaling pathways downstream of leptin receptor binding in POMC and AgRP/NPY neurons abolish the

changes in neuropeptide expression and secretion that normally occur in response to leptin (161). Cytokine receptors engage many of the downstream signaling pathways that leptin receptors utilize (64, 360), although it remains unclear if resistance to constant signaling by inflammatory cytokines develops in a manner similar to resistance to constant leptin signaling. Although it is currently unknown if constant cytokine signaling alters signaling pathways in POMC or AgRP/NPY neurons, in the periphery cytokines have been shown to potentiate signaling pathways in sensory neurons (361, 362). Compensatory hypersensitivity of the downstream melanocortin signaling pathway have been described in leptin-induced leptin resistant rats (358) and mice with diet-induced obesity (DIO) (161). Hypersensitivity in downstream melancortin signaling in DIO mice may in part be explained by the observed increase in the expression of MC4-R mRNA in the PVN (161). In our studies, we observed that IL-1β and LIF consistently induced dense c-fos immunoreactivity in hypothalamic and hindbrain nuclei where MC4-R mRNA is expressed including the PVN, DMH, LHA, NTS and DMV. Although we investigated the effect of individual cytokines and acute and chronic inflammation the regulation of POMC mRNA and AgRP mRNA, we did not extend these studies to investigating potential changes that these inflammatory paradigms might have had on MC4-R mRNA expression. Future studies investigating the effect of chronic inflammation on the basal activity of POMC and AgRP/NPY neurons, and the downstream signaling pathways that are engaged in by melanocortin peptides will help to further elucidate the response of the central melanocortin system to pathophysiological conditions.

Using double-label ISH, we have shown in this thesis work that POMC and AgRP neurons in the ARC co-express IL-1R and LIF-R (Chapter 2,3 and Appendix) suggesting that these neurons may be direct targets for the actions of IL-1β and LIF. However, despite the demonstrated expression of these receptors in the NTS (87, 363), our inability to reliably label NTS POMC neurons with a non-radioactive digoxigenin-labeled (DIG) riboprobe meant that we were unable to conclusively determine if NTS POMC neurons co-expressed either IL-1R, or LIF-R. In rare instances, we were able to successfully label NTS POMC neurons with a DIG riboprobe, but this labeling was never consistent enough to conduct a formal double-label ISH assay. The low sensitivity of non-radioactive riboprobes remains a critical shortcoming of this powerful experimental technique and continues to hinder our ability to characterize systems of interest. The continued disagreement concerning the regulation of NTS POMC neurons by leptin is a particularly relevant example. Ten years after the seminal paper by Cheung et. al. was published demonstrating that ARC POMC neurons co-express leptin receptors (154) we still don't know if NTS POMC neurons also co-express leptin receptors due to the inability to detect these neurons with non-radioactive probes. Activational studies in POMC-EGFP mice have failed to add clarity to this issue as conflicting reports of activation (167), or absence of activation (164) of NTS POMC neurons in response to leptin have been made. In the absence of leptin receptor co-expression data the effect of leptin on these neurons remains uncertain. Barring a significant advancement in the sensitivity of assays that rely upon the use of non-radioactive labeled riboprobes to label neurons, our ability to fully characterize neural systems, including the central melanocortin system, will require the development of new techniques to detect, or label cells expressing low abundance mRNA

transcripts. The increasing use and availability of transgenic animals that express flourescent proteins under the control of a known target gene promoter may facilitate new methods to perform co-expression assays. Microarray analysis of transcripts purified from mostly pure pools of fluorescent cells using automated flow cytometry and cell sorting (FACS) machines, or single-cell laser capture microdissection could identify co-expressed transcripts in a more rapid and cost-effective manner than traditional double-label ISH. Although these assays would have their own limitations including contamination by non-targeted cells and a loss of spatial resolution for heterogeneous populations of cells like ARC POMC and AgRP/NPY neurons, they nonetheless could represent a long overdue advancement in our ability to perform co-expression assays.

Our studies demonstrated that genetic (MC4-RKO mice) and pharmacologic (i.c.v. AgRP) blockade of central melanocortin signaling attenuated cardiac cachexia in rodent models of CHF. These studies suggest that increased central melanocortin signaling likely plays a role in the pathogenesis of cardiac cachexia and that compounds that inhibit central melanocortin signaling may have important pharmacotherapeutic benefit for cachectic CHF patients. Complications that may limit the use of compounds that antagonize melanocortin signaling to treat cardiac cachexia are the potential for these compounds to inhibit the normal anti-inflammatory role of melanocortins in the periphery and the demonstrated ability of melanocortin receptor antagonists to increase adiposity.

RT-PCR and western blotting have demonstrated that peripheral macrophages express MC3-R (364). Activation of MC3-R on macrophages by α-MSH inhibits macrophage

migration and suppresses their synthesis and release of cytokine and chemokines (365). Damage to the myocardium stimulates the infiltration of macrophages into the cardiac tissue and these macrophages are thought to be the primary source of the high levels of TNF-α measured in the myocardium of patients and animals with CHF (366, 367). Inhibition of macrophages in the heart by melanocortin peptides may play a key role in limiting myocardial damage as studies in mice and rats have demonstrated their ability to significantly reduce both heart ischemia/reperfusion injury (264) and size of the ischemic area induced by permanent coronary occlusion (368). The cardioprotective properties of melancortin peptides are likely mediated by the MC3-R and not MC4-R as the protective effects in mice are prevented by SHU9119, but not by the MC4-R selective anatagonist HS204 (264). Combined with previous studies demonstrating that blockade of central MC3-R signaling promotes increased anorexia and wasting in response to inflammation (207), these results further support the use of MC4-R specific antagonists for the treatment of cardiac cachexia.

Increased adiposity is recognized as an independent risk factor for cardiovascular disease (341, 342). Therefore, therapeutics that lead to increases in the adiposity of CHF patients could have the undesired effect of increasing the patients' risk for suffering additional cardiovascular events. Single injections of AgRP and specific MC4-R antagonists induce hyperphagia in rodents whereas repeated injections of AgRP causes obesity (206, 340). Our studies have shown that repeated AgRP injections also induce hyperphagia and increased adiposity in rats with CHF (Chapter 4). In our experiments, we administered 1.0 nmol doses of AgRP every other day (Chapter 4). However, increased food intake in

rats has been shown to persist for an entire week after a single third ventricular injection of AgRP (302). The possibility exists that by using a lower dose of AgRP and/or by giving fewer AgRP injections we might have been able to increase LBM without the simultaneous increase in adiposity. Surprisingly though, the ability of AgRP and potential therapeutic compounds with AgRP-like properties to increase both fat mass and LBM accumulation may actually prove beneficial to cardiac cachexia patients. Recent studies have shown that an inverse relationship exists between BMI and decreased mortality in CHF patients (343, 369). This inverse relationship, or "obesity paradox" extends beyond BMI as high levels of low-density lipoprotein and total cholesterol have also been associated with a survival advantage in CHF patients (370). Mechanistically, it is hypothesized that higher serum cholesterol and lipoprotein levels are beneficial to CHF patients by decreasing inflammation. Lipoproteins serve as effective scavengers that bind and neutralize bacterial endotoxins, including LPS, that are increased in the serum of CHF patients due to elevated pressure from increased bowel wall edema that develops in these patients (328, 370, 371). Although we have demonstrated that the central melanocortin system is responsive to peripheral injections of LPS, it is currently unknown if the increased circulating levels of LPS found in CHF patients are sufficient to drive increased central melanocortin signaling. Cumulatively, the available data suggests that blockade of central melanocortin signaling with therapeutics that specifically antagonize MC4-R signaling may be effective for the treatment of human patients with cardiac cachexia.

In summary, experiments conducted during the course of this thesis work have demonstrated that the central melanocortin system is a target for inflammatory cytokines. We have shown that inflammatory cytokines can regulate signaling of the hypothalamic melancortin system and that cytokine-mediated changes in melanocortin signaling likely play a key role in the development of anorexia and metabolic dysregulation in response to acute and chronic pathophysiological conditions (Figure 5-1). We have shown that pharmacologic blockade of central melanocortin signaling may have important therapeutic benefit for treatment of cachectic CHF patients. Collectively, these studies have provided strong experimental data in support of the hypothesis that the central melanocortin system plays a key role in both integrating and mediating the feeding and metabolic effects of inflammatory cytokines.

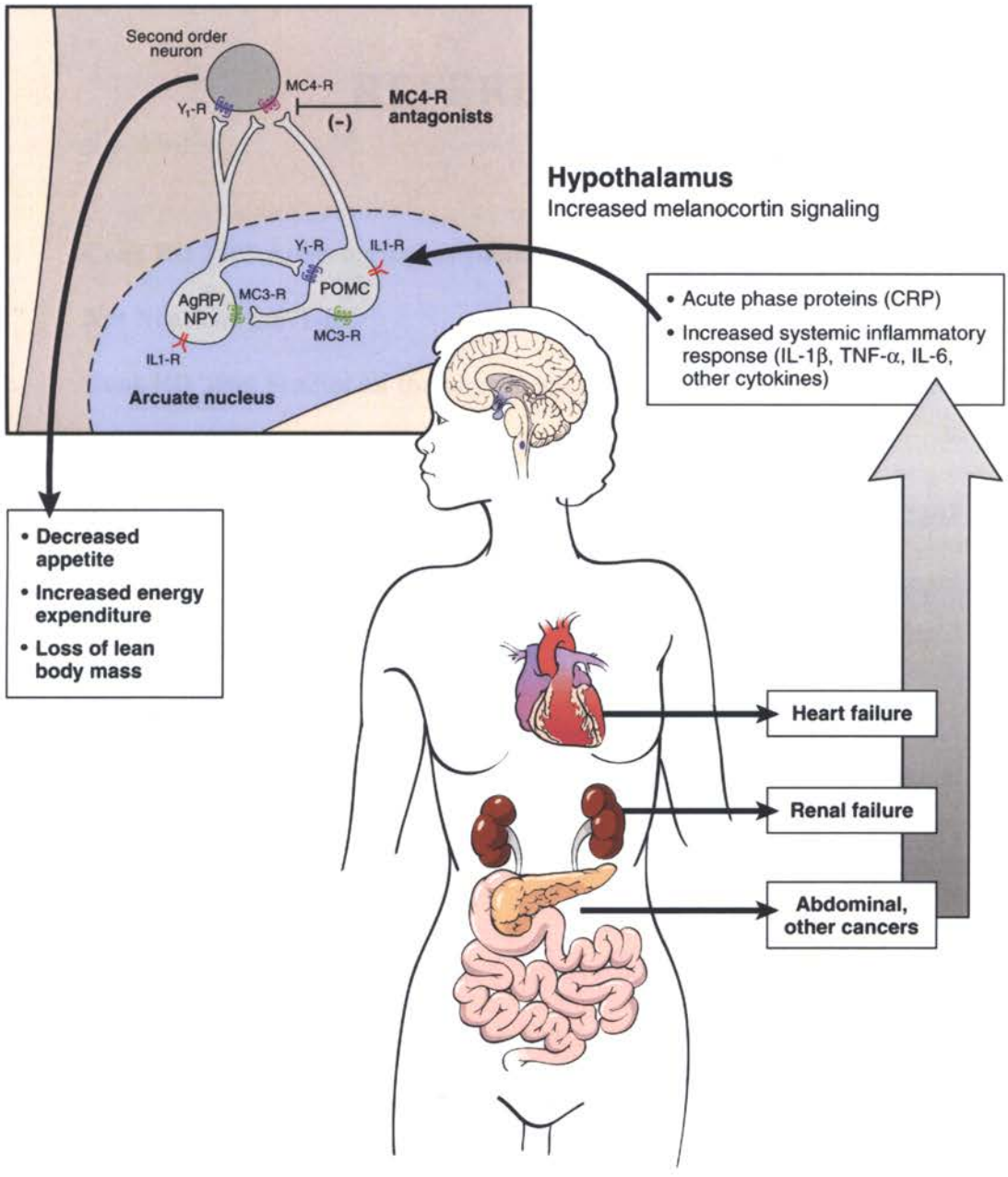

Figure 5-1. Theoretical model for the role of the central melanocortin system in illness-induced anorexia and cachexia of chronic disease.

REFERENCES

1. Cone RD 2005 Anatomy and regulation of the central melanocortin system. Nat Neurosci 8:571-8
2. Cone RD 2006 Studies on the physiological functions of the melanocortin system. Endocr Rev 27:736-49
3. Farooqi IS, Keogh JM, Yeo GS, Lank EJ, Cheetham T, O'Rahilly S 2003 Clinical spectrum of obesity and mutations in the melanocortin 4 receptor gene. N Engl J Med 348:1085-95
4. Tisdale MJ 1997 Biology of cachexia. J Natl Cancer Inst 89:1763-73
5. Barber MD, Ross JA, Fearon KC 1999 Changes in nutritional, functional, and inflammatory markers in advanced pancreatic cancer. Nutr Cancer 35:106-10
6. Gelin J, Moldawer LL, Lonnroth C, Sherry B, Chizzonite R, Lundholm K 1991 Role of endogenous tumor necrosis factor alpha and interleukin 1 for experimental tumor growth and the development of cancer cachexia. Cancer Res 51:415-21
7. Plata-Salaman CR 1991 Immunoregulators in the nervous system. Neurosci Biobehav Rev 15:185-215
8. Hart BL 1988 Biological basis of the behavior of sick animals. Neurosci Biobehav Rev 12:123-37

9. Ahima RS, Prabakaran D, Mantzoros C, Qu D, Lowell B, Maratos-Flier E, Flier JS 1996 Role of leptin in the neuroendocrine response to fasting. Nature 382:250-2

10. Konsman JP, Dantzer R 2001 How the immune and nervous systems interact during disease-associated anorexia. Nutrition 17:664-8

11. Romijn JA 2000 Substrate metabolism in the metabolic response to injury. Proc Nutr Soc 59:447-9

12. Dantzer R 2004 Cytokine-induced sickness behaviour: a neuroimmune response to activation of innate immunity. Eur J Pharmacol 500:399-411

13. Aubert A, Goodall G, Dantzer R 1995 Compared effects of cold ambient temperature and cytokines on macronutrient intake in rats. Physiol Behav 57:869-73

14. Aubert A, Vega C, Dantzer R, Goodall G 1995 Pyrogens specifically disrupt the acquisition of a task involving cognitive processing in the rat. Brain Behav Immun 9:129-48

15. Fantuzzi G, Faggioni R 2000 Leptin in the regulation of immunity, inflammation, and hematopoiesis. J Leukoc Biol 68:437-46

16. Bazar KA, Yun AJ, Lee PY 2005 "Starve a fever and feed a cold": feeding and anorexia may be adaptive behavioral modulators of autonomic and T helper balance. Med Hypotheses 64:1080-4

17. Morley JE, Thomas DR, Wilson MM 2006 Cachexia: pathophysiology and clinical relevance. Am J Clin Nutr 83:735-43

18. Laviano A, Meguid MM, Inui A, Muscaritoli M, Rossi-Fanelli F 2005 Therapy insight: Cancer anorexia-cachexia syndrome--when all you can eat is yourself. Nat Clin Pract Oncol 2:158-65

19. Tisdale MJ 2002 Cachexia in cancer patients. Nat Rev Cancer 2:862-71

20. Thomas DR 2002 Distinguishing starvation from cachexia. Clin Geriatr Med 18:883-91

21. Barber MD, Fearon KC, Delmore G, Loprinzi CL 1998 Should cancer patients with incurable disease receive parenteral or enteral nutritional support? Eur J Cancer 34:279-85

22. Bruera E 1997 ABC of palliative care. Anorexia, cachexia, and nutrition. Bmj 315:1219-22

23. Della Cuna GR, Pellegrini A, Piazzi M 1989 Effect of methylprednisolone sodium succinate on quality of life in preterminal cancer patients: a placebo-controlled, multicenter study. The Methylprednisolone Preterminal Cancer Study Group. Eur J Cancer Clin Oncol 25:1817-21

24. Moertel CG, Schutt AJ, Reitemeier RJ, Hahn RG 1974 Corticosteroid therapy of preterminal gastrointestinal cancer. Cancer 33:1607-9

25. Loprinzi CL, Schaid DJ, Dose AM, Burnham NL, Jensen MD 1993 Body-composition changes in patients who gain weight while receiving megestrol acetate. J Clin Oncol 11:152-4

26. Von Roenn JH, Armstrong D, Kotler DP, Cohn DL, Klimas NG, Tchekmedyian NS, Cone L, Brennan PJ, Weitzman SA 1994 Megestrol acetate in patients with AIDS-related cachexia. Ann Intern Med 121:393-9

27. Anker SD, Chua TP, Ponikowski P, Harrington D, Swan JW, Kox WJ, Poole-Wilson PA, Coats AJ 1997 Hormonal changes and catabolic/anabolic imbalance in chronic heart failure and their importance for cardiac cachexia. Circulation 96:526-34

28. Levine B, Kalman J, Mayer L, Fillit HM, Packer M 1990 Elevated circulating levels of tumor necrosis factor in severe chronic heart failure. N Engl J Med 323:236-41

29. Deans C, Wigmore SJ 2005 Systemic inflammation, cachexia and prognosis in patients with cancer. Curr Opin Clin Nutr Metab Care 8:265-9

30. Scott HR, McMillan DC, Crilly A, McArdle CS, Milroy R 1996 The relationship between weight loss and interleukin 6 in non-small-cell lung cancer. Br J Cancer 73:1560-2

31. Sonti G, Ilyin SE, Plata-Salaman CR 1996 Anorexia induced by cytokine interactions at pathophysiological concentrations. Am J Physiol 270:R1394-402

32. Plata-Salaman CR 1996 Anorexia induced by activators of the signal transducer gp 130. Neuroreport 7:841-4

33. Glass DJ 2003 Signalling pathways that mediate skeletal muscle hypertrophy and atrophy. Nat Cell Biol 5:87-90

34. Langen RC, Schols AM, Kelders MC, Wouters EF, Janssen-Heininger YM 2001 Inflammatory cytokines inhibit myogenic differentiation through activation of nuclear factor-kappaB. Faseb J 15:1169-80

35. Cai D, Frantz JD, Tawa NE, Jr., Melendez PA, Oh BC, Lidov HG, Hasselgren PO, Frontera WR, Lee J, Glass DJ, Shoelson SE 2004 IKKbeta/NF-kappaB activation causes severe muscle wasting in mice. Cell 119:285-98

36. Guttridge DC, Mayo MW, Madrid LV, Wang CY, Baldwin AS, Jr. 2000 NF-kappaB-induced loss of MyoD messenger RNA: possible role in muscle decay and cachexia. Science 289:2363-6

37. Stellar E 1994 The physiology of motivation. 1954. Psychol Rev 101:301-11

38. Elmquist JK, Elias CF, Saper CB 1999 From lesions to leptin: hypothalamic control of food intake and body weight. Neuron 22:221-32

39. Hervey GR 1957 Hypothalamic lesion in parabiotic rats. J. Physiol. 138:15-16P

40. Hervey GR 1959 The effects of lesions in the hypothalamus in parabiotic rats. J Physiol 145:336-52

41. Peruzzo B, Pastor FE, Blazquez JL, Schobitz K, Pelaez B, Amat P, Rodriguez EM 2000 A second look at the barriers of the medial basal hypothalamus. Exp Brain Res 132:10-26

42. Cone RD, Cowley MA, Butler AA, Fan W, Marks DL, Low MJ 2001 The arcuate nucleus as a conduit for diverse signals relevant to energy homeostasis. Int J Obes Relat Metab Disord 25 Suppl 5:S63-7

43. Hetherington AW, Ranson SW 1940 Hypothalamic lesions and adiposity in the rat. Anat. Rec. 78:149-172

44. Broberger C, Johansen J, Johansson C, Schalling M, Hokfelt T 1998 The neuropeptide Y/agouti gene-related protein (AGRP) brain circuitry in normal, anorectic, and monosodium glutamate-treated mice. Proc Natl Acad Sci U S A 95:15043-8

45. Jacobowitz DM, O'Donohue TL 1978 alpha-Melanocyte stimulating hormone: immunohistochemical identification and mapping in neurons of rat brain. Proc Natl Acad Sci U S A 75:6300-4

46. Kennedy GC 1953 The role of depot fat in the hypothalamic control of food intake in the rat. Proc R Soc Lond B Biol Sci 140:578-96

47. Coleman DL 1973 Effects of parabiosis of obese with diabetes and normal mice. Diabetologia 9:294-8

48. Coleman DL, Hummel KP 1969 Effects of parabiosis of normal with genetically diabetic mice. Am J Physiol 217:1298-304

49. Zhang Y, Proenca R, Maffei M, Barone M, Leopold L, Friedman JM 1994 Positional cloning of the mouse obese gene and its human homologue. Nature 372:425-32

50. Tartaglia LA, Dembski M, Weng X, Deng N, Culpepper J, Devos R, Richards GJ, Campfield LA, Clark FT, Deeds J, Muir C, Sanker S, Moriarty A, Moore KJ, Smutko JS, Mays GG, Wool EA, Monroe CA, Tepper RI 1995 Identification and expression cloning of a leptin receptor, OB-R. Cell 83:1263-71

51. Grill HJ, Kaplan JM 1992 Sham feeding in intact and chronic decerebrate rats. Am J Physiol 262:R1070-4

52. Norgren R 1978 Projections from the nucleus of the solitary tract in the rat. Neuroscience 3:207-18

53. Seeley RJ, Grill HJ, Kaplan JM 1994 Neurological dissociation of gastrointestinal and metabolic contributions to meal size control. Behav Neurosci 108:347-52

54. Miselis RR, Hyde TM, Shapiro RE 1984 Area postrema and adjacent solitary nucleus in water and energy balance. Fed Proc 43:2969-71

55. Shapiro RE, Miselis RR 1985 The central neural connections of the area postrema of the rat. J Comp Neurol 234:344-64

56. Harfstrand A, Fuxe K, Terenius L, Kalia M 1987 Neuropeptide Y-immunoreactive perikarya and nerve terminals in the rat medulla oblongata: relationship to cytoarchitecture and catecholaminergic cell groups. J Comp Neurol 260:20-35

57. Jin SL, Han VK, Simmons JG, Towle AC, Lauder JM, Lund PK 1988 Distribution of glucagonlike peptide I (GLP-I), glucagon, and glicentin in the rat brain: an immunocytochemical study. J Comp Neurol 271:519-32

58. Thomson A 1991 The Cytokine Handbook. Academic Press, London

59. Gass GH, Kaplan HM 1996 Handbook of Endocrinology. CRC Press, Boca Raton

60. Johnson RW, Arkins S, Dantzer R, Kelley KW 1997 Hormones, lymphohemopoietic cytokines and the neuroimmune axis. Comp Biochem Physiol A Physiol 116:183-201

61. Montgomery DW, LeFevre JA, Ulrich ED, Adamson CR, Zukoski CF 1990 Identification of prolactin-like proteins synthesized by normal murine lymphocytes. Endocrinology 127:2601-3

62. Smith EM, Blalock JE 1981 Human lymphocyte production of corticotropin and endorphin-like substances: association with leukocyte interferon. Proc Natl Acad Sci U S A 78:7530-4

63. Bajetto A, Bonavia R, Barbero S, Schettini G 2002 Characterization of chemokines and their receptors in the central nervous system: physiopathological implications. J Neurochem 82:1311-29

64. Chesnokova V, Melmed S 2002 Minireview: Neuro-immuno-endocrine modulation of the hypothalamic-pituitary-adrenal (HPA) axis by gp130 signaling molecules. Endocrinology 143:1571-4

65. Hopkins SJ 2007 Central nervous system recognition of peripheral inflammation: a neural, hormonal collaboration. Acta Biomed 78 Suppl 1:231-47

66. Kapsimalis F, Richardson G, Opp MR, Kryger M 2005 Cytokines and normal sleep. Curr Opin Pulm Med 11:481-4

67. Opp MR, Krueger JM 1994 Interleukin-1 is involved in responses to sleep deprivation in the rabbit. Brain Res 639:57-65

68. Chida D, Osaka T, Hashimoto O, Iwakura Y 2006 Combined interleukin-6 and interleukin-1 deficiency causes obesity in young mice. Diabetes 55:971-7

69. Garcia MC, Wernstedt I, Berndtsson A, Enge M, Bell M, Hultgren O, Horn M, Ahren B, Enerback S, Ohlsson C, Wallenius V, Jansson JO 2006 Mature-onset obesity in interleukin-1 receptor I knockout mice. Diabetes 55:1205-13

70. Somm E, Henrichot E, Pernin A, Juge-Aubry CE, Muzzin P, Dayer JM, Nicklin MJ, Meier CA 2005 Decreased fat mass in interleukin-1 receptor antagonist-deficient mice: impact on adipogenesis, food intake, and energy expenditure. Diabetes 54:3503-9

71. Wallenius V, Wallenius K, Ahren B, Rudling M, Carlsten H, Dickson SL, Ohlsson C, Jansson JO 2002 Interleukin-6-deficient mice develop mature-onset obesity. Nat Med 8:75-9

72. Dinarello CA 1991 The proinflammatory cytokines interleukin-1 and tumor necrosis factor and treatment of the septic shock syndrome. J Infect Dis 163:1177-84

73. Turrin NP, Plata-Salaman CR 2000 Cytokine-cytokine interactions and the brain. Brain Res Bull 51:3-9

74. Rothwell NJ 1991 Functions and mechanisms of interleukin 1 in the brain. Trends Pharmacol Sci 12:430-6

75. Rothwell NJ, Luheshi GN 2000 Interleukin 1 in the brain: biology, pathology and therapeutic target. Trends Neurosci 23:618-25

76. Webb AC, Collins KL, Auron PE, Eddy RL, Nakai H, Byers MG, Haley LL, Henry WM, Shows TB 1986 Interleukin-1 gene (IL1) assigned to long arm of human chromosome 2. Lymphokine Res 5:77-85

77. Hirsch E, Irikura VM, Paul SM, Hirsh D 1996 Functions of interleukin 1 receptor antagonist in gene knockout and overproducing mice. Proc Natl Acad Sci U S A 93:11008-13

78. Thornberry NA, Molineaux SM 1995 Interleukin-1 beta converting enzyme: a novel cysteine protease required for IL-1 beta production and implicated in programmed cell death. Protein Sci 4:3-12

79. Vitkovic L, Bockaert J, Jacque C 2000 "Inflammatory" cytokines: neuromodulators in normal brain? J Neurochem 74:457-71

80. Giulian D, Tapscott MJ 1988 Immunoregulation of cells within the central nervous system. Brain Behav Immun 2:352-8

81. Higgins GA, Olschowka JA 1991 Induction of interleukin-1 beta mRNA in adult rat brain. Brain Res Mol Brain Res 9:143-8

82. Stalder AK, Campbell IL 1994 Simultaneous analysis of multiple cytokine receptor mRNAs by RNase protection assay in LPS-induced endotoxemia. Lymphokine Cytokine Res 13:107-12

83. Turrin NP, Ilyin SE, Gayle DA, Plata-Salaman CR, Ramos EJ, Laviano A, Das UN, Inui A, Meguid MM 2004 Interleukin-1beta system in anorectic catabolic tumor-bearing rats. Curr Opin Clin Nutr Metab Care 7:419-26

84. Boraschi D, Tagliabue A 2006 The interleukin-1 receptor family. Vitam Horm 74:229-54

85. Sims JE, March CJ, Cosman D, Widmer MB, MacDonald HR, McMahan CJ, Grubin CE, Wignall JM, Jackson JL, Call SM, et al. 1988 cDNA

expression cloning of the IL-1 receptor, a member of the immunoglobulin superfamily. Science 241:585-9

86. Korherr C, Hofmeister R, Wesche H, Falk W 1997 A critical role for interleukin-1 receptor accessory protein in interleukin-1 signaling. Eur J Immunol 27:262-7

87. Ericsson A, Liu C, Hart RP, Sawchenko PE 1995 Type 1 interleukin-1 receptor in the rat brain: distribution, regulation, and relationship to sites of IL-1-induced cellular activation. J Comp Neurol 361:681-98

88. Parnet P, Kelley KW, Bluthe RM, Dantzer R 2002 Expression and regulation of interleukin-1 receptors in the brain. Role in cytokines-induced sickness behavior. J Neuroimmunol 125:5-14

89. Ilyin SE, Gayle D, Flynn MC, Plata-Salaman CR 1998 Interleukin-1beta system (ligand, receptor type I, receptor accessory protein and receptor antagonist), TNF-alpha, TGF-beta1 and neuropeptide Y mRNAs in specific brain regions during bacterial LPS-induced anorexia. Brain Res Bull 45:507-15

90. Gayle D, Ilyin SE, Plata-Salaman CR 1997 Central nervous system IL-1 beta system and neuropeptide Y mRNAs during IL-1 beta-induced anorexia in rats. Brain Res Bull 44:311-7

91. Kluger MJ 1991 Fever: role of pyrogens and cryogens. Physiol Rev 71:93-127

92. Hori T, Shibata M, Nakashima T, Yamasaki M, Asami A, Asami T, Koga H 1988 Effects of interleukin-1 and arachidonate on the preoptic and anterior hypothalamic neurons. Brain Res Bull 20:75-82

93. Li S, Ballou LR, Morham SG, Blatteis CM 2001 Cyclooxygenase-2 mediates the febrile response of mice to interleukin-1beta. Brain Res 910:163-73

94. Katsuura G, Gottschall PE, Dahl RR, Arimura A 1988 Adrenocorticotropin release induced by intracerebroventricular injection of recombinant human interleukin-1 in rats: possible involvement of prostaglandin. Endocrinology 122:1773-9

95. Dantzer R 2001 Cytokine-induced sickness behavior: where do we stand? Brain Behav Immun 15:7-24

96. Kent S, Bluthe RM, Dantzer R, Hardwick AJ, Kelley KW, Rothwell NJ, Vannice JL 1992 Different receptor mechanisms mediate the pyrogenic and behavioral effects of interleukin 1. Proc Natl Acad Sci U S A 89:9117-20

97. Shimizu H, Uehara Y, Shimomura Y, Kobayashi I 1991 Central administration of ibuprofen failed to block the anorexia induced by interleukin-1. Eur J Pharmacol 195:281-4

98. Shimomura Y, Inukai T, Kuwabara S, Shimizu H, Takahashi M, Sato N, Uehara Y, Tanaka Y, Kobayashi I 1992 Both cyclooxygenase and lipoxygenase inhibitor partially restore the anorexia by interleukin-1 beta. Life Sci 51:1419-26

99. Herkenham M, Lee HY, Baker RA 1998 Temporal and spatial patterns of c-fos mRNA induced by intravenous interleukin-1: a cascade of non-neuronal cellular activation at the blood-brain barrier. J Comp Neurol 400:175-96

100. Reyes TM, Sawchenko PE 2002 Involvement of the arcuate nucleus of the hypothalamus in interleukin-1-induced anorexia. J Neurosci 22:5091-9

101. Luheshi GN, Gardner JD, Rushforth DA, Loudon AS, Rothwell NJ 1999 Leptin actions on food intake and body temperature are mediated by IL-1. Proc Natl Acad Sci U S A 96:7047-52

102. Campfield LA, Smith FJ, Guisez Y, Devos R, Burn P 1995 Recombinant mouse OB protein: evidence for a peripheral signal linking adiposity and central neural networks. Science 269:546-9

103. Pelleymounter MA, Cullen MJ, Baker MB, Hecht R, Winters D, Boone T, Collins F 1995 Effects of the obese gene product on body weight regulation in ob/ob mice. Science 269:540-3

104. Montague CT, Farooqi IS, Whitehead JP, Soos MA, Rau H, Wareham NJ, Sewter CP, Digby JE, Mohammed SN, Hurst JA, Cheetham CH, Earley AR, Barnett AH, Prins JB, O'Rahilly S 1997 Congenital leptin deficiency is associated with severe early-onset obesity in humans. Nature 387:903-8

105. Farooqi IS, Matarese G, Lord GM, Keogh JM, Lawrence E, Agwu C, Sanna V, Jebb SA, Perna F, Fontana S, Lechler RI, DePaoli AM, O'Rahilly S 2002 Beneficial effects of leptin on obesity, T cell hyporesponsiveness, and neuroendocrine/metabolic dysfunction of human congenital leptin deficiency. J Clin Invest 110:1093-103

106. Chen H, Charlat O, Tartaglia LA, Woolf EA, Weng X, Ellis SJ, Lakey ND, Culpepper J, Moore KJ, Breitbart RE, Duyk GM, Tepper RI, Morgenstern JP 1996 Evidence that the diabetes gene encodes the leptin receptor: identification of a mutation in the leptin receptor gene in db/db mice. Cell 84:491-5

107. Lee GH, Proenca R, Montez JM, Carroll KM, Darvishzadeh JG, Lee JI, Friedman JM 1996 Abnormal splicing of the leptin receptor in diabetic mice. Nature 379:632-5

108. Fei H, Okano HJ, Li C, Lee GH, Zhao C, Darnell R, Friedman JM 1997 Anatomic localization of alternatively spliced leptin receptors (Ob-R) in mouse brain and other tissues. Proc Natl Acad Sci U S A 94:7001-5

109. Guan XM, Hess JF, Yu H, Hey PJ, van der Ploeg LH 1997 Differential expression of mRNA for leptin receptor isoforms in the rat brain. Mol Cell Endocrinol 133:1-7

110. Mercer JG, Moar KM, Hoggard N 1998 Localization of leptin receptor (Ob-R) messenger ribonucleic acid in the rodent hindbrain. Endocrinology 139:29-34

111. Schwartz MW, Seeley RJ, Campfield LA, Burn P, Baskin DG 1996 Identification of targets of leptin action in rat hypothalamus. J Clin Invest 98:1101-6

112. Burguera B, Couce ME, Long J, Lamsam J, Laakso K, Jensen MD, Parisi JE, Lloyd RV 2000 The long form of the leptin receptor (OB-Rb) is widely expressed in the human brain. Neuroendocrinology 71:187-95

113. Clement K, Vaisse C, Lahlou N, Cabrol S, Pelloux V, Cassuto D, Gourmelen M, Dina C, Chambaz J, Lacorte JM, Basdevant A, Bougneres P, Lebouc Y, Froguel P, Guy-Grand B 1998 A mutation in the human leptin receptor gene causes obesity and pituitary dysfunction. Nature 392:398-401

114. Jackson IJ, Budd P, Horn JM, Johnson R, Raymond S, Steel K 1994 Genetics and molecular biology of mouse pigmentation. Pigment Cell Res 7:73-80

115. Geschwind, II, Huseby RA, Nishioka R 1972 The effect of melanocyte-stimulating hormone on coat color in the mouse. Recent Prog Horm Res 28:91-130

116. Lamoreux ML, Mayer TC 1975 Site of gene action in the development of hair pigment in recessive yellow (e/e) mice. Dev Biol 46:160-6

117. Duhl DM, Stevens ME, Vrieling H, Saxon PJ, Miller MW, Epstein CJ, Barsh GS 1994 Pleiotropic effects of the mouse lethal yellow (Ay) mutation explained by deletion of a maternally expressed gene and the simultaneous production of agouti fusion RNAs. Development 120:1695-708

118. Yen TT, Gill AM, Frigeri LG, Barsh GS, Wolff GL 1994 Obesity, diabetes, and neoplasia in yellow A(vy)/- mice: ectopic expression of the agouti gene. Faseb J 8:479-88

119. Robbins LS, Nadeau JH, Johnson KR, Kelly MA, Roselli-Rehfuss L, Baack E, Mountjoy KG, Cone RD 1993 Pigmentation phenotypes of variant extension locus alleles result from point mutations that alter MSH receptor function. Cell 72:827-34

120. Lu D, Vage DI, Cone RD 1998 A ligand-mimetic model for constitutive activation of the melanocortin-1 receptor. Mol Endocrinol 12:592-604

121. Bultman SJ, Michaud EJ, Woychik RP 1992 Molecular characterization of the mouse agouti locus. Cell 71:1195-204

122. Miller MW, Duhl DM, Vrieling H, Cordes SP, Ollmann MM, Winkes BM, Barsh GS 1993 Cloning of the mouse agouti gene predicts a secreted protein ubiquitously expressed in mice carrying the lethal yellow mutation. Genes Dev 7:454-67

123. Lu D, Willard D, Patel IR, Kadwell S, Overton L, Kost T, Luther M, Chen W, Woychik RP, Wilkison WO, et al. 1994 Agouti protein is an antagonist of the melanocyte-stimulating-hormone receptor. Nature 371:799-802

124. Magenis RE, Smith L, Nadeau JH, Johnson KR, Mountjoy KG, Cone RD 1994 Mapping of the ACTH, MSH, and neural (MC3 and MC4) melanocortin receptors in the mouse and human. Mamm Genome 5:503-8

125. Mountjoy KG, Mortrud MT, Low MJ, Simerly RB, Cone RD 1994 Localization of the melanocortin-4 receptor (MC4-R) in neuroendocrine and autonomic control circuits in the brain. Mol Endocrinol 8:1298-308

126. Bertagna X 1994 Proopiomelanocortin-derived peptides. Endocrinol Metab Clin North Am 23:467-85

127. Benjannet S, Rondeau N, Day R, Chretien M, Seidah NG 1991 PC1 and PC2 are proprotein convertases capable of cleaving proopiomelanocortin at distinct pairs of basic residues. Proc Natl Acad Sci U S A 88:3564-8

128. Cone RD 1999 The Central Melanocortin System and Energy Homeostasis. Trends Endocrinol Metab 10:211-216

129. Bronstein DM, Schafer MK, Watson SJ, Akil H 1992 Evidence that beta-endorphin is synthesized in cells in the nucleus tractus solitarius: detection of POMC mRNA. Brain Res 587:269-75

130. Ollmann MM, Wilson BD, Yang YK, Kerns JA, Chen Y, Gantz I, Barsh GS 1997 Antagonism of central melanocortin receptors in vitro and in vivo by agouti-related protein. Science 278:135-8

131. Backberg M, Collin M, Ovesjo ML, Meister B 2003 Chemical coding of GABA(B) receptor-immunoreactive neurones in hypothalamic regions regulating body weight. J Neuroendocrinol 15:1-14

132. Hahn TM, Breininger JF, Baskin DG, Schwartz MW 1998 Coexpression of Agrp and NPY in fasting-activated hypothalamic neurons. Nat Neurosci 1:271-2

133. Gropp E, Shanabrough M, Borok E, Xu AW, Janoschek R, Buch T, Plum L, Balthasar N, Hampel B, Waisman A, Barsh GS, Horvath TL, Bruning JC 2005 Agouti-related peptide-expressing neurons are mandatory for feeding. Nat Neurosci 8:1289-91

134. Bagnol D, Lu XY, Kaelin CB, Day HE, Ollmann M, Gantz I, Akil H, Barsh GS, Watson SJ 1999 Anatomy of an endogenous antagonist: relationship between Agouti-related protein and proopiomelanocortin in brain. J Neurosci 19:RC26

135. Cowley MA, Smart JL, Rubinstein M, Cerdan MG, Diano S, Horvath TL, Cone RD, Low MJ 2001 Leptin activates anorexigenic POMC neurons through a neural network in the arcuate nucleus. Nature 411:480-4

136. Pinto S, Roseberry AG, Liu H, Diano S, Shanabrough M, Cai X, Friedman JM, Horvath TL 2004 Rapid rewiring of arcuate nucleus feeding circuits by leptin. Science 304:110-5

137. Fan W, Ellacott KL, Halatchev IG, Takahashi K, Yu P, Cone RD 2004 Cholecystokinin-mediated suppression of feeding involves the brainstem melanocortin system. Nat Neurosci 7:335-6

138. Heisler LK, Cowley MA, Tecott LH, Fan W, Low MJ, Smart JL, Rubinstein M, Tatro JB, Marcus JN, Holstege H, Lee CE, Cone RD, Elmquist JK 2002 Activation of central melanocortin pathways by fenfluramine. Science 297:609-11

139. Batterham RL, Cowley MA, Small CJ, Herzog H, Cohen MA, Dakin CL, Wren AM, Brynes AE, Low MJ, Ghatei MA, Cone RD, Bloom SR 2002 Gut hormone PYY(3-36) physiologically inhibits food intake. Nature 418:650-4

140. Butler AA, Kesterson RA, Khong K, Cullen MJ, Pelleymounter MA, Dekoning J, Baetscher M, Cone RD 2000 A unique metabolic syndrome causes obesity in the melanocortin-3 receptor-deficient mouse. Endocrinology 141:3518-21

141. Chen AS, Marsh DJ, Trumbauer ME, Frazier EG, Guan XM, Yu H, Rosenblum CI, Vongs A, Feng Y, Cao L, Metzger JM, Strack AM, Camacho RE, Mellin TN, Nunes CN, Min W, Fisher J, Gopal-Truter S, MacIntyre DE, Chen HY, Van der Ploeg LH 2000 Inactivation of the mouse melanocortin-3 receptor results in increased fat mass and reduced lean body mass. Nat Genet 26:97-102

142. Chen W, Kelly MA, Opitz-Araya X, Thomas RE, Low MJ, Cone RD 1997 Exocrine gland dysfunction in MC5-R-deficient mice: evidence for

coordinated regulation of exocrine gland function by melanocortin peptides. Cell 91:789-98

143. Huszar D, Lynch CA, Fairchild-Huntress V, Dunmore JH, Fang Q, Berkemeier LR, Gu W, Kesterson RA, Boston BA, Cone RD, Smith FJ, Campfield LA, Burn P, Lee F 1997 Targeted disruption of the melanocortin-4 receptor results in obesity in mice. Cell 88:131-41

144. Yaswen L, Diehl N, Brennan MB, Hochgeschwender U 1999 Obesity in the mouse model of pro-opiomelanocortin deficiency responds to peripheral melanocortin. Nat Med 5:1066-70

145. Marsh DJ, Hollopeter G, Huszar D, Laufer R, Yagaloff KA, Fisher SL, Burn P, Palmiter RD 1999 Response of melanocortin-4 receptor-deficient mice to anorectic and orexigenic peptides. Nat Genet 21:119-22

146. Fan W, Boston BA, Kesterson RA, Hruby VJ, Cone RD 1997 Role of melanocortinergic neurons in feeding and the agouti obesity syndrome. Nature 385:165-8

147. Krude H, Biebermann H, Luck W, Horn R, Brabant G, Gruters A 1998 Severe early-onset obesity, adrenal insufficiency and red hair pigmentation caused by POMC mutations in humans. Nat Genet 19:155-7

148. Lubrano-Berthelier C, Durand E, Dubern B, Shapiro A, Dazin P, Weill J, Ferron C, Froguel P, Vaisse C 2003 Intracellular retention is a common characteristic of childhood obesity-associated MC4R mutations. Hum Mol Genet 12:145-53

149. Swarbrick MM, Vaisse C 2003 Emerging trends in the search for genetic variants predisposing to human obesity. Curr Opin Clin Nutr Metab Care 6:369-75

150. Vaisse C, Clement K, Durand E, Hercberg S, Guy-Grand B, Froguel P 2000 Melanocortin-4 receptor mutations are a frequent and heterogeneous cause of morbid obesity. J Clin Invest 106:253-62

151. Yeo GS, Farooqi IS, Challis BG, Jackson RS, O'Rahilly S 2000 The role of melanocortin signalling in the control of body weight: evidence from human and murine genetic models. Qjm 93:7-14

152. Yeo GS, Lank EJ, Farooqi IS, Keogh J, Challis BG, O'Rahilly S 2003 Mutations in the human melanocortin-4 receptor gene associated with severe familial obesity disrupts receptor function through multiple molecular mechanisms. Hum Mol Genet 12:561-74

153. Seeley RJ, Yagaloff KA, Fisher SL, Burn P, Thiele TE, van Dijk G, Baskin DG, Schwartz MW 1997 Melanocortin receptors in leptin effects. Nature 390:349

154. Cheung CC, Clifton DK, Steiner RA 1997 Proopiomelanocortin neurons are direct targets for leptin in the hypothalamus. Endocrinology 138:4489-92

155. Mercer JG, Hoggard N, Williams LM, Lawrence CB, Hannah LT, Morgan PJ, Trayhurn P 1996 Coexpression of leptin receptor and preproneuropeptide Y mRNA in arcuate nucleus of mouse hypothalamus. J Neuroendocrinol 8:733-5

156. Mizuno TM, Kleopoulos SP, Bergen HT, Roberts JL, Priest CA, Mobbs CV 1998 Hypothalamic pro-opiomelanocortin mRNA is reduced by fasting and [corrected] in ob/ob and db/db mice, but is stimulated by leptin. Diabetes 47:294-7

157. Swart I, Jahng JW, Overton JM, Houpt TA 2002 Hypothalamic NPY, AGRP, and POMC mRNA responses to leptin and refeeding in mice. Am J Physiol Regul Integr Comp Physiol 283:R1020-6

158. Thornton JE, Cheung CC, Clifton DK, Steiner RA 1997 Regulation of hypothalamic proopiomelanocortin mRNA by leptin in ob/ob mice. Endocrinology 138:5063-6

159. Munzberg H, Huo L, Nillni EA, Hollenberg AN, Bjorbaek C 2003 Role of signal transducer and activator of transcription 3 in regulation of hypothalamic proopiomelanocortin gene expression by leptin. Endocrinology 144:2121-31

160. Elias CF, Aschkenasi C, Lee C, Kelly J, Ahima RS, Bjorbaek C, Flier JS, Saper CB, Elmquist JK 1999 Leptin differentially regulates NPY and POMC neurons projecting to the lateral hypothalamic area. Neuron 23:775-86

161. Enriori PJ, Evans AE, Sinnayah P, Jobst EE, Tonelli-Lemos L, Billes SK, Glavas MM, Grayson BE, Perello M, Nillni EA, Grove KL, Cowley MA 2007 Diet-induced obesity causes severe but reversible leptin resistance in arcuate melanocortin neurons. Cell Metab 5:181-94

162. Watanobe H, Habu S 2002 Leptin regulates growth hormone-releasing factor, somatostatin, and alpha-melanocyte-stimulating hormone but not

neuropeptide Y release in rat hypothalamus in vivo: relation with growth hormone secretion. J Neurosci 22:6265-71

163. Mizuno TM, Mobbs CV 1999 Hypothalamic agouti-related protein messenger ribonucleic acid is inhibited by leptin and stimulated by fasting. Endocrinology 140:814-7

164. Huo L, Grill HJ, Bjorbaek C 2006 Divergent regulation of proopiomelanocortin neurons by leptin in the nucleus of the solitary tract and in the arcuate hypothalamic nucleus. Diabetes 55:567-73

165. Perello M, Stuart RC, Nillni EA 2007 Differential effects of fasting and leptin on proopiomelanocortin peptides in the arcuate nucleus and in the nucleus of the solitary tract. Am J Physiol Endocrinol Metab 292:E1348-57

166. Bjorbaek C, Kahn BB 2004 Leptin signaling in the central nervous system and the periphery. Recent Prog Horm Res 59:305-31

167. Ellacott KL, Halatchev IG, Cone RD 2006 Characterization of leptin-responsive neurons in the caudal brainstem. Endocrinology 147:3190-5

168. Woods SC, Benoit SC, Clegg DJ 2006 The brain-gut-islet connection. Diabetes 55 Suppl 2:S114-21

169. Marks JL, Porte D, Jr., Stahl WL, Baskin DG 1990 Localization of insulin receptor mRNA in rat brain by in situ hybridization. Endocrinology 127:3234-6

170. Benoit SC, Air EL, Coolen LM, Strauss R, Jackman A, Clegg DJ, Seeley RJ, Woods SC 2002 The catabolic action of insulin in the brain is mediated by melanocortins. J Neurosci 22:9048-52

171. Mizuno TM, Makimura H, Silverstein J, Roberts JL, Lopingco T, Mobbs CV 1999 Fasting regulates hypothalamic neuropeptide Y, agouti-related peptide, and proopiomelanocortin in diabetic mice independent of changes in leptin or insulin. Endocrinology 140:4551-7

172. Larsson LI, Rehfeld JF 1978 Distribution of gastrin and CCK cells in the rat gastrointestinal tract. Evidence for the occurrence of three distinct cell types storing COOH-terminal gastrin immunoreactivity. Histochemistry 58:23-31

173. Straus E, Yalow RS 1979 Cholecystokinin in the brains of obese and nonobese mice. Science 203:68-9

174. Gibbs J, Smith GP 1977 Cholecystokinin and satiety in rats and rhesus monkeys. Am J Clin Nutr 30:758-61

175. Maddison S 1977 Intraperitoneal and intracranial cholecystokinin depress operant responding for food. Physiol Behav 19:819-24

176. Moran TH, Ameglio PJ, Schwartz GJ, McHugh PR 1992 Blockade of type A, not type B, CCK receptors attenuates satiety actions of exogenous and endogenous CCK. Am J Physiol 262:R46-50

177. Lodge DJ, Lawrence AJ 2001 Comparative analysis of the central CCK system in Fawn Hooded and Wistar Kyoto rats: extended localisation of CCK-A receptors throughout the rat brain using a novel radioligand. Regul Pept 99:191-201

178. Appleyard SM, Bailey TW, Doyle MW, Jin YH, Smart JL, Low MJ, Andresen MC 2005 Proopiomelanocortin neurons in nucleus tractus

solitarius are activated by visceral afferents: regulation by cholecystokinin and opioids. J Neurosci 25:3578-85

179. Casanueva FF, Dieguez C 1999 Growth Hormone Secretagogues: Physiological Role and Clinical Utility. Trends Endocrinol Metab 10:30-38

180. Kojima M, Hosoda H, Date Y, Nakazato M, Matsuo H, Kangawa K 1999 Ghrelin is a growth-hormone-releasing acylated peptide from stomach. Nature 402:656-60

181. Cowley MA, Smith RG, Diano S, Tschop M, Pronchuk N, Grove KL, Strasburger CJ, Bidlingmaier M, Esterman M, Heiman ML, Garcia-Segura LM, Nillni EA, Mendez P, Low MJ, Sotonyi P, Friedman JM, Liu H, Pinto S, Colmers WF, Cone RD, Horvath TL 2003 The distribution and mechanism of action of ghrelin in the CNS demonstrates a novel hypothalamic circuit regulating energy homeostasis. Neuron 37:649-61

182. Lu S, Guan JL, Wang QP, Uehara K, Yamada S, Goto N, Date Y, Nakazato M, Kojima M, Kangawa K, Shioda S 2002 Immunocytochemical observation of ghrelin-containing neurons in the rat arcuate nucleus. Neurosci Lett 321:157-60

183. Hosoda H, Kojima M, Kangawa K 2006 Biological, physiological, and pharmacological aspects of ghrelin. J Pharmacol Sci 100:398-410

184. Zigman JM, Jones JE, Lee CE, Saper CB, Elmquist JK 2006 Expression of ghrelin receptor mRNA in the rat and the mouse brain. J Comp Neurol 494:528-48

185. Cummings DE, Purnell JQ, Frayo RS, Schmidova K, Wisse BE, Weigle DS 2001 A preprandial rise in plasma ghrelin levels suggests a role in meal initiation in humans. Diabetes 50:1714-9

186. Tschop M, Smiley DL, Heiman ML 2000 Ghrelin induces adiposity in rodents. Nature 407:908-13

187. Toshinai K, Mondal MS, Nakazato M, Date Y, Murakami N, Kojima M, Kangawa K, Matsukura S 2001 Upregulation of Ghrelin expression in the stomach upon fasting, insulin-induced hypoglycemia, and leptin administration. Biochem Biophys Res Commun 281:1220-5

188. Lawrence CB, Snape AC, Baudoin FM, Luckman SM 2002 Acute central ghrelin and GH secretagogues induce feeding and activate brain appetite centers. Endocrinology 143:155-62

189. Wren AM, Seal LJ, Cohen MA, Brynes AE, Frost GS, Murphy KG, Dhillo WS, Ghatei MA, Bloom SR 2001 Ghrelin enhances appetite and increases food intake in humans. J Clin Endocrinol Metab 86:5992

190. Wren AM, Small CJ, Abbott CR, Dhillo WS, Seal LJ, Cohen MA, Batterham RL, Taheri S, Stanley SA, Ghatei MA, Bloom SR 2001 Ghrelin causes hyperphagia and obesity in rats. Diabetes 50:2540-7

191. Hewson AK, Dickson SL 2000 Systemic administration of ghrelin induces Fos and Egr-1 proteins in the hypothalamic arcuate nucleus of fasted and fed rats. J Neuroendocrinol 12:1047-9

192. Wang L, Saint-Pierre DH, Tache Y 2002 Peripheral ghrelin selectively increases Fos expression in neuropeptide Y - synthesizing neurons in mouse hypothalamic arcuate nucleus. Neurosci Lett 325:47-51

193. Kamegai J, Tamura H, Shimizu T, Ishii S, Sugihara H, Wakabayashi I 2001 Chronic central infusion of ghrelin increases hypothalamic neuropeptide Y and Agouti-related protein mRNA levels and body weight in rats. Diabetes 50:2438-43

194. Chen HY, Trumbauer ME, Chen AS, Weingarth DT, Adams JR, Frazier EG, Shen Z, Marsh DJ, Feighner SD, Guan XM, Ye Z, Nargund RP, Smith RG, Van der Ploeg LH, Howard AD, MacNeil DJ, Qian S 2004 Orexigenic action of peripheral ghrelin is mediated by neuropeptide Y and agouti-related protein. Endocrinology 145:2607-12

195. Nagaya N, Uematsu M, Kojima M, Ikeda Y, Yoshihara F, Shimizu W, Hosoda H, Hirota Y, Ishida H, Mori H, Kangawa K 2001 Chronic administration of ghrelin improves left ventricular dysfunction and attenuates development of cardiac cachexia in rats with heart failure. Circulation 104:1430-5

196. Deboer MD, Zhu XX, Levasseur P, Meguid MM, Suzuki S, Inui A, Taylor JE, Halem HA, Dong JZ, Datta R, Culler MD, Marks DL 2007 Ghrelin treatment causes increased food intake and retention of lean body mass in a rat model of cancer cachexia. Endocrinology 148:3004-12

197. Sergeyev V, Broberger C, Hokfelt T 2001 Effect of LPS administration on the expression of POMC, NPY, galanin, CART and MCH mRNAs in the rat hypothalamus. Brain Res Mol Brain Res 90:93-100

198. Endo M, Masaki T, Seike M, Yoshimatsu H 2007 Involvement of stomach ghrelin and hypothalamic neuropeptides in tumor necrosis factor-alpha-induced hypophagia in mice. Regul Pept 140:94-100

199. Espat NJ, Auffenberg T, Rosenberg JJ, Rogy M, Martin D, Fang CH, Hasselgren PO, Copeland EM, Moldawer LL 1996 Ciliary neurotrophic factor is catabolic and shares with IL-6 the capacity to induce an acute phase response. Am J Physiol 271:R185-90

200. Henderson JT, Seniuk NA, Richardson PM, Gauldie J, Roder JC 1994 Systemic administration of ciliary neurotrophic factor induces cachexia in rodents. J Clin Invest 93:2632-8

201. Richardson PM 1994 Ciliary neurotrophic factor: a review. Pharmacol Ther 63:187-98

202. MacLennan AJ, Vinson EN, Marks L, McLaurin DL, Pfeifer M, Lee N 1996 Immunohistochemical localization of ciliary neurotrophic factor receptor alpha expression in the rat nervous system. J Neurosci 16:621-30

203. Bjorbaek C, Elmquist JK, El-Haschimi K, Kelly J, Ahima RS, Hileman S, Flier JS 1999 Activation of SOCS-3 messenger ribonucleic acid in the hypothalamus by ciliary neurotrophic factor. Endocrinology 140:2035-43

204. Kelly JF, Elias CF, Lee CE, Ahima RS, Seeley RJ, Bjorbaek C, Oka T, Saper CB, Flier JS, Elmquist JK 2004 Ciliary neurotrophic factor and leptin induce

distinct patterns of immediate early gene expression in the brain. Diabetes 53:911-20

205. Janoschek R, Plum L, Koch L, Munzberg H, Diano S, Shanabrough M, Muller W, Horvath TL, Bruning JC 2006 gp130 signaling in proopiomelanocortin neurons mediates the acute anorectic response to centrally applied ciliary neurotrophic factor. Proc Natl Acad Sci U S A 103:10707-12

206. Joppa MA, Ling N, Chen C, Gogas KR, Foster AC, Markison S 2005 Central administration of peptide and small molecule MC4 receptor antagonists induce hyperphagia in mice and attenuate cytokine-induced anorexia. Peptides 26:2294-301

207. Marks DL, Butler AA, Turner R, Brookhart G, Cone RD 2003 Differential role of melanocortin receptor subtypes in cachexia. Endocrinology 144:1513-23

208. Marks DL, Ling N, Cone RD 2001 Role of the central melanocortin system in cachexia. Cancer Res 61:1432-8

209. Clark JT, Kalra PS, Crowley WR, Kalra SP 1984 Neuropeptide Y and human pancreatic polypeptide stimulate feeding behavior in rats. Endocrinology 115:427-9

210. Stanley BG, Kyrkouli SE, Lampert S, Leibowitz SF 1986 Neuropeptide Y chronically injected into the hypothalamus: a powerful neurochemical inducer of hyperphagia and obesity. Peptides 7:1189-92

211. Zarjevski N, Cusin I, Vettor R, Rohner-Jeanrenaud F, Jeanrenaud B 1993 Chronic intracerebroventricular neuropeptide-Y administration to normal rats mimics hormonal and metabolic changes of obesity. Endocrinology 133:1753-8

212. Katsuura G, Asakawa A, Inui A 2002 Roles of pancreatic polypeptide in regulation of food intake. Peptides 23:323-9

213. Naveilhan P, Hassani H, Canals JM, Ekstrand AJ, Larefalk A, Chhajlani V, Arenas E, Gedda K, Svensson L, Thoren P, Ernfors P 1999 Normal feeding behavior, body weight and leptin response require the neuropeptide Y Y2 receptor. Nat Med 5:1188-93

214. Ueno N, Inui A, Iwamoto M, Kaga T, Asakawa A, Okita M, Fujimiya M, Nakajima Y, Ohmoto Y, Ohnaka M, Nakaya Y, Miyazaki JI, Kasuga M 1999 Decreased food intake and body weight in pancreatic polypeptide-overexpressing mice. Gastroenterology 117:1427-32

215. Polidori C, Ciccocioppo R, Regoli D, Massi M 2000 Neuropeptide Y receptor(s) mediating feeding in the rat: characterization with antagonists. Peptides 21:29-35

216. Wieland HA, Engel W, Eberlein W, Rudolf K, Doods HN 1998 Subtype selectivity of the novel nonpeptide neuropeptide Y Y1 receptor antagonist BIBO 3304 and its effect on feeding in rodents. Br J Pharmacol 125:549-55

217. Yokosuka M, Kalra PS, Kalra SP 1999 Inhibition of neuropeptide Y (NPY)-induced feeding and c-Fos response in magnocellular paraventricular

nucleus by a NPY receptor antagonist: a site of NPY action. Endocrinology 140:4494-500

218. Calza L, Giardino L, Battistini N, Zanni M, Galetti S, Protopapa F, Velardo A 1989 Increase of neuropeptide Y-like immunoreactivity in the paraventricular nucleus of fasting rats. Neurosci Lett 104:99-104

219. Dube MG, Sahu A, Kalra PS, Kalra SP 1992 Neuropeptide Y release is elevated from the microdissected paraventricular nucleus of food-deprived rats: an in vitro study. Endocrinology 131:684-8

220. Sahu A 1998 Leptin decreases food intake induced by melanin-concentrating hormone (MCH), galanin (GAL) and neuropeptide Y (NPY) in the rat. Endocrinology 139:4739-42

221. Gayle D, Ilyin SE, Flynn MC, Plata-Salaman CR 1998 Lipopolysaccharide (LPS)- and muramyl dipeptide (MDP)-induced anorexia during refeeding following acute fasting: characterization of brain cytokine and neuropeptide systems mRNAs. Brain Res 795:77-86

222. Gayle D, Ilyin SE, Romanovitch AE, Peloso E, Satinoff E, Plata-Salaman CR 1999 Basal and IL-1beta-stimulated cytokine and neuropeptide mRNA expression in brain regions of young and old Long-Evans rats. Brain Res Mol Brain Res 70:92-100

223. King PJ, Widdowson PS, Doods H, Williams G 2000 Effect of cytokines on hypothalamic neuropeptide Y release in vitro. Peptides 21:143-6

224. Chance WT, Balasubramaniam A, Thompson H, Mohapatra B, Ramo J, Fischer JE 1996 Assessment of feeding response of tumor-bearing rats to hypothalamic injection and infusion of neuropeptide Y. Peptides 17:797-801

225. Chance WT, Sheriff S, Kasckow JW, Regmi A, Balasubramaniam A 1998 NPY messenger RNA is increased in medial hypothalamus of anorectic tumor-bearing rats. Regul Pept 75-76:347-53

226. Bittencourt JC, Presse F, Arias C, Peto C, Vaughan J, Nahon JL, Vale W, Sawchenko PE 1992 The melanin-concentrating hormone system of the rat brain: an immuno- and hybridization histochemical characterization. J Comp Neurol 319:218-45

227. Gomori A, Ishihara A, Ito M, Mashiko S, Matsushita H, Yumoto M, Ito M, Tanaka T, Tokita S, Moriya M, Iwaasa H, Kanatani A 2003 Chronic intracerebroventricular infusion of MCH causes obesity in mice. Melanin-concentrating hormone. Am J Physiol Endocrinol Metab 284:E583-8

228. Ito M, Gomori A, Ishihara A, Oda Z, Mashiko S, Matsushita H, Yumoto M, Ito M, Sano H, Tokita S, Moriya M, Iwaasa H, Kanatani A 2003 Characterization of MCH-mediated obesity in mice. Am J Physiol Endocrinol Metab 284:E940-5

229. Shimada M, Tritos NA, Lowell BB, Flier JS, Maratos-Flier E 1998 Mice lacking melanin-concentrating hormone are hypophagic and lean. Nature 396:670-4

230. Skofitsch G, Jacobowitz DM, Zamir N 1985 Immunohistochemical localization of a melanin concentrating hormone-like peptide in the rat brain. Brain Res Bull 15:635-49

231. Chambers J, Ames RS, Bergsma D, Muir A, Fitzgerald LR, Hervieu G, Dytko GM, Foley JJ, Martin J, Liu WS, Park J, Ellis C, Ganguly S, Konchar S, Cluderay J, Leslie R, Wilson S, Sarau HM 1999 Melanin-concentrating hormone is the cognate ligand for the orphan G-protein-coupled receptor SLC-1. Nature 400:261-5

232. Hill J, Duckworth M, Murdock P, Rennie G, Sabido-David C, Ames RS, Szekeres P, Wilson S, Bergsma DJ, Gloger IS, Levy DS, Chambers JK, Muir AI 2001 Molecular cloning and functional characterization of MCH2, a novel human MCH receptor. J Biol Chem 276:20125-9

233. Hervieu GJ, Cluderay JE, Harrison D, Meakin J, Maycox P, Nasir S, Leslie RA 2000 The distribution of the mRNA and protein products of the melanin-concentrating hormone (MCH) receptor gene, slc-1, in the central nervous system of the rat. Eur J Neurosci 12:1194-216

234. Elmquist JK, Bjorbaek C, Ahima RS, Flier JS, Saper CB 1998 Distributions of leptin receptor mRNA isoforms in the rat brain. J Comp Neurol 395:535-47

235. Sailer AW, Sano H, Zeng Z, McDonald TP, Pan J, Pong SS, Feighner SD, Tan CP, Fukami T, Iwaasa H, Hreniuk DL, Morin NR, Sadowski SJ, Ito M, Ito M, Bansal A, Ky B, Figueroa DJ, Jiang Q, Austin CP, MacNeil DJ, Ishihara A, Ihara M, Kanatani A, Van der Ploeg LH, Howard AD, Liu Q

2001 Identification and characterization of a second melanin-concentrating hormone receptor, MCH-2R. Proc Natl Acad Sci U S A 98:7564-9

236. Qu D, Ludwig DS, Gammeltoft S, Piper M, Pelleymounter MA, Cullen MJ, Mathes WF, Przypek R, Kanarek R, Maratos-Flier E 1996 A role for melanin-concentrating hormone in the central regulation of feeding behaviour. Nature 380:243-7

237. Tritos NA, Mastaitis JW, Kokkotou E, Maratos-Flier E 2001 Characterization of melanin concentrating hormone and preproorexin expression in the murine hypothalamus. Brain Res 895:160-6

238. Hanada R, Nakazato M, Matsukura S, Murakami N, Yoshimatsu H, Sakata T 2000 Differential regulation of melanin-concentrating hormone and orexin genes in the agouti-related protein/melanocortin-4 receptor system. Biochem Biophys Res Commun 268:88-91

239. Abbott CR, Kennedy AR, Wren AM, Rossi M, Murphy KG, Seal LJ, Todd JF, Ghatei MA, Small CJ, Bloom SR 2003 Identification of hypothalamic nuclei involved in the orexigenic effect of melanin-concentrating hormone. Endocrinology 144:3943-9

240. Douglass J, McKinzie AA, Couceyro P 1995 PCR differential display identifies a rat brain mRNA that is transcriptionally regulated by cocaine and amphetamine. J Neurosci 15:2471-81

241. Hunter RG, Philpot K, Vicentic A, Dominguez G, Hubert GW, Kuhar MJ 2004 CART in feeding and obesity. Trends Endocrinol Metab 15:454-9

242. Kristensen P, Judge ME, Thim L, Ribel U, Christjansen KN, Wulff BS, Clausen JT, Jensen PB, Madsen OD, Vrang N, Larsen PJ, Hastrup S 1998 Hypothalamic CART is a new anorectic peptide regulated by leptin. Nature 393:72-6

243. Broberger C 1999 Hypothalamic cocaine- and amphetamine-regulated transcript (CART) neurons: histochemical relationship to thyrotropin-releasing hormone, melanin-concentrating hormone, orexin/hypocretin and neuropeptide Y. Brain Res 848:101-13

244. Elias CF, Saper CB, Maratos-Flier E, Tritos NA, Lee C, Kelly J, Tatro JB, Hoffman GE, Ollmann MM, Barsh GS, Sakurai T, Yanagisawa M, Elmquist JK 1998 Chemically defined projections linking the mediobasal hypothalamus and the lateral hypothalamic area. J Comp Neurol 402:442-59

245. Zheng H, Patterson LM, Berthoud HR 2002 CART in the dorsal vagal complex: sources of immunoreactivity and effects on Fos expression and food intake. Brain Res 957:298-310

246. Shimomura Y, Inukai T, Kuwabara A, Shimizu H, Sato N, Uehara Y, Kobayashi I, Kobayashi S 1991 Enhanced sensitivity to anorexia and consumption of drinking water induced by interleukin-1 beta in obese yellow mice. Eur J Pharmacol 209:15-8

247. Friedman JM 1997 The alphabet of weight control. Nature 385:119-20

248. Ebihara K, Ogawa Y, Katsuura G, Numata Y, Masuzaki H, Satoh N, Tamaki M, Yoshioka T, Hayase M, Matsuoka N, Aizawa-Abe M, Yoshimasa Y, Nakao K 1999 Involvement of agouti-related protein, an endogenous

antagonist of hypothalamic melanocortin receptor, in leptin action. Diabetes 48:2028-33

249. Huang QH, Hruby VJ, Tatro JB 1999 Role of central melanocortins in endotoxin-induced anorexia. Am J Physiol 276:R864-71

250. Lawrence CB, Rothwell NJ 2001 Anorexic but not pyrogenic actions of interleukin-1 are modulated by central melanocortin-3/4 receptors in the rat. J Neuroendocrinol 13:490-5

251. Wisse BE, Frayo RS, Schwartz MW, Cummings DE 2001 Reversal of cancer anorexia by blockade of central melanocortin receptors in rats. Endocrinology 142:3292-301

252. Cheung W, Yu PX, Little BM, Cone RD, Marks DL, Mak RH 2005 Role of leptin and melanocortin signaling in uremia-associated cachexia. J Clin Invest 115:1659-65

253. Mikkelsen S, Wall M, Zhu X, DiLorenzo M, Marks DL Cachexia in the mouse agar bead model of infection. Pediatric Pulmonology, 2004, p 297

254. Markison S, Foster AC, Chen C, Brookhart GB, Hesse A, Hoare SR, Fleck BA, Brown BT, Marks DL 2005 The regulation of feeding and metabolic rate and the prevention of murine cancer cachexia with a small-molecule melanocortin-4 receptor antagonist. Endocrinology 146:2766-73

255. Vos TJ, Caracoti A, Che JL, Dai M, Farrer CA, Forsyth NE, Drabic SV, Horlick RA, Lamppu D, Yowe DL, Balani S, Li P, Zeng H, Joseph IB, Rodriguez LE, Maguire MP, Patane MA, Claiborne CF 2004 Identification of 2-[2-[2-(5-bromo-2- methoxyphenyl)-ethyl]-3-fluorophenyl]-4,5-dihydro-

1H-imidazole (ML00253764), a small molecule melanocortin 4 receptor antagonist that effectively reduces tumor-induced weight loss in a mouse model. J Med Chem 47:1602-4

256. Getting SJ, Allcock GH, Flower R, Perretti M 2001 Natural and synthetic agonists of the melanocortin receptor type 3 possess anti-inflammatory properties. J Leukoc Biol 69:98-104

257. Adachi S, Morii E, Kim D, Ogihara H, Jippo T, Ito A, Lee YM, Kitamura Y 2000 Involvement of mi-transcription factor in expression of alpha-melanocyte-stimulating hormone receptor in cultured mast cells of mice. J Immunol 164:855-60

258. Luger TA, Bhardwaj RS, Grabbe S, Schwarz T 1996 Regulation of the immune response by epidermal cytokines and neurohormones. J Dermatol Sci 13:5-10

259. Ichiyama T, Sakai T, Catania A, Barsh GS, Furukawa S, Lipton JM 1999 Inhibition of peripheral NF-kappaB activation by central action of alpha-melanocyte-stimulating hormone. J Neuroimmunol 99:211-7

260. Ichiyama T, Zhao H, Catania A, Furukawa S, Lipton JM 1999 alpha-melanocyte-stimulating hormone inhibits NF-kappaB activation and IkappaBalpha degradation in human glioma cells and in experimental brain inflammation. Exp Neurol 157:359-65

261. Baeuerle PA, Baltimore D 1996 NF-kappa B: ten years after. Cell 87:13-20

262. Gantz I, Miwa H, Konda Y, Shimoto Y, Tashiro T, Watson SJ, DelValle J, Yamada T 1993 Molecular cloning, expression, and gene localization of a fourth melanocortin receptor. J Biol Chem 268:15174-9

263. Mountjoy KG, Jenny Wu CS, Dumont LM, Wild JM 2003 Melanocortin-4 receptor messenger ribonucleic acid expression in rat cardiorespiratory, musculoskeletal, and integumentary systems. Endocrinology 144:5488-96

264. Getting SJ, Di Filippo C, Christian HC, Lam CW, Rossi F, D'Amico M, Perretti M 2004 MC-3 receptor and the inflammatory mechanisms activated in acute myocardial infarct. J Leukoc Biol 76:845-53

265. Mioni C, Giuliani D, Cainazzo MM, Leone S, Bazzani C, Grieco P, Novellino E, Tomasi A, Bertolini A, Guarini S 2003 Further evidence that melanocortins prevent myocardial reperfusion injury by activating melanocortin MC3 receptors. Eur J Pharmacol 477:227-34

266. Rheins LA, Cotleur AL, Kleier RS, Hoppenjans WB, Saunder DN, Nordlund JJ 1989 Alpha-melanocyte stimulating hormone modulates contact hypersensitivity responsiveness in C57/BL6 mice. J Invest Dermatol 93:511-7

267. Raap U, Brzoska T, Sohl S, Path G, Emmel J, Herz U, Braun A, Luger T, Renz H 2003 Alpha-melanocyte-stimulating hormone inhibits allergic airway inflammation. J Immunol 171:353-9

268. Maaser C, Kannengiesser K, Specht C, Lugering A, Brzoska T, Luger TA, Domschke W, Kucharzik T 2006 Crucial role of the melanocortin receptor MC1R in experimental colitis. Gut 55:1415-22

269. Elmquist JK, Scammell TE, Saper CB 1997 Mechanisms of CNS response to systemic immune challenge: the febrile response. Trends Neurosci 20:565-70

270. Plata-Salaman C, Turrin N 1999 Cytokine action in the brain. Mol Psychiatry 4:302

271. Hart BL 1990 Behavioral adaptations to pathogens and parasites: five strategies. Neurosci Biobehav Rev 14:273-94

272. Murray MJ, Murray AB 1979 Anorexia of infection as a mechanism of host defense. Am J Clin Nutr 32:593-6

273. Ramos EJ, Suzuki S, Marks D, Inui A, Asakawa A, Meguid MM 2004 Cancer anorexia-cachexia syndrome: cytokines and neuropeptides. Curr Opin Clin Nutr Metab Care 7:427-34

274. Haskell-Luevano C, Chen P, Li C, Chang K, Smith MS, Cameron JL, Cone RD 1999 Characterization of the neuroanatomical distribution of agouti-related protein immunoreactivity in the rhesus monkey and the rat. Endocrinology 140:1408-15

275. Baskin DG, Hahn TM, Schwartz MW 1999 Leptin sensitive neurons in the hypothalamus. Horm Metab Res 31:345-50

276. Niswender KD, Baskin DG, Schwartz MW 2004 Insulin and its evolving partnership with leptin in the hypothalamic control of energy homeostasis. Trends Endocrinol Metab 15:362-9

277. Zhang F, Chen Y, Heiman M, Dimarchi R 2005 Leptin: structure, function and biology. Vitam Horm 71:345-72

278. Mercer JG, Hoggard N, Williams LM, Lawrence CB, Hannah LT, Trayhurn P 1996 Localization of leptin receptor mRNA and the long form splice variant (Ob-Rb) in mouse hypothalamus and adjacent brain regions by in situ hybridization. FEBS Lett 387:113-6

279. Rothwell NJ, Luheshi G 1994 Pharmacology of interleukin-1 actions in the brain. Adv Pharmacol 25:1-20

280. Plata-Salaman CR 1998 Cytokine-induced anorexia. Behavioral, cellular, and molecular mechanisms. Ann N Y Acad Sci 856:160-70

281. Ericsson A, Kovacs KJ, Sawchenko PE 1994 A functional anatomical analysis of central pathways subserving the effects of interleukin-1 on stress-related neuroendocrine neurons. J Neurosci 14:897-913

282. Labow M, Shuster D, Zetterstrom M, Nunes P, Terry R, Cullinan EB, Bartfai T, Solorzano C, Moldawer LL, Chizzonite R, McIntyre KW 1997 Absence of IL-1 signaling and reduced inflammatory response in IL-1 type I receptor-deficient mice. J Immunol 159:2452-61

283. Paxinos G, Franklin K 2001 The Mouse Brain in Stereotaxic Coordinates (2nd ed). Academic Press, Orlando, FL

284. Cunningham MJ, Scarlett JM, Steiner RA 2002 Cloning and distribution of galanin-like peptide mRNA in the hypothalamus and pituitary of the macaque. Endocrinology 143:755-63

285. Paxinos G, Watson C 1998 The Rat Brain in Stereotaxic Coordinates (4th ed.). Academic Press, Orlando, FL

286. Cartmell T, Southgate T, Rees GS, Castro MG, Lowenstein PR, Luheshi GN 1999 Interleukin-1 mediates a rapid inflammatory response after injection of adenoviral vectors into the brain. J Neurosci 19:1517-23

287. Inui A 1999 Cancer anorexia-cachexia syndrome: are neuropeptides the key? Cancer Res 59:4493-501

288. Wisse BE 2004 The inflammatory syndrome: the role of adipose tissue cytokines in metabolic disorders linked to obesity. J Am Soc Nephrol 15:2792-800

289. Ek M, Kurosawa M, Lundeberg T, Ericsson A 1998 Activation of vagal afferents after intravenous injection of interleukin-1beta: role of endogenous prostaglandins. J Neurosci 18:9471-9

290. Bluthe RM, Michaud B, Kelley KW, Dantzer R 1996 Vagotomy attenuates behavioural effects of interleukin-1 injected peripherally but not centrally. Neuroreport 7:1485-8

291. Ericsson A, Arias C, Sawchenko PE 1997 Evidence for an intramedullary prostaglandin-dependent mechanism in the activation of stress-related neuroendocrine circuitry by intravenous interleukin-1. J Neurosci 17:7166-79

292. Elander L, Engstrom L, Hallbeck M, Blomqvist A 2006 IL-1{beta} and LPS induce anorexia by distinct mechanisms differentially dependent on microsomal prostaglandin E synthase-1. Am J Physiol Regul Integr Comp Physiol

293. Ferri CC, Yuill EA, Ferguson AV 2005 Interleukin-1beta depolarizes magnocellular neurons in the paraventricular nucleus of the hypothalamus through prostaglandin-mediated activation of a non selective cationic conductance. Regul Pept 129:63-71

294. Tabarean IV, Korn H, Bartfai T 2006 Interleukin-1beta induces hyperpolarization and modulates synaptic inhibition in preoptic and anterior hypothalamic neurons. Neuroscience

295. Cowley MA, Pronchuk N, Fan W, Dinulescu DM, Colmers WF, Cone RD 1999 Integration of NPY, AGRP, and melanocortin signals in the hypothalamic paraventricular nucleus: evidence of a cellular basis for the adipostat. Neuron 24:155-63

296. Sonti G, Ilyin SE, Plata-Salaman CR 1996 Neuropeptide Y blocks and reverses interleukin-1 beta-induced anorexia in rats. Peptides 17:517-20

297. Plata-Salaman CR 2000 Central nervous system mechanisms contributing to the cachexia-anorexia syndrome. Nutrition 16:1009-12

298. Kalra SP, Dube MG, Pu S, Xu B, Horvath TL, Kalra PS 1999 Interacting appetite-regulating pathways in the hypothalamic regulation of body weight. Endocr Rev 20:68-100

299. Stutz AM, Morrison CD, Argyropoulos G 2005 The Agouti-related protein and its role in energy homeostasis. Peptides 26:1771-81

300. Arora S, Anubhuti 2006 Role of neuropeptides in appetite regulation and obesity - A review. Neuropeptides

301. Rossi M, Kim MS, Morgan DG, Small CJ, Edwards CM, Sunter D, Abusnana S, Goldstone AP, Russell SH, Stanley SA, Smith DM, Yagaloff K, Ghatei MA, Bloom SR 1998 A C-terminal fragment of Agouti-related protein increases feeding and antagonizes the effect of alpha-melanocyte stimulating hormone in vivo. Endocrinology 139:4428-31

302. Hagan MM, Rushing PA, Pritchard LM, Schwartz MW, Strack AM, Van Der Ploeg LH, Woods SC, Seeley RJ 2000 Long-term orexigenic effects of AgRP-(83---132) involve mechanisms other than melanocortin receptor blockade. Am J Physiol Regul Integr Comp Physiol 279:R47-52

303. Graham M, Shutter JR, Sarmiento U, Sarosi I, Stark KL 1997 Overexpression of Agrt leads to obesity in transgenic mice. Nat Genet 17:273-4

304. Friedman JM 1999 Leptin and the regulation of body weight. Harvey Lect 95:107-36

305. Woods SC, Seeley RJ, Porte D, Jr., Schwartz MW 1998 Signals that regulate food intake and energy homeostasis. Science 280:1378-83

306. Tartaglia LA 1997 The leptin receptor. J Biol Chem 272:6093-6

307. Wilson BD, Bagnol D, Kaelin CB, Ollmann MM, Gantz I, Watson SJ, Barsh GS 1999 Physiological and anatomical circuitry between Agouti-related protein and leptin signaling. Endocrinology 140:2387-97

308. Breen TL, Conwell IM, Wardlaw SL 2005 Effects of fasting, leptin, and insulin on AGRP and POMC peptide release in the hypothalamus. Brain Res 1032:141-8

309. Busbridge NJ, Dascombe MJ, Rothwell NJ 1993 Chronic effects of interleukin-1 beta on fever, oxygen consumption and food intake in the rat. Horm Metab Res 25:222-7

310. Scarlett JM, Jobst EE, Enriori PJ, Bowe DD, Batra AK, Grant WF, Cowley MA, Marks DL 2007 Regulation of central melanocortin signaling by interleukin-1{beta}. Endocrinology doi:10.1210/en.2007-0017

311. Sato T, Meguid MM, Fetissov SO, Chen C, Zhang L 2001 Hypothalamic dopaminergic receptor expressions in anorexia of tumor-bearing rats. Am J Physiol Regul Integr Comp Physiol 281:R1907-16

312. Ramos EJ, Middleton FA, Laviano A, Sato T, Romanova I, Das UN, Chen C, Qi Y, Meguid MM 2004 Effects of omega-3 fatty acid supplementation on tumor-bearing rats. J Am Coll Surg 199:716-23

313. Korner J, Savontaus E, Chua SC, Jr., Leibel RL, Wardlaw SL 2001 Leptin regulation of Agrp and Npy mRNA in the rat hypothalamus. J Neuroendocrinol 13:959-66

314. Ziotopoulou M, Erani DM, Hileman SM, Bjorbaek C, Mantzoros CS 2000 Unlike leptin, ciliary neurotrophic factor does not reverse the starvation-induced changes of serum corticosterone and hypothalamic neuropeptide levels but induces expression of hypothalamic inhibitors of leptin signaling. Diabetes 49:1890-6

315. Faggioni R, Fantuzzi G, Fuller J, Dinarello CA, Feingold KR, Grunfeld C 1998 IL-1 beta mediates leptin induction during inflammation. Am J Physiol 274:R204-8

316. Grunfeld C, Zhao C, Fuller J, Pollack A, Moser A, Friedman J, Feingold KR 1996 Endotoxin and cytokines induce expression of leptin, the ob gene product, in hamsters. J Clin Invest 97:2152-7

317. Leyva F, Anker SD, Egerer K, Stevenson JC, Kox WJ, Coats AJ 1998 Hyperleptinaemia in chronic heart failure. Relationships with insulin. Eur Heart J 19:1547-51

318. Merabet E, Dagogo-Jack S, Coyne DW, Klein S, Santiago JV, Hmiel SP, Landt M 1997 Increased plasma leptin concentration in end-stage renal disease. J Clin Endocrinol Metab 82:847-50

319. Sarraf P, Frederich RC, Turner EM, Ma G, Jaskowiak NT, Rivet DJ, 3rd, Flier JS, Lowell BB, Fraker DL, Alexander HR 1997 Multiple cytokines and acute inflammation raise mouse leptin levels: potential role in inflammatory anorexia. J Exp Med 185:171-5

320. Sahu A, Kalra PS, Kalra SP 1988 Food deprivation and ingestion induce reciprocal changes in neuropeptide Y concentrations in the paraventricular nucleus. Peptides 9:83-6

321. Schwartz MW, Erickson JC, Baskin DG, Palmiter RD 1998 Effect of fasting and leptin deficiency on hypothalamic neuropeptide Y gene transcription in vivo revealed by expression of a lacZ reporter gene. Endocrinology 139:2629-35

322. Widdowson PS, Upton R, Henderson L, Buckingham R, Wilson S, Williams G 1997 Reciprocal regional changes in brain NPY receptor density during dietary restriction and dietary-induced obesity in the rat. Brain Res 774:1-10

323. McCarthy HD, Dryden S, Williams G 1995 Interleukin-1 beta-induced anorexia and pyrexia in rat: relationship to hypothalamic neuropeptide Y. Am J Physiol 269:E852-7

324. Chance WT, Balasubramaniam A, Dayal R, Brown J, Fischer JE 1994 Hypothalamic concentration and release of neuropeptide Y into microdialysates is reduced in anorectic tumor-bearing rats. Life Sci 54:1869-74

325. Bergen HT, Mizuno TM, Taylor J, Mobbs CV 1998 Hyperphagia and weight gain after gold-thioglucose: relation to hypothalamic neuropeptide Y and proopiomelanocortin. Endocrinology 139:4483-8

326. Pittman JG, Cohen P 1964 The Pathogenesis Of Cardiac Cachexia. N Engl J Med 271:403-9 CONTD

327. Anker SD, Ponikowski P, Varney S, Chua TP, Clark AL, Webb-Peploe KM, Harrington D, Kox WJ, Poole-Wilson PA, Coats AJ 1997 Wasting as independent risk factor for mortality in chronic heart failure. Lancet 349:1050-3

328. Davos CH, Doehner W, Rauchhaus M, Cicoira M, Francis DP, Coats AJ, Clark AL, Anker SD 2003 Body mass and survival in patients with chronic heart failure without cachexia: the importance of obesity. J Card Fail 9:29-35

329. Anker SD, Ponikowski PP, Clark AL, Leyva F, Rauchhaus M, Kemp M, Teixeira MM, Hellewell PG, Hooper J, Poole-Wilson PA, Coats AJ 1999 Cytokines and neurohormones relating to body composition alterations in the wasting syndrome of chronic heart failure. Eur Heart J 20:683-93

330. Dutka DP, Elborn JS, Delamere F, Shale DJ, Morris GK 1993 Tumour necrosis factor alpha in severe congestive cardiac failure. Br Heart J 70:141-3

331. Plata-Salaman CR 2001 Cytokines and feeding. Int J Obes Relat Metab Disord 25 Suppl 5:S48-52

332. Plata-Salaman CR, Sonti G, Borkoski JP, Wilson CD, French-Mullen JMb 1996 Anorexia induced by chronic central administration of cytokines at estimated pathophysiological concentrations. Physiol Behav 60:867-75

333. Campbell IL 1998 Transgenic mice and cytokine actions in the brain: bridging the gap between structural and functional neuropathology. Brain Res Brain Res Rev 26:327-36

334. Foster AC, Joppa M, Markison S, Gogas KR, Fleck BA, Murphy BJ, Wolff M, Cismowski MJ, Ling N, Goodfellow VS, Chen C, Saunders J, Conlon PJ 2003 Body weight regulation by selective MC4 receptor agonists and antagonists. Ann N Y Acad Sci 994:103-10

335. Joppa MA, Gogas KR, Foster AC, Markison S 2007 Central infusion of the melanocortin receptor antagonist agouti-related peptide (AgRP(83-132)) prevents cachexia-related symptoms induced by radiation and colon-26 tumors in mice. Peptides

336. Kamegai J, Tamura H, Shimizu T, Ishii S, Sugihara H, Wakabayashi I 2000 Central effect of ghrelin, an endogenous growth hormone secretagogue, on hypothalamic peptide gene expression. Endocrinology 141:4797-800

337. Helies-Toussaint C, Moinard C, Rasmusen C, Tabbi-Anneni I, Cynober L, Grynberg A 2005 Aortic banding in rat as a model to investigate malnutrition associated with heart failure. Am J Physiol Regul Integr Comp Physiol 288:R1325-31

338. Tinsley FC, Taicher GZ, Heiman ML 2004 Evaluation of a quantitative magnetic resonance method for mouse whole body composition analysis. Obes Res 12:150-60

339. Anker SD, Coats AJ 1999 Cardiac cachexia: a syndrome with impaired survival and immune and neuroendocrine activation. Chest 115:836-47

340. Small CJ, Kim MS, Stanley SA, Mitchell JR, Murphy K, Morgan DG, Ghatei MA, Bloom SR 2001 Effects of chronic central nervous system administration of agouti-related protein in pair-fed animals. Diabetes 50:248-54

341. Kenchaiah S, Evans JC, Levy D, Wilson PW, Benjamin EJ, Larson MG, Kannel WB, Vasan RS 2002 Obesity and the risk of heart failure. N Engl J Med 347:305-13

342. Poirier P, Giles TD, Bray GA, Hong Y, Stern JS, Pi-Sunyer FX, Eckel RH 2006 Obesity and cardiovascular disease: pathophysiology, evaluation, and effect of weight loss: an update of the 1997 American Heart Association Scientific Statement on Obesity and Heart Disease from the Obesity Committee of the Council on Nutrition, Physical Activity, and Metabolism. Circulation 113:898-918

343. Curtis JP, Selter JG, Wang Y, Rathore SS, Jovin IS, Jadbabaie F, Kosiborod M, Portnay EL, Sokol SI, Bader F, Krumholz HM 2005 The obesity paradox: body mass index and outcomes in patients with heart failure. Arch Intern Med 165:55-61

344. Albarado DC, McClaine J, Stephens JM, Mynatt RL, Ye J, Bannon AW, Richards WG, Butler AA 2004 Impaired coordination of nutrient intake and substrate oxidation in melanocortin-4 receptor knockout mice. Endocrinology 145:243-52

345. Nagaya N, Moriya J, Yasumura Y, Uematsu M, Ono F, Shimizu W, Ueno K, Kitakaze M, Miyatake K, Kangawa K 2004 Effects of ghrelin administration on left ventricular function, exercise capacity, and muscle wasting in patients with chronic heart failure. Circulation 110:3674-9

346. Schwartz GJ 2000 The role of gastrointestinal vagal afferents in the control of food intake: current prospects. Nutrition 16:866-73

347. Thaler CD, Suhr L, Ip N, Katz DM 1994 Leukemia inhibitory factor and neurotrophins support overlapping populations of rat nodose sensory neurons in culture. Dev Biol 161:338-44

348. Day HE, Akil H 1996 Differential pattern of c-fos mRNA in rat brain following central and systemic administration of interleukin-1-beta: implications for mechanism of action. Neuroendocrinology 63:207-18

349. Akasaka S, Nomura M, Nishii H, Fujimoto N, Ueta Y, Tsutsui M, Shimokawa H, Yanagihara N, Matsumoto T 2006 The hypothalamo-

pituitary axis responses to lipopolysaccharide-induced endotoxemia in mice lacking inducible nitric oxide synthase. Brain Res 1089:1-9

350. Bajetto A, Bonavia R, Barbero S, Florio T, Schettini G 2001 Chemokines and their receptors in the central nervous system. Front Neuroendocrinol 22:147-84

351. Mantovani A 1999 The chemokine system: redundancy for robust outputs. Immunol Today 20:254-7

352. Banisadr G, Queraud-Lesaux F, Boutterin MC, Pelaprat D, Zalc B, Rostene W, Haour F, Parsadaniantz SM 2002 Distribution, cellular localization and functional role of CCR2 chemokine receptors in adult rat brain. J Neurochem 81:257-69

353. Horuk R, Martin AW, Wang Z, Schweitzer L, Gerassimides A, Guo H, Lu Z, Hesselgesser J, Perez HD, Kim J, Parker J, Hadley TJ, Peiper SC 1997 Expression of chemokine receptors by subsets of neurons in the central nervous system. J Immunol 158:2882-90

354. Minano FJ, Myers RD 1991 Anorexia and adipsia: dissociation from fever after MIP-1 injection in ventromedial hypothalamus and preoptic area of rats. Brain Res Bull 27:273-8

355. Plata-Salaman CR, Borkoski JP 1994 Chemokines/intercrines and central regulation of feeding. Am J Physiol 266:R1711-5

356. Weisberg SP, Hunter D, Huber R, Lemieux J, Slaymaker S, Vaddi K, Charo I, Leibel RL, Ferrante AW, Jr. 2006 CCR2 modulates inflammatory and metabolic effects of high-fat feeding. J Clin Invest 116:115-24

357. Kim YW, Kim JY, Park YH, Park SY, Won KC, Choi KH, Huh JY, Moon KH 2006 Metformin restores leptin sensitivity in high-fat-fed obese rats with leptin resistance. Diabetes 55:716-24

358. Scarpace PJ, Matheny M, Zolotukhin S, Tumer N, Zhang Y 2003 Leptin-induced leptin resistant rats exhibit enhanced responses to the melanocortin agonist MT II. Neuropharmacology 45:211-9

359. Tulipano G, Vergoni AV, Soldi D, Muller EE, Cocchi D 2004 Characterization of the resistance to the anorectic and endocrine effects of leptin in obesity-prone and obesity-resistant rats fed a high-fat diet. J Endocrinol 183:289-98

360. Emanuelli B, Glondu M, Filloux C, Peraldi P, Van Obberghen E 2004 The potential role of SOCS-3 in the interleukin-1beta-induced desensitization of insulin signaling in pancreatic beta-cells. Diabetes 53 Suppl 3:S97-S103

361. Liu L, Yang TM, Liedtke W, Simon SA 2006 Chronic IL-1beta signaling potentiates voltage-dependent sodium currents in trigeminal nociceptive neurons. J Neurophysiol 95:1478-90

362. Obreja O, Rathee PK, Lips KS, Distler C, Kress M 2002 IL-1 beta potentiates heat-activated currents in rat sensory neurons: involvement of IL-1RI, tyrosine kinase, and protein kinase C. Faseb J 16:1497-503

363. Yamakuni H, Minami M, Satoh M 1996 Localization of mRNA for leukemia inhibitory factor receptor in the adult rat brain. J Neuroimmunol 70:45-53

364. Getting SJ 2002 Melanocortin peptides and their receptors: new targets for anti-inflammatory therapy. Trends Pharmacol Sci 23:447-9

365. Getting SJ, Gibbs L, Clark AJ, Flower RJ, Perretti M 1999 POMC gene-derived peptides activate melanocortin type 3 receptor on murine macrophages, suppress cytokine release, and inhibit neutrophil migration in acute experimental inflammation. J Immunol 162:7446-53

366. Frangogiannis NG, Smith CW, Entman ML 2002 The inflammatory response in myocardial infarction. Cardiovasc Res 53:31-47

367. Sharma R, Coats AJ, Anker SD 2000 The role of inflammatory mediators in chronic heart failure: cytokines, nitric oxide, and endothelin-1. Int J Cardiol 72:175-86

368. Bazzani C, Guarini S, Botticelli AR, Zaffe D, Tomasi A, Bini A, Cainazzo MM, Ferrazza G, Mioni C, Bertolini A 2001 Protective effect of melanocortin peptides in rat myocardial ischemia. J Pharmacol Exp Ther 297:1082-7

369. Horwich TB, Fonarow GC, Hamilton MA, MacLellan WR, Woo MA, Tillisch JH 2001 The relationship between obesity and mortality in patients with heart failure. J Am Coll Cardiol 38:789-95

370. Rauchhaus M, Clark AL, Doehner W, Davos C, Bolger A, Sharma R, Coats AJ, Anker SD 2003 The relationship between cholesterol and survival in patients with chronic heart failure. J Am Coll Cardiol 42:1933-40

371. Mari D, Di Berardino F, Cugno M 2002 Chronic heart failure and the immune system. Clin Rev Allergy Immunol 23:325-40

APPENDIX

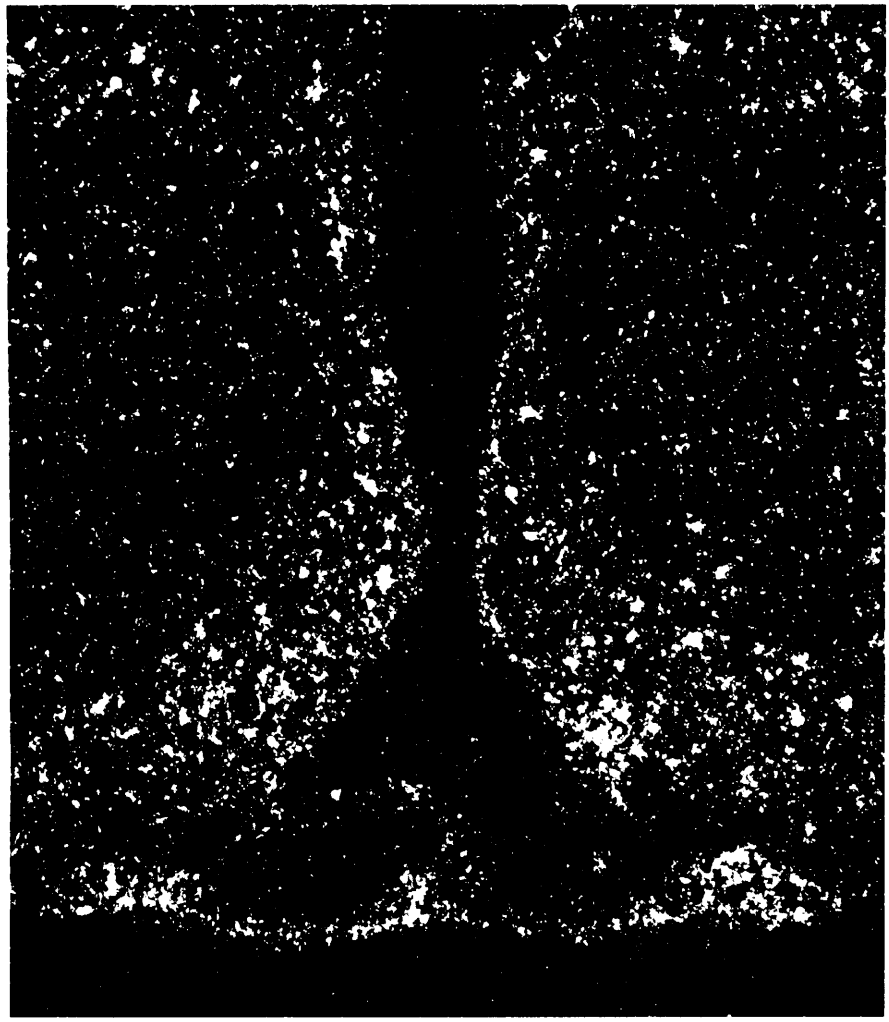

Figure A-1. Representative darkfield photomicrograph showing the distribution of LIF-R mRNA (white silver grain clusters) in the ARC of wild-type rats.

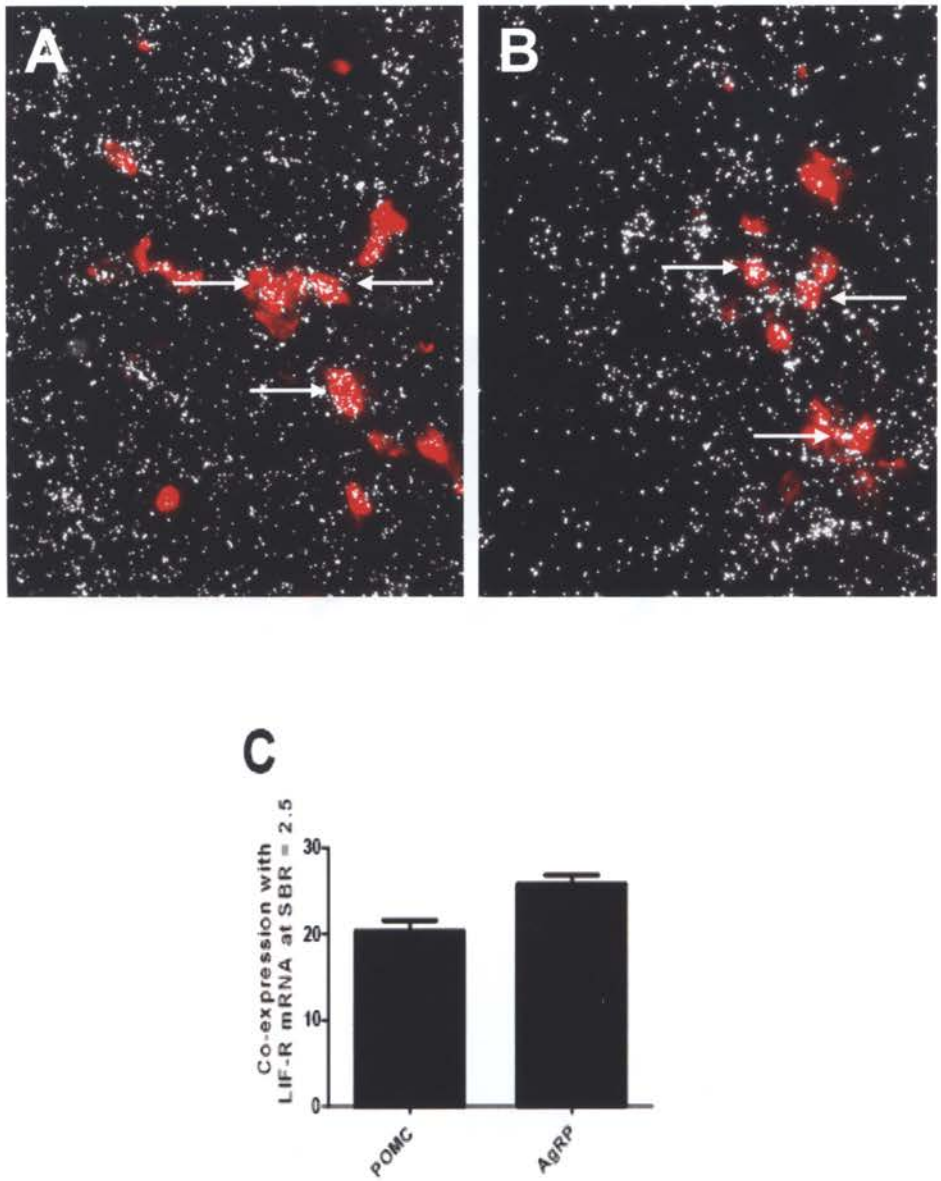

Figure A-2. Co-expression of POMC mRNA and AgRP mRNA with LIF-R mRNA in the ARC of wild-type rats. Double-label ISH was performed on rat hypothalamic sections using digoxigenin-labed POMC (n = 6), or AgRP (n = 6) riboprobes and ^{33}P-labeled rat LIF-R (861 base-pairs) riboprobe. (**A**) Co-expression of ARC POMC mRNA-expressing neurons (red precipitate) with LIF-R mRNA-expressing cells (clusters of silver grains). *Arrows* point to POMC neurons that co-expresses LIF-R mRNA. (**B**) Co-expression of AgRP mRNA-expressing neurons (red precipitate) with LIF-R mRNA-expressing cells (clusters of silver grains). *Arrows* point to AgRP neurons that co-expresses LIF-R mRNA. (**C**) Relative co-expression of LIF-R by POMC and AgRP neurons with the threshold for co-expression set at a signal-to-background ratio of 2.5

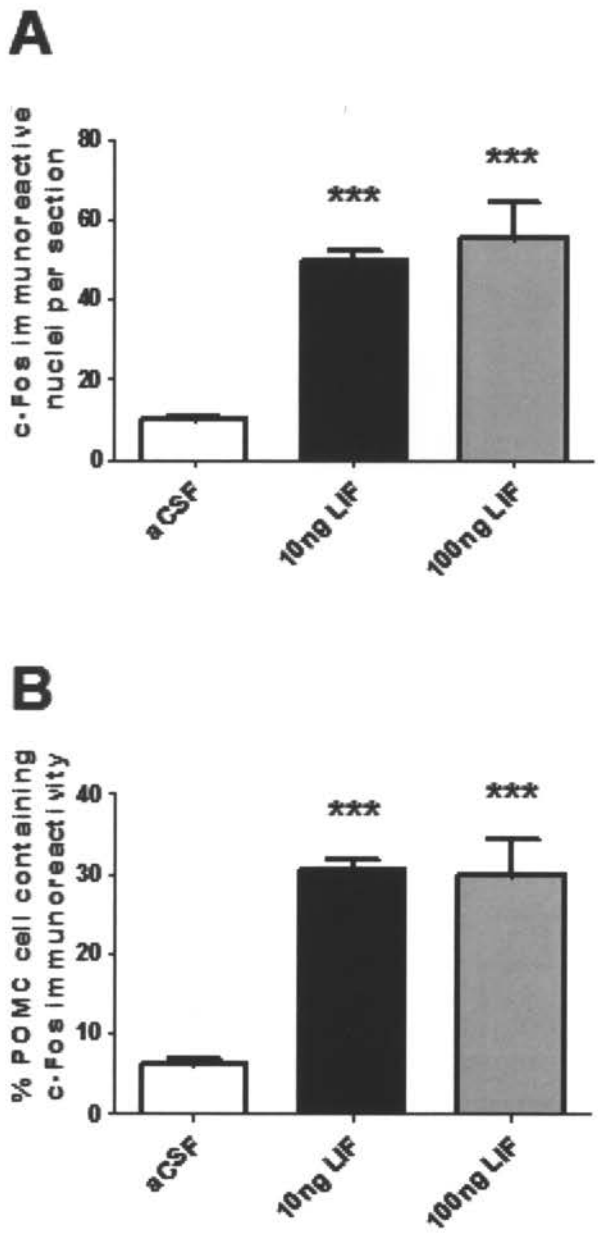

Figure A-3. LIF activates POMC-EGFP neurons in the hypothalamus. (**A**) LIF (10ng, i.c.v., n=4) increases the expression of c-Fos in the ARC. Increased doses of LIF (100ng, i.c.v., n=3) do not increase c-Fos expression vs. the lower dose (one-way ANOVA, ***$p<0.0001$ vs. aCSF). (**B**) ~31% of POMC neurons are activated by i.c.v. LIF (10ng and 100ng, one-way ANOVA, ***$p<0.0001$ vs. aCSF).

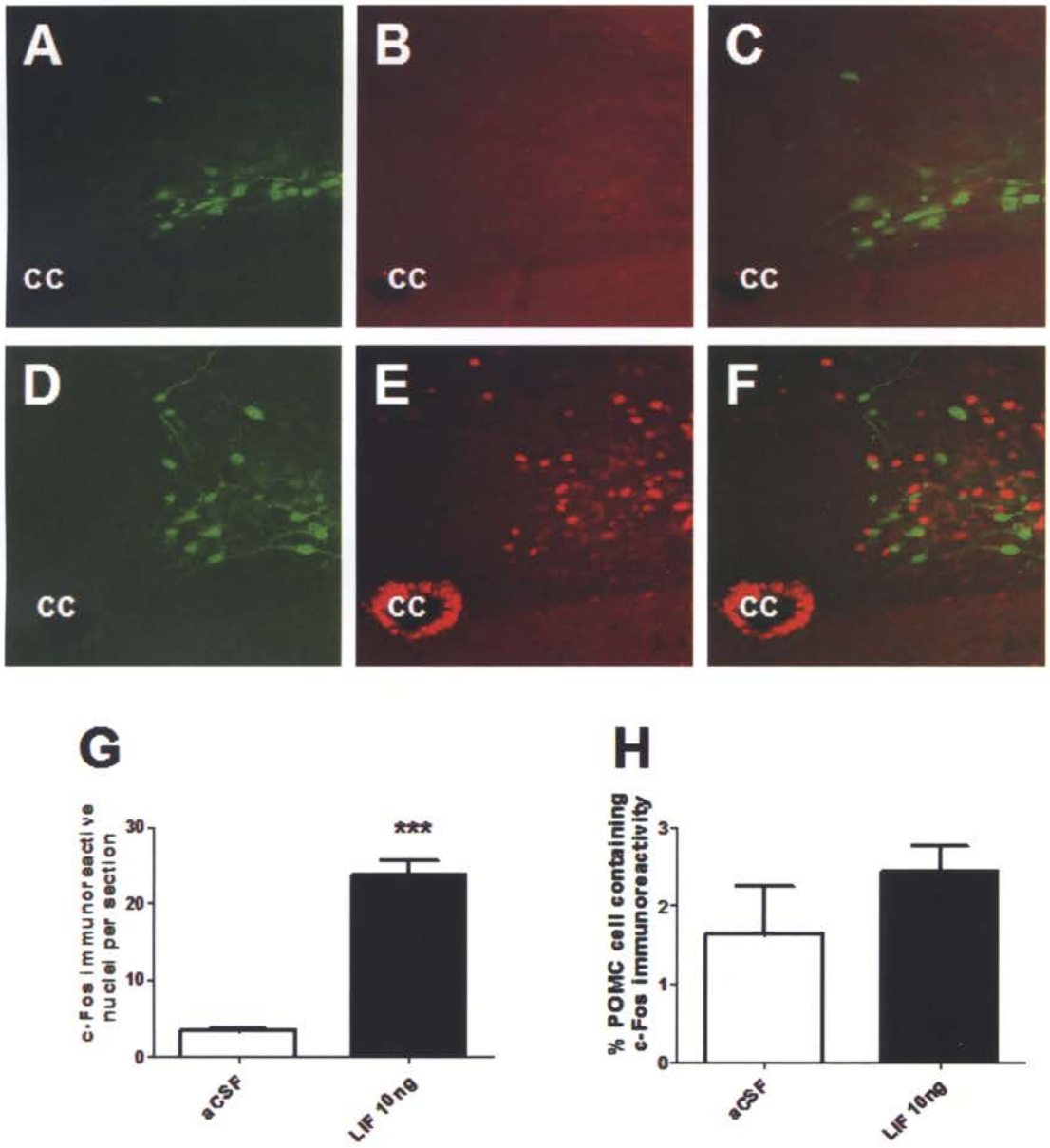

Figure A-4. LIF does not activate POMC-EGFP neurons in the NTS. (**A,D**) Expression of EGFP in the NTS of POMC-EGFP mice. (**B**) Expression of c-Fos (red) in aCSF-treated animals (i.c.v., n=4) is very low. (**C**) Few POMC neurons express c-Fos following aCSF treatment. (**E**) Expression of c-Fos in LIF-treated animals (10ng, i.c.v., n=5) is increased. (**F**) LIF does not activate c-Fos in NTS POMC-EGFP neurons. (**G**) LIF increases the expression of c-Fos in the NTS by ~7 fold (two-tailed Student's t-test, ***$p<0.0001$ vs. aCSF). (**H**) LIF does not increase the number POMC neurons activated in the NTS (two-tailed Student's t-test, p = ns vs. aCSF). CC = central canal.